

CONFIDENTIAL

Copy 5  
RM A53E12

NACA RM A53E12

AUG 12 1953



# RESEARCH MEMORANDUM

THE EFFECTS OF LEADING-EDGE EXTENSIONS, A TRAILING-EDGE  
EXTENSION, AND A FENCE ON THE STATIC LONGITUDINAL  
STABILITY OF A WING-FUSELAGE-TAIL COMBINATION  
HAVING A WING WITH  $35^\circ$  OF SWEEPBACK AND AN  
ASPECT RATIO OF 4.5

By Ralph Selan and Angelo Bandettini

Ames Aeronautical Laboratory  
Moffett Field, Calif.

CLASSIFICATION CANCELLED

Authority NACA Reg. 60s Date 5/14/56  
KN 101  
By MDA 6/1/56 See \_\_\_\_\_

CLASSIFIED DOCUMENT

This material contains information affecting the National Defense of the United States within the meaning of the espionage laws, Title 18, U.S.C., Secs. 793 and 794, the transmission or revelation of which in any manner to an unauthorized person is prohibited by law.

## NATIONAL ADVISORY COMMITTEE FOR AERONAUTICS

WASHINGTON

August 7, 1953

CONFIDENTIAL

NACA LIBRARY  
LANGLEY AERONAUTICAL LABORATORY  
Moffett Field, Calif.



## NATIONAL ADVISORY COMMITTEE FOR AERONAUTICS

RESEARCH MEMORANDUMTHE EFFECTS OF LEADING-EDGE EXTENSIONS, A TRAILING-EDGE  
EXTENSION, AND A FENCE ON THE STATIC LONGITUDINAL  
STABILITY OF A WING-FUSELAGE-TAIL COMBINATION  
HAVING A WING WITH  $35^\circ$  OF SWEEPBACK AND AN  
ASPECT RATIO OF 4.5

By Ralph Selan and Angelo Bandettini


## SUMMARY

An investigation has been made of leading-edge extensions, a trailing-edge extension, and a fence on the static longitudinal stability of a wing-fuselage-tail combination having a wing with  $35^\circ$  of sweepback and an aspect ratio of 4.5. The investigation involved the use of force measurements and tuft studies of the stall progression.

The results of tests of the semispan model without any wing modifications indicated large forward movements of the aerodynamic center at moderate angles of attack up to a Mach number of 0.90. A leading-edge chord extension with the inner discontinuity at 58 percent of the wing semispan proved effective up to 0.85 Mach number in increasing the lift coefficient at which this large forward movement in aerodynamic center occurred and caused no adverse effects at a Mach number of 0.92. The leading-edge chord extensions with the inner discontinuity at 77 percent of the wing semispan proved ineffective. A fence at 58 percent of the semispan improved the longitudinal stability at Mach numbers below 0.85, but did not change the aerodynamic characteristics of the model at the higher Mach numbers. A trailing-edge extension was, in general, ineffective in improving the stability of the model at all Mach numbers at which tests were conducted.

## INTRODUCTION

Swept-wing airplanes having wings of moderate or high aspect ratio tend to experience reductions in static longitudinal stability within a limited range of angles of attack at both subsonic and transonic Mach numbers. The alleviation of this reduction in stability has been the object of numerous wind-tunnel and flight investigations such as those



reported in references 1 through 6. The severity of the variations in stability differs considerably between various airplane configurations, depending primarily upon the character of the flow separation on the wing and, also, upon the distribution and strength of the wing downwash in the region of the tail.

Improvements in the static longitudinal stability have been obtained by the use of various devices for controlling flow separation. These devices include leading-edge slats, flaps, fences, vortex generators, leading-edge suction, and chord extensions (see, e.g., refs. 1, 5, and 7). Some of these devices improve only the low-speed-stall characteristics of a wing. Some of the devices, although effective in improving the static longitudinal-stability characteristics, are objectionable because of excessive mechanical complication and weight or because they increase the drag.

Tests of leading-edge chord extensions (ref. 3) have shown that this type of wing modification may be effective in improving the longitudinal stability for a large range of subsonic Mach numbers. Furthermore, there is little, if any, drag penalty involved in such a wing modification at low to moderate lift coefficients, and the drag is often decreased at the higher lift coefficients. Tests have indicated that the effectiveness of such a wing-leading-edge modification depends upon the geometry of the original wing, the type and spanwise location of the initial flow separation on the wing, and upon the geometry, size, and location of the leading-edge chord extension.

Tests were conducted in the 12-foot pressure wind tunnel to determine the effects of various leading-edge chord extensions on a model which was longitudinally unstable within a limited angle-of-attack range below maximum lift for Mach numbers up to about 0.90 (refs. 8 and 9). The model had a wing which was similar to that of an existing airplane (ref. 4). The effects of a trailing-edge extension and a leading-edge fence were also investigated.

#### NOTATION

All areas and dimensions used in the following symbols refer to the unmodified wing:

- b    wing span
- c    local wing chord parallel to the plane of symmetry

$\bar{c}$	wing mean aerodynamic chord, $\frac{\int_0^{b/2} c^2 dy}{\int_0^{b/2} c dy}$
$c^i$	wing chord at the inner end of the long-span leading-edge extension
$c''$	wing chord at the inner end of the short-span leading-edge extension
$c_t$	wing chord at the tip
$C_D$	drag coefficient, $\frac{\text{drag}}{qS}$
$C_L$	lift coefficient, $\frac{\text{lift}}{qS}$
$C_m$	pitching-moment coefficient about the quarter point of the wing mean aerodynamic chord, $\frac{\text{pitching moment}}{qS\bar{c}}$
$l$	length of body
$l_t$	tail length, distance from the quarter point of the wing mean aerodynamic chord to the quarter point of the horizontal-tail mean aerodynamic chord
$M$	free-stream Mach number
$q$	free-stream dynamic pressure
$R$	Reynolds number based on wing mean aerodynamic chord
$r$	local radius of body
$r_0$	maximum radius of body
$S$	area of semispan wing
$y$	coordinate in the lateral direction, normal to the plane of symmetry
$\alpha$	angle of attack measured from body center line, deg

$\left(\frac{dC_L}{d\alpha}\right)_{C_L=0}$  lift-curve slope at zero lift, per deg

$\left(\frac{dC_m}{dC_L}\right)_{C_L=0}$  pitching-moment-curve slope at zero lift

## MODEL DESCRIPTION

### Basic Model

The model used in this investigation (fig. 1) employed the solid steel semispan wing used in the tests reported in reference 8. This basic wing, referred to in the report as the unmodified wing, had the quarter-chord line swept back  $35^\circ$ , and had a taper ratio of 0.5 and an aspect ratio of 4.5. The wing sections in planes perpendicular to the quarter-chord line were the NACA 64A010. The model had a full-span trailing-edge flap but for this investigation this flap was locked at  $0^\circ$ , and all gaps at the hinge line were sealed. The horizontal tail was not swept and had an aspect ratio of 4.3 and a taper ratio of 1.0. The sections of the tail were the NACA 63A004.

The body consisted of a cast-aluminum shell on a steel spar. Coordinates for the body, which had a fineness ratio of 12.5, were determined from the equation given in figure 1(a). A mahogany fairing was used at the juncture between the horizontal stabilizer and the supporting pylon (fig. 2). Both the fairing and pylon remained in place during the tests when the horizontal stabilizer was removed. A description of the geometry of the basic model is given in table I and figure 1(a).

### Leading-Edge Extensions

The leading-edge extensions (fig. 1(b)) were machined from solid steel. Their profiles faired into the original wing at approximately 39 percent of the chord and were similar to the forward part of the original airfoil, except for reduced thickness ratios and nose radii (table II). The inner ends of the extensions were plane surfaces parallel to the plane of symmetry. The various leading-edge extensions, which varied in spanwise location and chordwise dimension, are described in the following paragraphs.

Long-span leading-edge extensions.- Leading-edge chord extensions having spanwise dimensions that were 42 percent of the wing semispan and located between 58 percent of the wing semispan and the tip are referred to as long-span leading-edge extensions (figs. 1(b) and 2(c)). The chordwise dimension of one of these extensions varied from 10 percent of the local wing chord at its inner end to 0 at the tip; whereas a second extension varied from 15 percent of the local wing chord at its inner end to 0 at the tip. A third long-span extension, which increased the original wing area by 5 percent, had a chordwise dimension equal to 15 percent of the local wing chord over its entire span.

Short-span leading-edge extensions.- Leading-edge chord extensions having spans equal to 23 percent of the wing semispan and located between 77 percent of the semispan and the tip are referred to as short-span leading-edge extensions (see figs. 1(b) and 2(d)). Except for the span of these extensions and the location of their inner ends, the geometry of the short-span leading-edge extensions was similar to that of the long-span extensions.

Inner leading-edge extension.- An inner leading-edge extension which increased the wing chord by 15 percent of the original local wing chord was located between 58 percent and 77 percent of the semispan (figs. 1(b) and 2(e)).

Double, tapered leading-edge extension.- The double, tapered leading-edge extension consisted of two extensions installed so as to produce discontinuities of the leading edge at 58 and 77 percent of the semispan. Each of the two parts of this extension tapered from 15 percent of the local wing chord at its inner end to 0 at its outer end (figs. 1(b) and 2(f)).

#### Trailing-Edge Extension

A trailing-edge extension consisting of a solid, wedge-shaped, mahogany fairing covered on both upper and lower surfaces with plastic-impregnated glass fabric was also added to the wing. The straight, unswept trailing edge of this extension intersected the original trailing edge 45 percent of the semispan out from the model center line, thereby increasing the wing root chord at the model center line by 36.8 percent, increasing the wing area by 11 percent, and moving the centroid of area rearward 2.74 percent of  $\bar{c}$  (figs. 1(b) and 2(g)). The coordinates of the trailing-edge extension are given in table II.

### Fence

The model was also tested with a boundary-layer fence. The fence (figs. 1(a) and 2(h)) was at 58 percent of the semispan and extended from 5 percent of the chord on the lower surface of the wing around the leading edge to 66 percent of the chord on the upper surface. The fence extended 3.75 percent of the local chord above the wing and 4.19 percent of the local chord ahead of the wing.

### TESTS

Tests of the model were conducted with and without the horizontal tail and employing various leading-edge extensions, a trailing-edge extension, and a fence. A combination of the leading-edge and trailing-edge extensions was also tested. Lift, drag, and pitching moment were measured at Mach numbers ranging from 0.20 to 0.92 at a Reynolds number of 2,000,000. Additional data were obtained at a Reynolds number of 11,000,000 and a Mach number of 0.20 to study the effects of Reynolds number variation.


The angle of attack was varied from  $-4^\circ$  to  $24^\circ$ , except at the higher Mach numbers where the range was reduced due to wind-tunnel choking and to power limitations. In all cases, the horizontal stabilizer was maintained at  $0^\circ$  incidence with respect to the body center line.

### CORRECTIONS TO DATA

The data have been corrected for jet-boundary effects, for constriction due to the tunnel walls, and for model-support tare forces.

Corrections to the data to account for jet-boundary effects due to lift on the wing have been computed by the methods given in reference 10. The corrections, which were added to the angles of attack, drag coefficients, and the pitching-moment coefficients are shown in table III. The data have been corrected for the constriction due to the tunnel walls by the methods of reference 11 and are listed in table III. The effect of the sweep on these corrections has not been taken into account.

Tare corrections to account for the drag due to the exposed area of the turntable were subtracted from the measured drag coefficients and are also shown in table III. No evaluation was made of the interference between the model and the turntable, and no compensation was



made for the tunnel-floor boundary layer which had a displacement thickness of 1/2 inch at the turntable.

## RESULTS AND DISCUSSION

### Model With Unmodified Wing

Figure 3 shows the effects of Mach number, at a Reynolds number of 2,000,000, on the lift, drag, and pitching moment of the model without modifications. The pitching-moment data (fig. 3(b)) indicate that at Mach numbers below 0.90, the center of pressure moved forward with increasing lift coefficient within a lift-coefficient range that varied to some extent with Mach number. Observations of tufts, which will be discussed later, indicate that initial separation occurred near the leading edge below a Mach number of 0.90; whereas above this Mach number, initial separation occurred near the trailing edge.

Figure 4 shows the lift, pitching-moment, and drag data for the unmodified model without the horizontal tail, but with the tail fairing in place. A comparison of figures 3(b) and 4(b) shows that although the tail contributed to the longitudinal stability at low and moderate angles of attack, its contribution was small or negative at lift coefficients where model instability occurred. The model with the tail removed became unstable at about the same angles of attack as the complete model, but the extent of the center-of-pressure movement was not as large. Initial instability of the complete model can be attributed to the pitching-moment characteristics of the wing-fuselage combination, but the extent of the loss in stability with increasing angle of attack was augmented by a decrease in horizontal-tail effectiveness.

### The Effect of Leading-Edge Modifications

Experience has shown that a variety of devices can be used to remedy the low-speed longitudinal instability occurring at the higher lift coefficients for an airplane having a sweptback wing. However, few of these devices have been successful in contributing to the stability at high subsonic speeds. Therefore, initial tests were conducted at Mach numbers of 0.80, 0.85, and 0.92 to determine the effects on the stability characteristics of variation of leading-edge-extension geometry, size, and location along the span.

Mach number of 0.80.- Figures 5, 6, and 7 show the lift, drag, and pitching-moment data obtained with the leading-edge extensions and the fence, at a Mach number of 0.80. Comparison of the pitching-moment data



for the original model and for the model with the long-span, leading-edge extensions (fig. 5(a)) shows that with the extensions added, there was an increase in the lift coefficient at which a forward movement of the center of pressure occurred. A rearward center-of-pressure movement corresponding to a maximum increment in pitching-moment coefficient of -0.05 resulted from the addition of these extensions. From figure 6(a), it is apparent that the short extensions merely decreased slightly the forward movement of the center of pressure. Results of testing the inner extension, the double, tapered extension, and the fence (fig. 7) indicate that these two leading-edge extensions were more effective than the fence. The leading-edge extensions with the inner discontinuity at 58 percent of the semispan proved most effective at a Mach number of 0.80.

Mach number of 0.85.- Lift, drag, and pitching-moment data obtained at a Mach number of 0.85 are shown in figures 8, 9, and 10 for the model with the leading-edge extensions and the fence. For the range of lift coefficients between 0.60 and 0.78, the long-span extensions improved the pitching-moment characteristics of the original model, but to a lesser extent than at a Mach number of 0.80 (fig. 5(a)). Figure 9(a) shows that the short extensions had little effect on the pitching-moment characteristics. Both the short, inner extension and the double, tapered extension delayed the forward movement of the center of pressure which occurred at a lift coefficient of about 0.60 on the original model; whereas the fence was completely ineffective. As was the case for a Mach number of 0.80, the extensions having their inner discontinuity at 58 percent of the semispan proved most effective.

Mach number of 0.92.- Figures 11, 12, and 13 show the aerodynamic characteristics obtained at a Mach number of 0.92 for the model with the leading-edge extensions and the fence. The addition of these leading-edge modifications did not result in significant adverse changes in the pitching-moment characteristics of the original model.

The effects of Mach number for the model with chord extensions extending to  $0.58 b/2$ .- Since the results presented previously indicated that the leading-edge extensions with their inner ends at 58 percent of the wing semispan were the most effective in improving the longitudinal stability of the original model, further tests were conducted with the long-span and the inner, constant-percent-chord extensions.

Lift, pitching-moment, and drag data for the complete model with the long leading-edge extension are shown in figure 14. Data for the model with the horizontal tail removed are shown in figure 15. It can be seen from figure 15(b) that the effect of adding the long-span leading-edge extension to the model without the tail was to eliminate or delay to higher lift coefficients the forward center-of-pressure movement at all the test Mach numbers up to 0.90. Comparison of the data for the complete model with those for the model with the tail

removed indicates that the loss in tail effectiveness at high angles of attack was not as great as in the case of the original model. Addition of the leading-edge extension resulted in little or no change in the values of pitching moment at zero lift for the various test Mach numbers.

Accompanying the improvement in the longitudinal stability of the original model, the data indicate reductions in drag at the higher lift coefficients and little or no increase at lower lift coefficients as a result of adding the long-span leading-edge extensions to the wing. In connection with the drag reductions, tuft studies indicated reductions in the areas of flow separation.

Data obtained at several Mach numbers with the original model modified by the addition of the short, 15-percent-chord extension at the inner location are shown in figure 16. Comparison of figures 16(b) and 14(b) shows that the stability improvements due to the short-span inner extension closely approach those contributed by the long-span leading-edge extension. (Both the long and short extensions had their inner ends  $0.58 b/2$  from the body center line.)

The effects of a long-span chord extension at low speed and a Reynolds number of 11,000,000.- The effects of adding the long-span chord extension at a Reynolds number of 11,000,000 and a Mach number of 0.20 are shown in figure 17. Comparison of figures 3 and 17(a) indicates that increasing the Reynolds number from 2,000,000 to 11,000,000 increased the angle-of-attack range for which the lift and pitching-moment curves remained essentially linear.

Tests of both the long, constant 15-percent-chord, leading-edge extension and the long, tapered, 10-percent-chord extension indicated that these extensions eliminated the forward center-of-pressure movement present with the original model and increased the maximum lift coefficient by nearly 0.20. In addition, the shapes of the lift curves near maximum lift were not altered (fig. 17(a)).

Tests of the wing-body combination with the long ( $0.42 b/2$ ), constant 15-percent-chord, leading-edge extension (fig. 17(b)) indicate that the improvement in longitudinal stability was primarily due to the beneficial effects of the leading-edge extension upon the wing-fuselage characteristics.

#### The Effects of a Trailing-Edge Extension and of a Trailing-Edge and Leading-Edge Extension Combined

Effects of Mach number.- Figure 18 shows the effects of a trailing-edge extension on the aerodynamic characteristics of the basic model at

Mach numbers up to 0.92. Similar data are shown in figure 19 for the model without the horizontal tail. The trailing-edge extension was not effective in improving the pitching-moment characteristics of the model.

The effect of adding both a leading-edge extension and a trailing-edge extension to the basic model is shown in figures 20 and 21. Comparison of the data in figure 20 with similar data for the wing with only the leading-edge extension (fig. 14) indicates that the improvement in stability was due almost entirely to the leading-edge chord extension.

Reynolds number of 11,000,000.- Lift, drag, and pitching-moment data obtained at a Reynolds number of 11,000,000 and a Mach number of 0.20 for the complete model with the trailing-edge extension in combination with the long-span, constant-percent-chord, leading-edge extension and for the unmodified model are shown in figure 22. As was the case at a Reynolds number of 2,000,000, the trailing-edge extension had little effect on the characteristics of either the plain wing or the wing with a leading-edge extension (cf. figs. 22 and 17(a)).

#### The Effects of the Fence

The effects of Mach number.- Lift, pitching-moment, and drag data for the complete model with a fence are compared with data for the unmodified model at Mach numbers from 0.20 to 0.92 in figure 23. It is seen in figure 23(b) that at Mach numbers of 0.80 and less, the fence increased the lift coefficients at which a sudden loss in longitudinal stability occurred. At Mach numbers of 0.85 and 0.90, the fence was completely ineffective. At a Mach number of 0.92, the addition of the fence resulted in no changes in the stability of the original model. Figures 23(a) and 23(c) show that the lift was increased and the drag was generally decreased at the Mach numbers (0.20 to 0.80) and lift coefficients at which the stability was improved by addition of the fence. Similar gains resulting from the use of a leading-edge fence were shown in reference 3.

Comparison of data obtained with the horizontal tail removed from the model (fig. 24) and data for the complete model (fig. 23) reveals that the addition of the fence had little effect on the flow at the horizontal tail.

Reynolds number of 11,000,000.- Shown in figures 25 and 26 are the lift, drag, and pitching-moment data for the model with the leading-edge fence at a Reynolds number of 11,000,000. These data indicate that adding the fence eliminated the large forward movement of the wing center of pressure, increased the maximum lift coefficient approximately

0.13, and did not alter the shape of the lift curve near maximum lift. Comparison of figure 17(a) and figure 25 indicates that the effects of the leading-edge extension and of the fence are similar at this Mach number and Reynolds number.

### Summary of the Effects of Compressibility

The variation with Mach number of lift-curve slope, pitching-moment-curve slope, and drag coefficient is shown in figure 27 for the original model with the unmodified wing and the model with the long-span, constant 15-percent-chord, leading-edge extension. It is seen that, in general, the variation of the above-mentioned parameters with Mach number is about the same for the modified and unmodified models. Addition of the leading-edge extension caused little or no increase in drag at the lower lift coefficients; whereas it caused a reduction in drag at a lift coefficient of 0.6.

### Remarks on Flow Separation

Some indication of the effects of the leading-edge chord extension and of the fence on the flow over the wing and on the stall progression was provided by observation of tufts on the wing. At all the test Mach numbers below 0.85, flow separation on the original wing first occurred near the leading edge. At the higher Mach numbers, 0.90 and 0.92, the flow separated first near the trailing edge on the outer portion of the span and, as the angle of attack increased, the separation spread forward and inward. The wing modifications were most effective in improving the model stability and in altering the areas of flow separation when the leading-edge type of separation was present.

Mach number of 0.20 to 0.80.- At a Reynolds number of 11,000,000 and a Mach number of 0.20, the initial separation occurred close to the leading edge and was accompanied by a pronounced outflow in the narrow region of separation. When the fence was added, the initial separation near the leading edge occurred at about the same angle of attack as on the unmodified model, but was reduced in chordwise extent, except at the tip and just inboard of the fence. When the chord extension was added to the wing leading edge, the areas of flow separation were similar to those on the wing with the fence.

At a Reynolds number of 2,000,000 and at Mach numbers from 0.20 to 0.80, separation on the original wing followed patterns similar to those at a Reynolds number of 11,000,000, except that extensive separation began at much lower angles of attack and progressed more gradually

over the rest of the wing. In each case, the forward movement of the center of pressure indicated by the pitching-moment data was accompanied by a chordwise and spanwise spreading of the region of separation. At angles of attack below those at which longitudinal instability occurred, leading-edge separation was observed along a large portion of the span. The separation extended from the leading edge back a very short distance along the chord at the inner extremity, but widened to extend over an increasingly large part of the chord toward the tip. The region of separated flow near the leading edge remained small, and early reattachment occurred behind this region near the root. The boundary-layer control was due to the three-dimensional nature of the flow; in regions along the span where this condition existed, outflow within the separated region removed some of the separated flow and permitted reattachment near the leading edge, thus avoiding the sudden, rapid, rearward extension of separation that is typical of a two-dimensional flow with similar initial separation.

When the fence was added to the wing, the section just outboard of the fence presumably benefitted from the favorable effects of three-dimensional flow in the same manner as did portions of the unmodified wing near the root. Although local separation occurred at the leading edge, the point of reattachment remained near the leading edge of the wing just outboard of the fence. Immediately inside the fence, no favorable control of the boundary layer was present and separation extended over most of the chord.

As with the fence, the chord extensions apparently prevented the flow within the region of leading-edge separation (on the inner portion of the wing) from continuing spanwise across the leading-edge discontinuity. As a result, the wing immediately outboard of the discontinuity benefitted from boundary-layer control due to outflow in the region of leading-edge separation on the outer portion of the wing. Elimination of spanwise flow at the discontinuity can be attributed to the effect of a vortex generated by the discontinuity which streamed over the upper surface of the wing, thus introducing an aerodynamic barrier to interrupt the outflow and deflect it rearward and also energizing the boundary layer by introducing into it air from the stream outside the boundary layer. The inner face of the leading-edge extension may also have acted as a physical barrier to the spanwise flow in much the same manner as the fence.

Mach number of 0.85.- Examination of tuft photographs indicates that at a Mach number of 0.85, the flow separation on the original wing first occurred near the midchord at the tip and then spread progressively inward. The growth of the regions of separation did not appear to be directly associated with a spanwise flow in the boundary layer at this Mach number. Addition of the fence had practically no effect upon the location of the separation, or upon the static longitudinal stability.

Adding the chord extension, however, delayed the static instability and resulted in flow patterns which appeared to be similar to those at lower Mach numbers with the chord extension on the wing.

Mach numbers of 0.90 and 0.92.- At Mach numbers of 0.90 and 0.92, the tuft data indicated that separation initially occurred on the original wing near the trailing edge. However, no abrupt shift in center of pressure occurred on the original wing at a Mach number of 0.92. Neither the fence nor the leading-edge chord extension significantly affected the stability of the model. The areas of separation were practically unaffected by the addition of the fence, but addition of the leading-edge chord extensions eliminated some of the separated flow just outside the leading-edge discontinuity. This elimination or reduction of separation at this spanwise location was an effect of the chord extension that was observed at relatively high angles of attack at all the Mach numbers of the test, which may account for the reduction in drag mentioned previously.

#### CONCLUDING REMARKS

Test results have been presented to show the effects of various modifications including several leading-edge extensions, a trailing-edge extension, and a fence on the static longitudinal stability of a model with a 35° sweptback wing.

The data from the tests indicate the following:

1. The forward movement of the center of pressure with increasing angle of attack, which occurred at Mach numbers below 0.90, could be substantially decreased or delayed to higher lift coefficients by the addition of a leading-edge chord extension. Tuft studies indicated that initial separation occurred near the leading edge below a Mach number of 0.90.

2. The leading-edge extensions with the inner discontinuity at 58 percent of the semispan eliminated or reduced the forward movement of the center of pressure at moderate lift coefficients for Mach numbers of 0.80 and 0.85, whereas the leading-edge extensions with the inner discontinuity at 77 percent of the wing semispan were comparatively ineffective at these Mach numbers.

3. Addition of the leading-edge fence to the wing at 58 percent of the wing semispan improved the longitudinal stability at moderate lift coefficients at Mach numbers below 0.85, while at Mach numbers of 0.85 and above the stability characteristics differed little from those of the original model.

4. At a Reynolds number of 11,000,000 and a Mach number of 0.20, the addition of either a long span leading-edge chord extension or a fence increased the maximum lift coefficient, eliminated the forward movement of center of pressure at the stall, and did not change the shape of the lift curve near maximum lift.

5. The trailing-edge extension was, in general, ineffective in improving the stability of the original model at the Mach numbers and Reynolds numbers at which tests were conducted.

6. The addition of the long-span, constant-percent-chord, leading-edge extension to the original model caused a reduction in drag at high lift coefficients and little or no increase in drag at low lift coefficients.

Ames Aeronautical Laboratory  
National Advisory Committee for Aeronautics  
Moffett Field, Calif., May 12, 1953

#### REFERENCES

1. Maki, Ralph L.: Full-Scale Wind-Tunnel Investigation of the Effects of Wing Modifications and Horizontal-Tail Location on the Low-Speed Static Longitudinal Characteristics of a  $35^\circ$  Swept-Wing Airplane. NACA RM A52B05, 1952.
2. Morrill, Charles P., Jr., and Boddy, Lee E.: High-Speed Stability and Control Characteristics of a Fighter Airplane Model With a Swept-Back Wing and Tail. NACA RM A7K28, 1948.
3. Goodson, Kenneth W., and Few, Albert G., Jr.: Effect of Leading-Edge Chord-Extensions on Subsonic and Transonic Aerodynamic Characteristics of Three Models Having  $45^\circ$  Sweptback Wings of Aspect Ratio 4. NACA RM L52K21, 1952.
4. Anderson, Seth B., and Bray, Richard S.: A Flight Evaluation of the Longitudinal Stability Characteristics Associated With the Pitch-Up of a Swept-Wing Airplane in Maneuvering Flight at Transonic Speeds. NACA RM A51I12, 1951.
5. Jaquet, Byron M.: Effects of Chord Discontinuities and Chordwise Fences on Low-Speed Static Longitudinal Stability of an Airplane Model Having a  $35^\circ$  Sweptback Wing. NACA RM L52C25, 1952.

6. Fischel, Jack, and Nugent, Jack: Flight Determination of the Longitudinal Stability in Accelerated Maneuvers at Transonic Speeds for the Douglas D-558-II Research Airplane Including the Effects of an Outboard Wing Fence. NACA RM L53A16, 1953.
7. Goodson, Kenneth W., and Few, Albert G., Jr.: Low-Speed Aerodynamic Characteristics of a Model With Leading-Edge Chord Extensions Incorporated on a  $40^\circ$  Sweptback Circular-Arc Wing of Aspect Ratio 4 and Taper Ratio 0.50. NACA RM L52I18, 1952.
8. Tinling, Bruce E., and Dickson, Jerald K.: Tests of a Model Horizontal Tail of Aspect Ratio 4.5 in the Ames 12-Foot Pressure Wind Tunnel. I - Quarter-Chord Line Swept Back  $35^\circ$ . NACA RM A9G13, 1949.
9. Demele, Fred A., and Sutton, Fred B.: The Effects of Increasing the Leading-Edge Radius and Adding Forward Camber on the Aerodynamic Characteristics of a Wing with  $35^\circ$  of Sweepback. NACA RM A50K28a, 1951.
10. Sivells, James C., and Salmi, Rachel M.: Jet-Boundary Corrections for Complete and Semispan Swept Wings in Closed Circular Wind Tunnels. NACA TN 2454, 1951.
11. Herriot, John G.: Blockage Corrections for Three-Dimensional-Flow Closed-Throat Wind Tunnels With Consideration of the Effect of Compressibility. NACA Rep. 995, 1950 (Formerly NACA RM A7B28).



TABLE I.- GEOMETRY OF BASIC MODEL

Wing (without leading- or trailing-edge extensions)	
Aspect ratio . . . . .	4.5
Taper ratio . . . . .	0.5
Sweep of quarter-chord line, deg . . . . .	35
Section normal to quarter-chord line . . . . .	NACA 64A010
Area (semispan), sq ft . . . . .	4.443
Mean aerodynamic chord, ft . . . . .	1.458
Dihedral, deg . . . . .	0
Incidence, deg . . . . .	0.5
Position on body . . . . .	midwing
Body	
Fineness ratio . . . . .	12.5
Length, ft . . . . .	7.292
Frontal area/wing area . . . . .	0.0303
Horizontal Tail	
Aspect ratio . . . . .	4.333
Taper ratio . . . . .	1.0
Sweep, deg . . . . .	0
Section . . . . .	NACA 63A004
Area (semispan), sq ft . . . . .	0.542
Tail length ( $l_t$ ), ft . . . . .	3.267
Incidence, deg . . . . .	0
Vertical distance above wing-chord plane extended . . . . .	0.218 $b/2$



TABLE II.- COORDINATES OF SECTIONS IN STREAM DIRECTION<sup>1</sup>  
[All dimensions in percent of chord of original section]

Original section (streamwise direction)		Section with 10% chord L.E.extension(inboard end)		Section with 15% chord L.E.extension(inboard end)		Section with T.E.extension (root station)	
Station	Ordinate Upper or lower	Station	Ordinate Upper or lower	Station	Ordinate Upper or lower	Station	Ordinate Upper or lower
0	0	-10.000	0	-15.000	0		
.100	.300	-9.875	.300	-14.863	.300		
.200	.438	-9.750	.438	-14.725	.438		
.300	.537	-9.625	.538	-14.587	.538		
.578	.732	-9.275	.731	-14.200	.731		
.866	.881	-8.919	.881	-13.800	.881		
1.200	1.019	-8.494	1.019	-13.338	1.019		
1.442	1.113	-8.194	1.113	-13.006	1.113		
2.000	1.288	-7.488	1.288	-12.225	1.288		
2.877	1.531	-6.381	1.531	-11.000	1.531		
4.000	1.781	-4.975	1.781	-9.450	1.781		
5.730	2.103	-2.794	2.106	-7.044	2.106	(Same as orig. sec.)	(Same as orig. sec.)
8.562	2.525	.756	2.525	3.125	2.525		
11.372	2.869	4.288	2.869	.781	2.869		
16.929	3.394	11.281	3.394	8.500	3.394		
22.402	3.774	18.150	3.775	16.081	3.775		
27.794	4.038	24.938	4.038	23.575	4.038		
33.106	4.210	31.606	4.213	30.944	4.213		
38.340	4.292	36.000	4.288	36.000	4.288		
38.760	4.294	38.181	4.294	38.206	4.294		
43.492	4.284						
48.582	4.167						
53.592	3.959					53.538	3.956
58.531	3.683					62.342	3.539
63.400	3.351					71.067	3.121
68.201	2.976	(Same as orig. sec.)	(Same as orig. sec.)	(Same as orig. sec.)	(Same as orig. sec.)	79.702	2.708
72.935	2.570					88.178	2.304
77.603	2.140					96.486	1.909
82.207	1.704					104.788	1.514
86.748	1.273					112.847	1.132
91.227	.849					120.906	.746
95.646	.430					128.796	.373
100.000	0					136.605	0

<sup>1</sup>Also describes the section at all stations of the constant-chord 15-percent leading-edge extensions.

TABLE III. - CORRECTIONS TO DATA

## (a) Corrections for Jet-Boundary Effects

M	$\Delta\alpha/C_L$	$\Delta C_D/C_L^2$	$\Delta C_m/C_L$	
			Wing-body	Wing-body-tail
0.20	0.384	0.00590	0.0010	0.0044
.60	.397	.00600	.0016	.0061
.80	.415	.00607	.0020	.0077
.85	.424	.00605	.0023	.0084
.90	.438	.00602	.0027	.0097
.92	.445	.00601	.0031	.0104

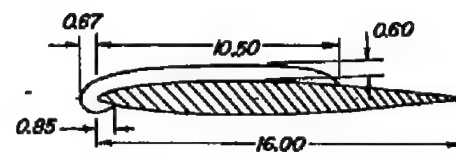
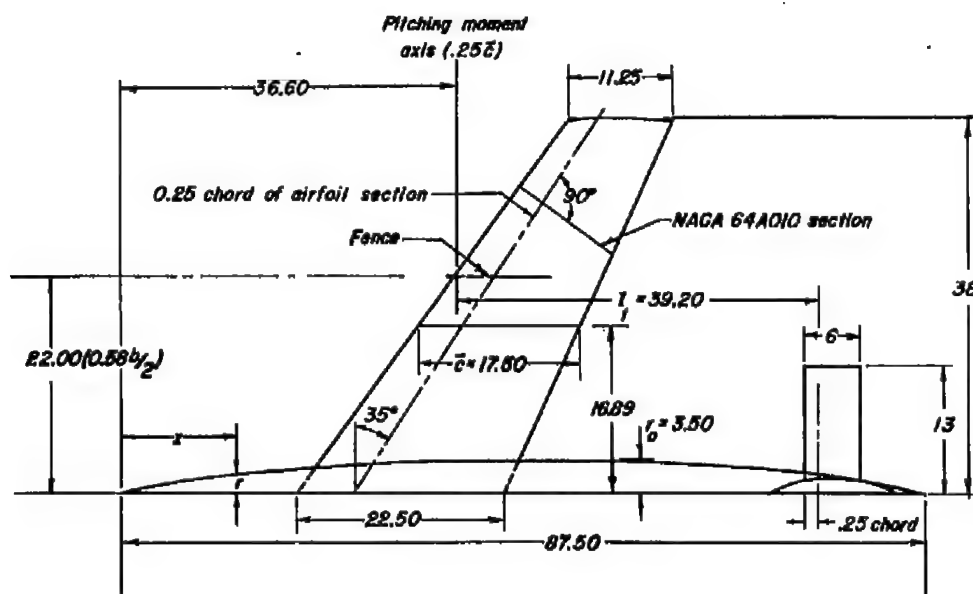
## (b) Corrections for Constriction Due to Tunnel Walls

Corrected Mach number	Uncorrected Mach number	$\frac{q_{\text{corrected}}}{q_{\text{uncorrected}}}$
0.200	0.200	1.002
.600	.599	1.003
.800	.797	1.005
.850	.846	1.006
.900	.892	1.010
.920	.909	1.012

## (c) Tare Corrections

$R \times 10^{-6}$	M	$C_{D\text{Tare}}$
11	0.20	0.0043
2	.20	.0045
↓	.60	.0045
	.80	.0050
	.85	.0053
	.90	.0057
	.92	.0060

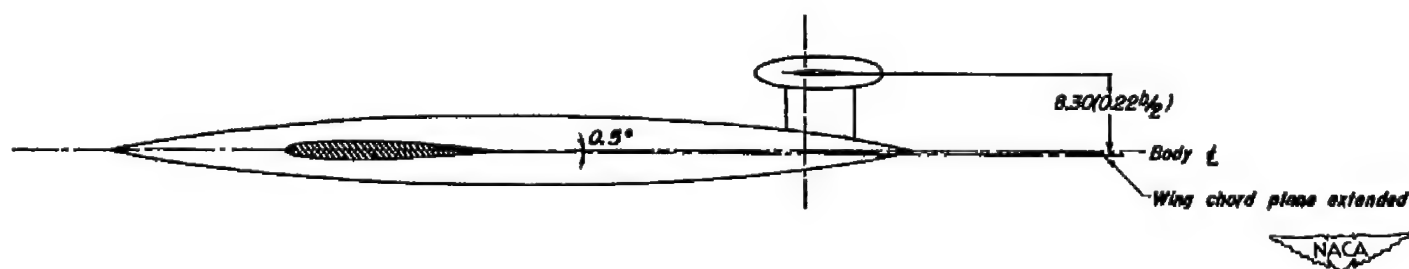




Fence detail

Equation of Body ordinates

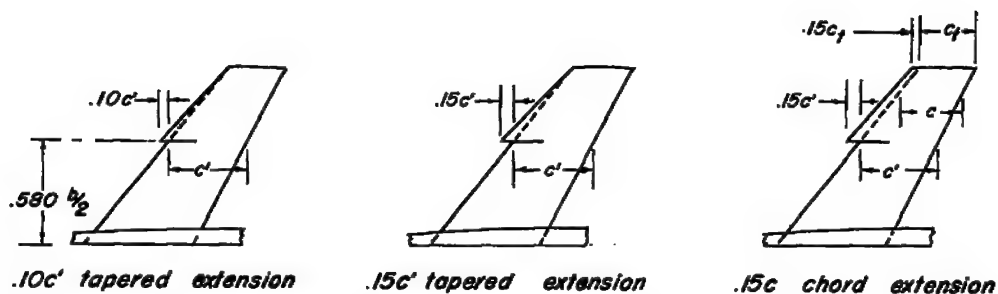
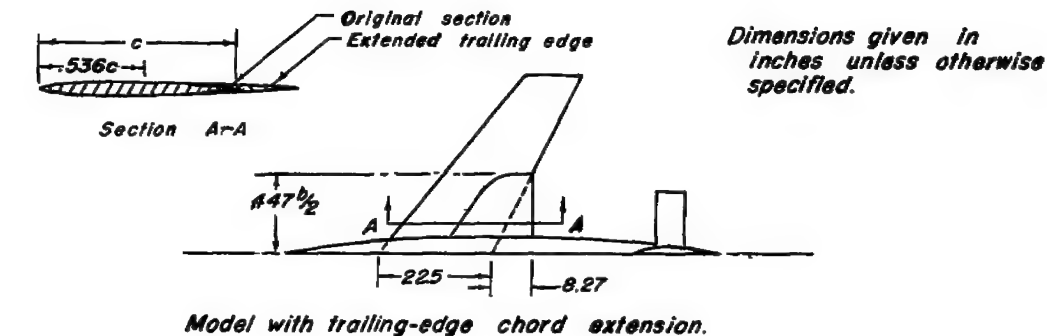
$$\frac{r}{r_o} = \left[ 1 - \left( 1 - \frac{2x}{l} \right)^2 \right]^{3/4}$$



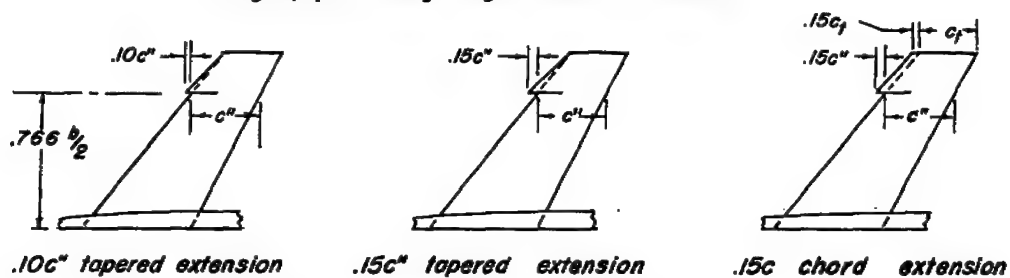
(a) Complete model.

Figure 1.- Drawings of the model.

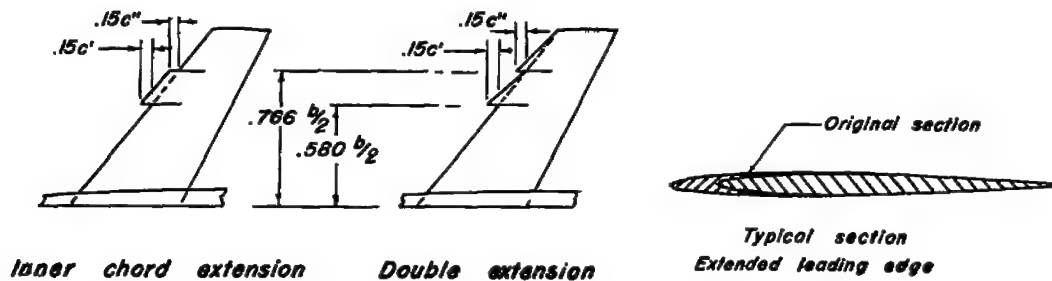
Note: Dimensions given in inches unless otherwise specified.



Long span leading-edge chord extensions



Short span leading-edge chord extensions

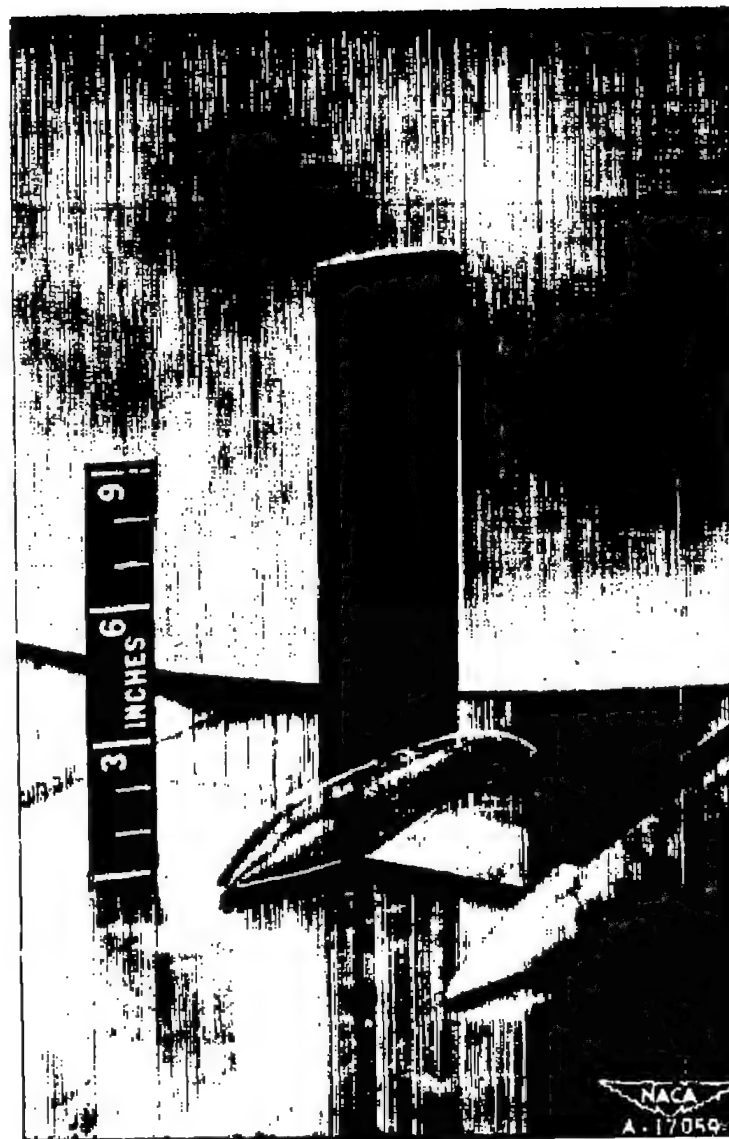


(b) Wing leading- and trailing-edge modifications.

Figure 1.- Concluded.



(a) Complete model.

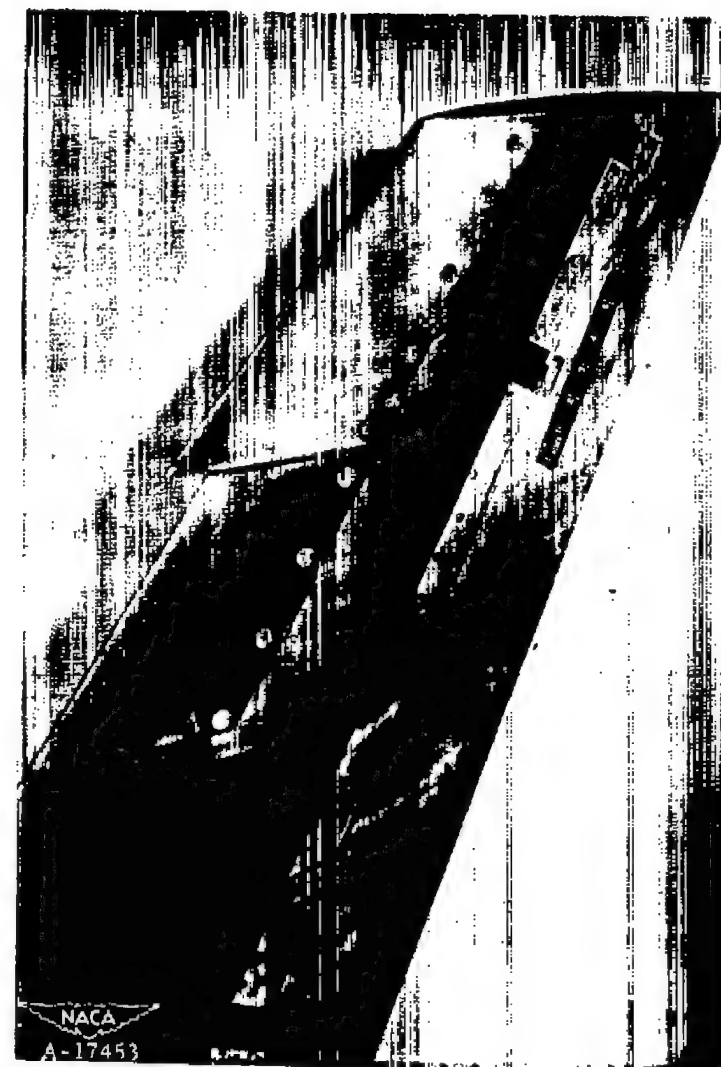


(b) Tail.

Figure 2.- Photographs of the model and modifications.



(c) Long, constant 15-percent-chord,  
leading-edge extension.

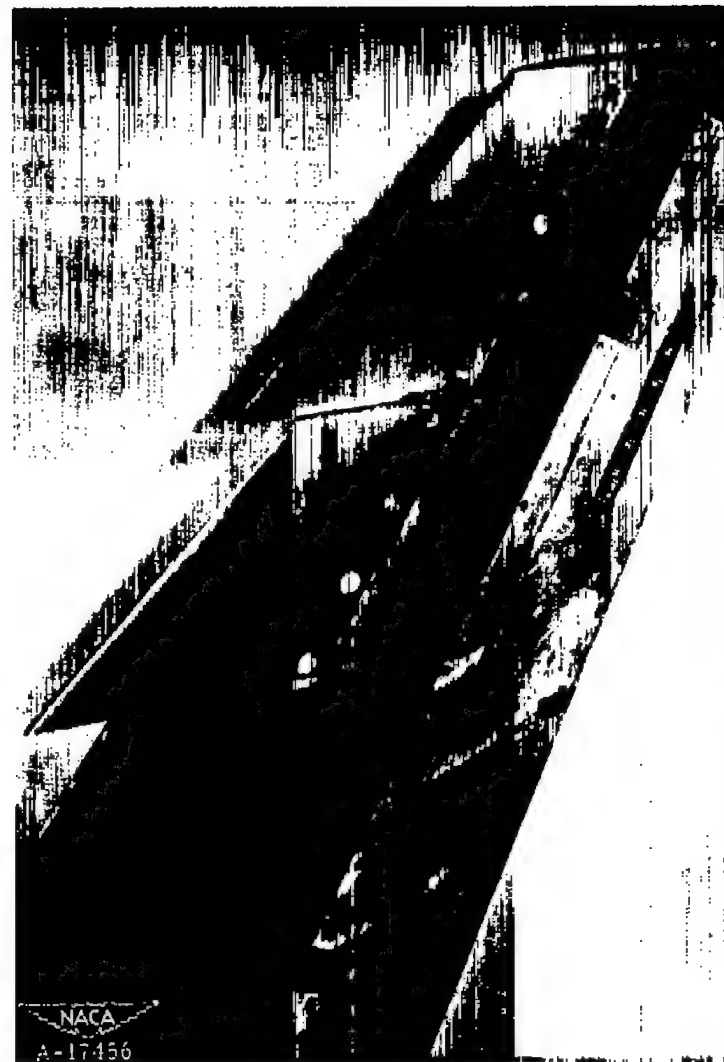


(d) Short, tapered, 10 percent-chord,  
leading-edge extension.

Figure 2.- Continued.



(e) Short, inner leading-edge extension.



(f) Double, tapered leading-edge extension.

Figure 2.- Continued.





(g) Model with leading-edge and trailing-edge extensions.



(h) Fence.

Figure 2.- Concluded.

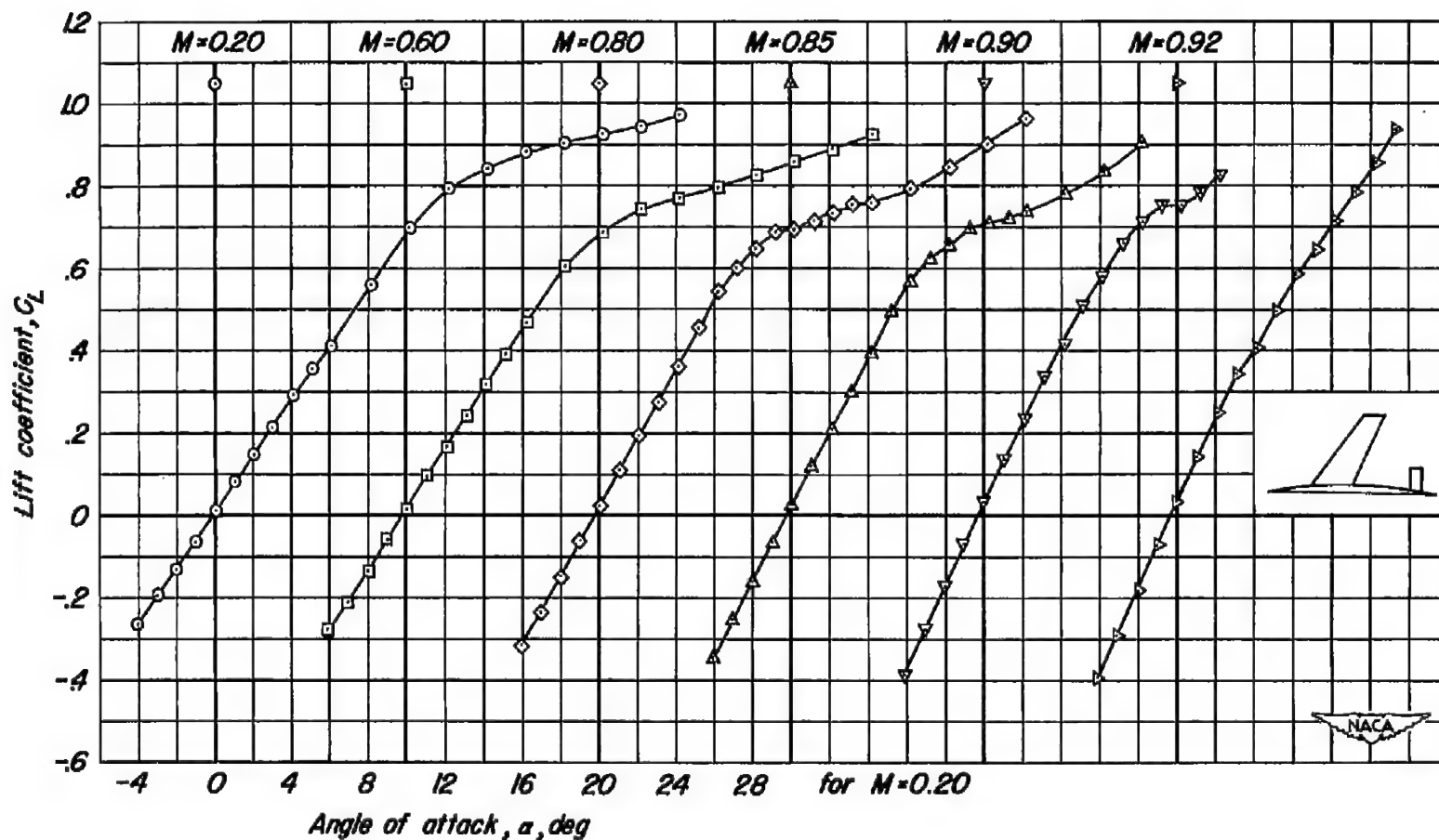
(a)  $C_L$  vs  $\alpha$ 

Figure 3.- The effect of Mach number on the aerodynamic characteristics of the complete model.  $R$ , 2,000,000.

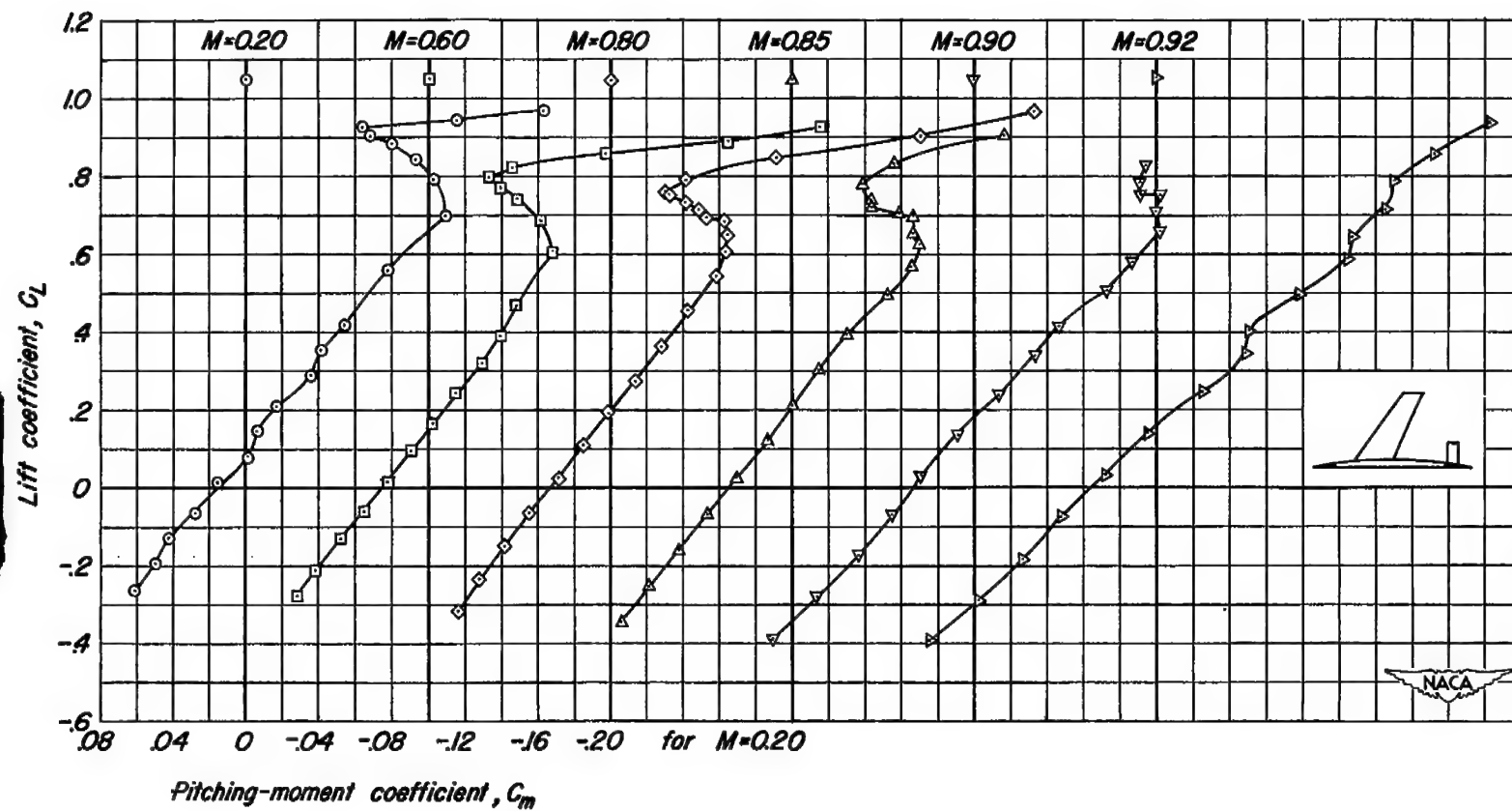
(b)  $C_L$  vs  $C_m$ 

Figure 3.- Continued.

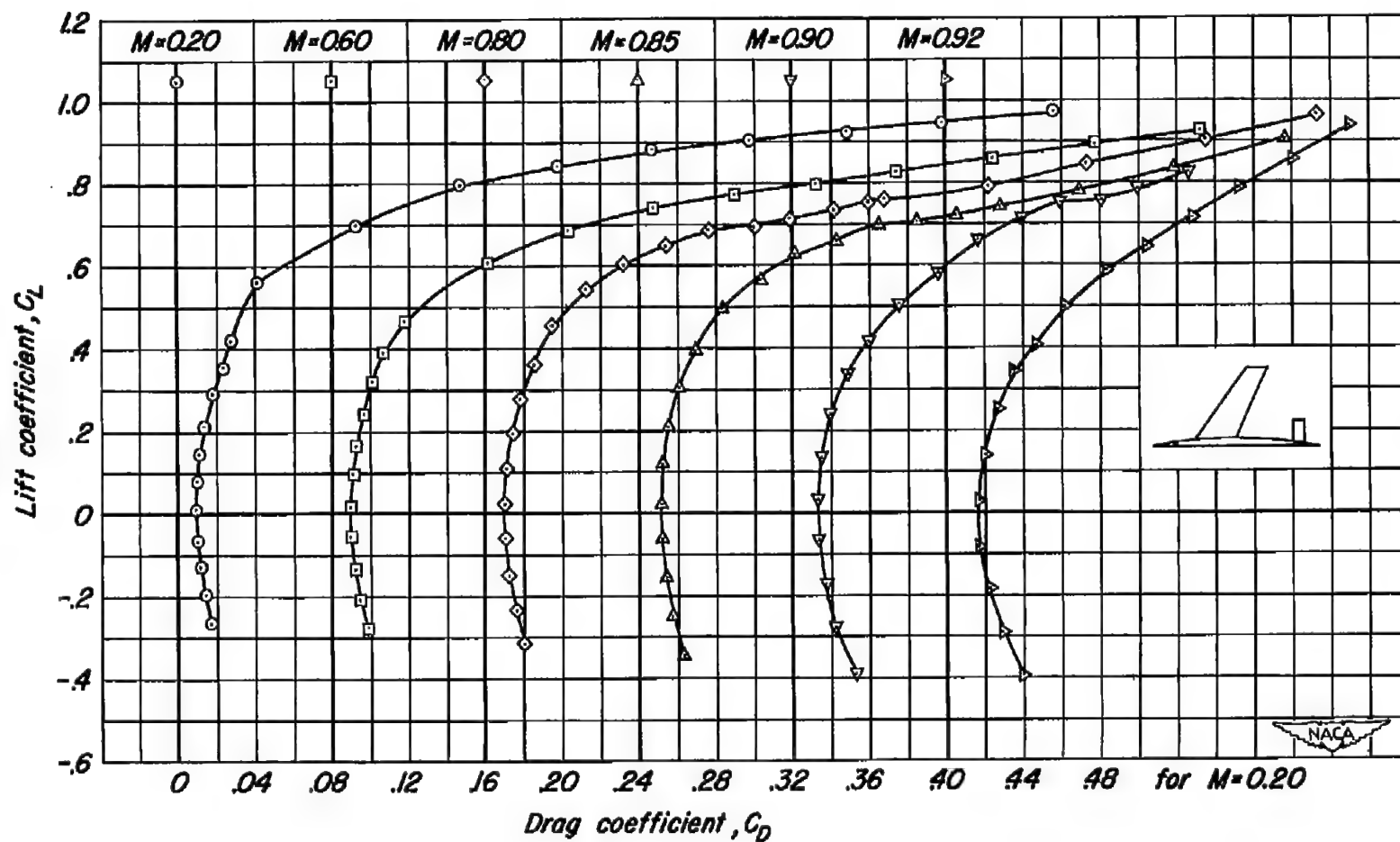
(c)  $C_L$  vs  $C_D$ 

Figure 3.- Concluded.

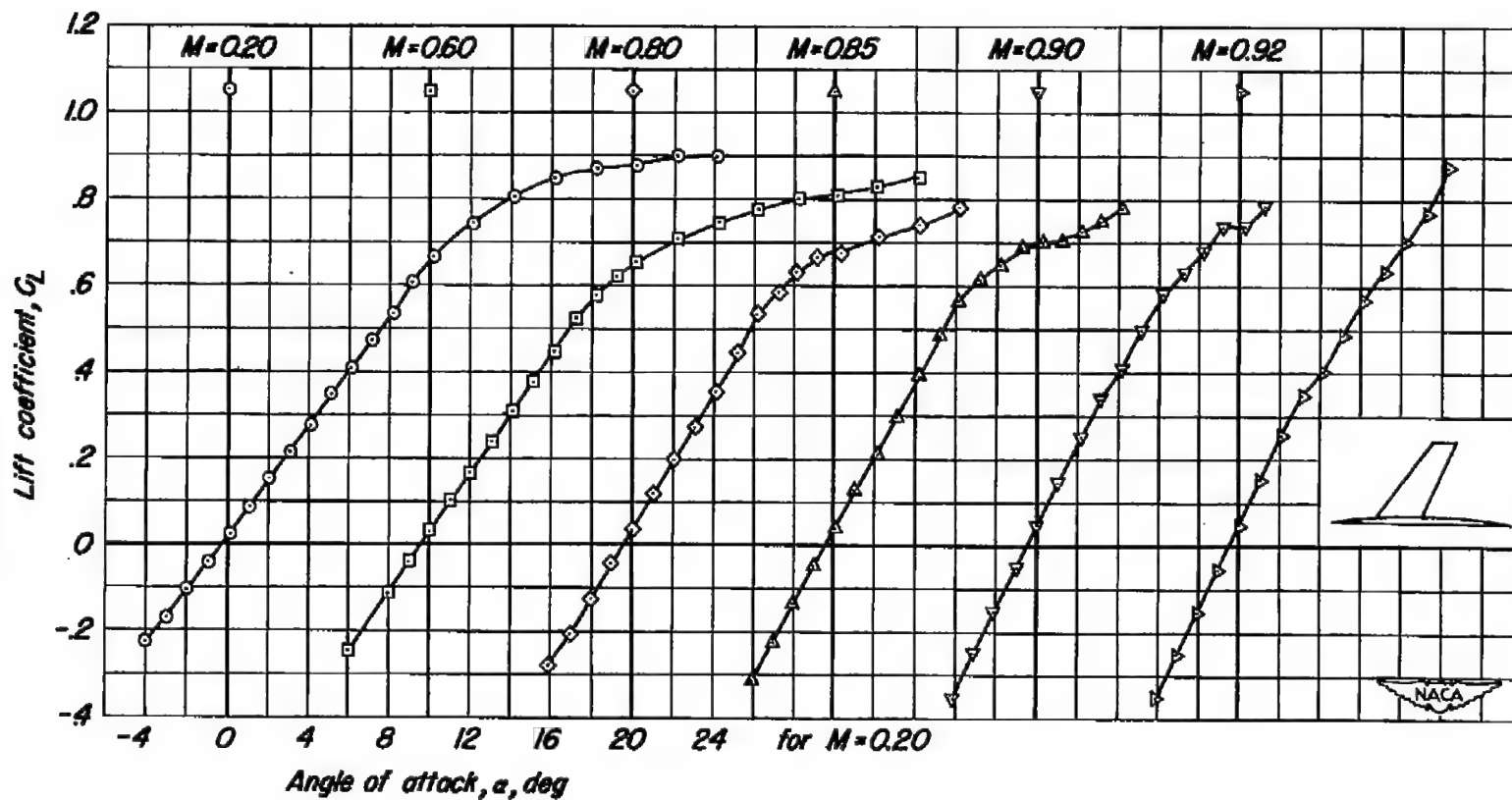
(a)  $C_L$  vs  $\alpha$ 

Figure 4.- The effect of Mach number on the aerodynamic characteristics of the model without tail.  $R$ , 2,000,000.

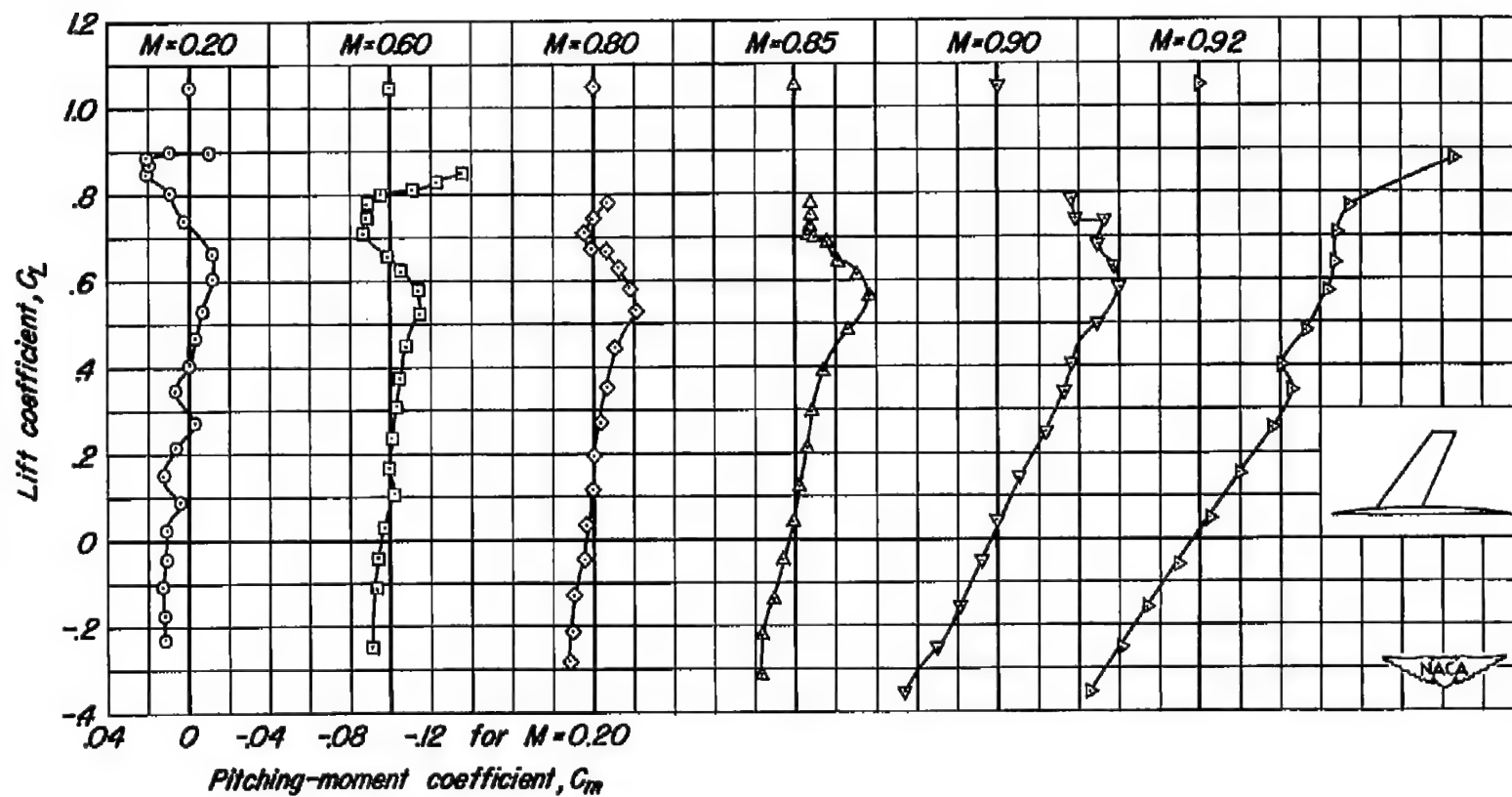
(b)  $C_L$  vs  $C_m$ 

Figure 4.- Continued.

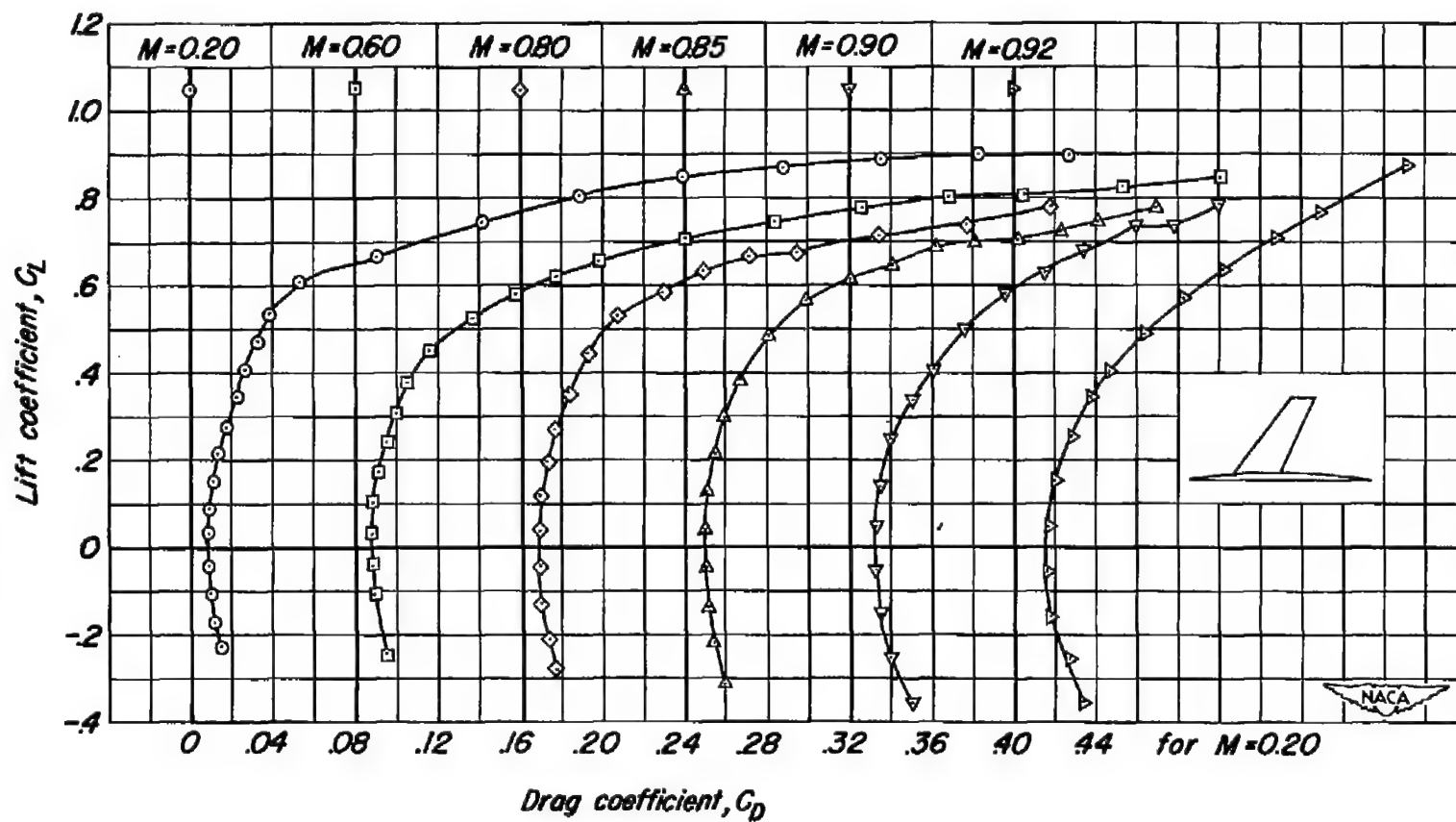
(c)  $C_L$  vs  $C_D$ 

Figure 4.- Concluded.

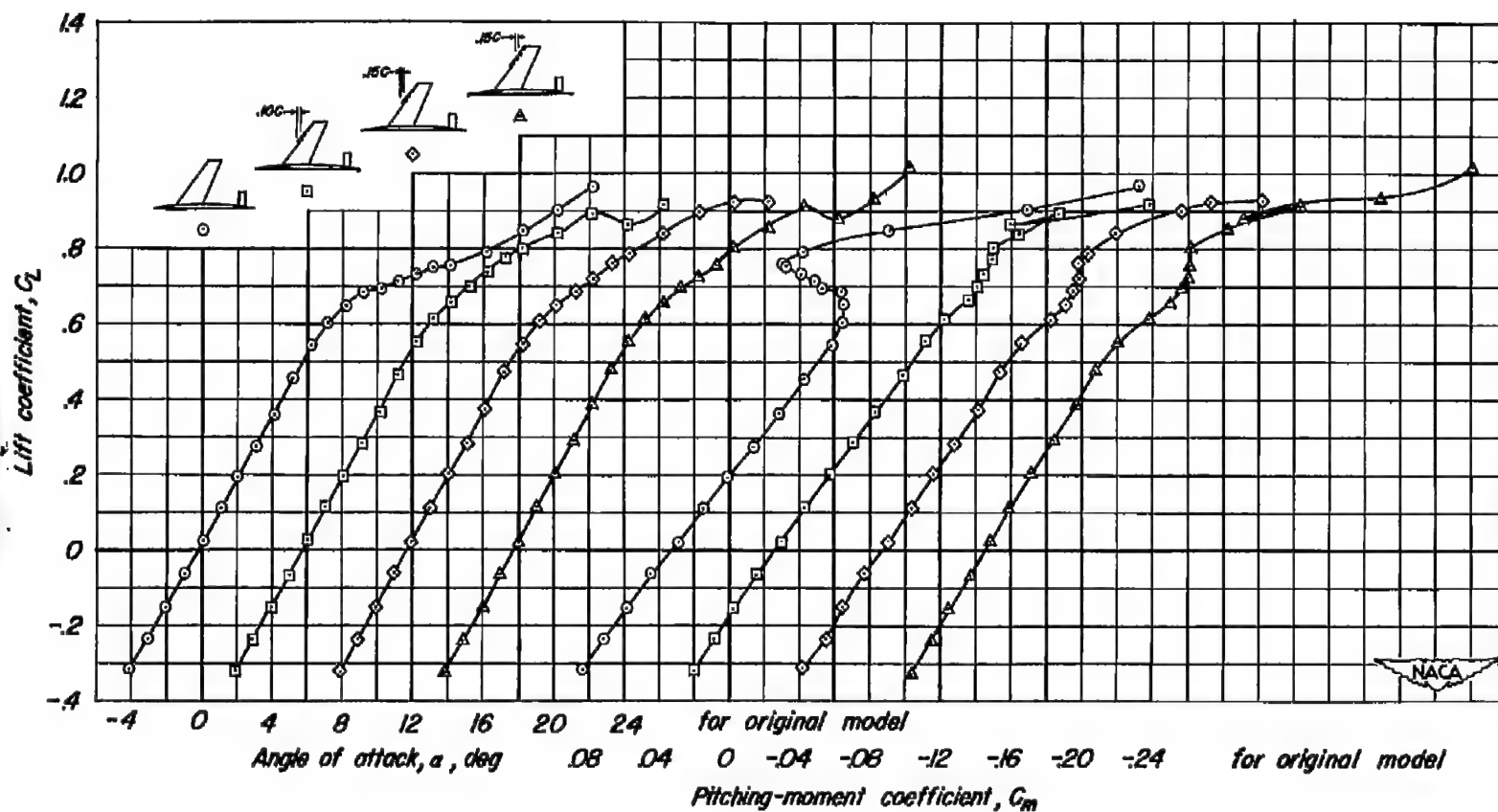
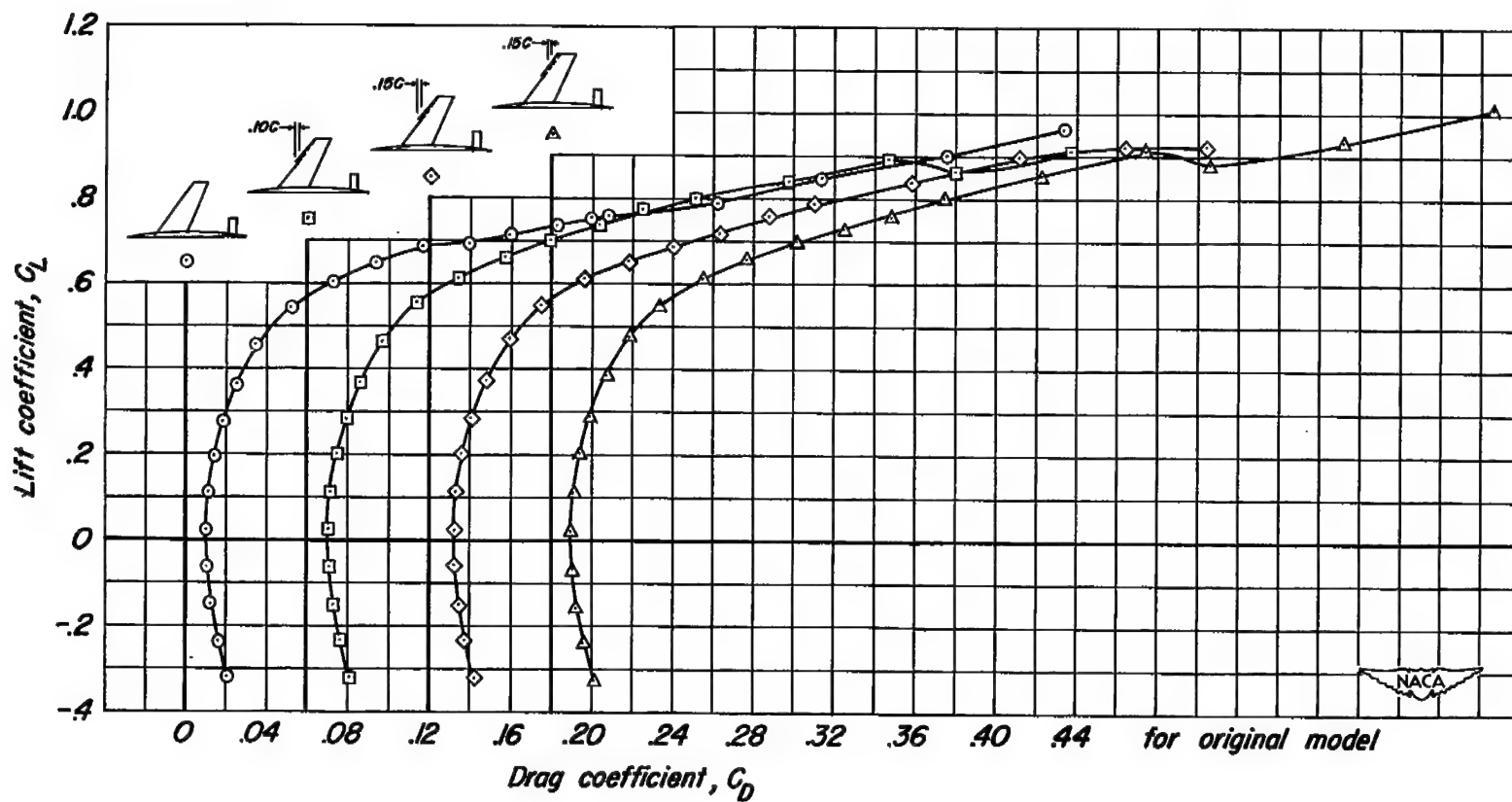
(a)  $C_L$  vs  $\alpha$ ;  $C_L$  vs  $C_m$ 

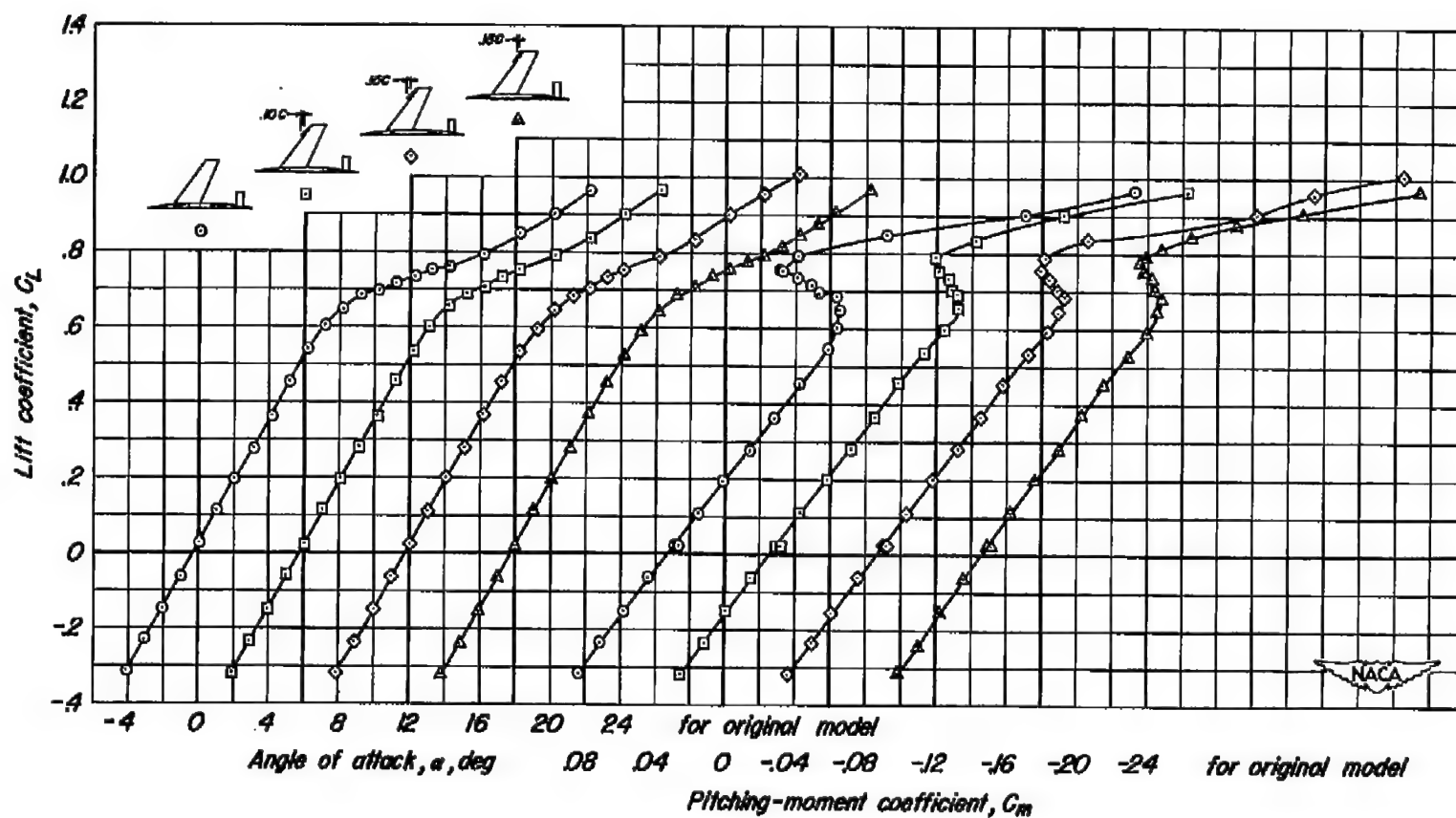
Figure 5.- The aerodynamic characteristics of the complete model with long-span leading-edge extensions at a Mach number of 0.80.  $R$ , 2,000,000.





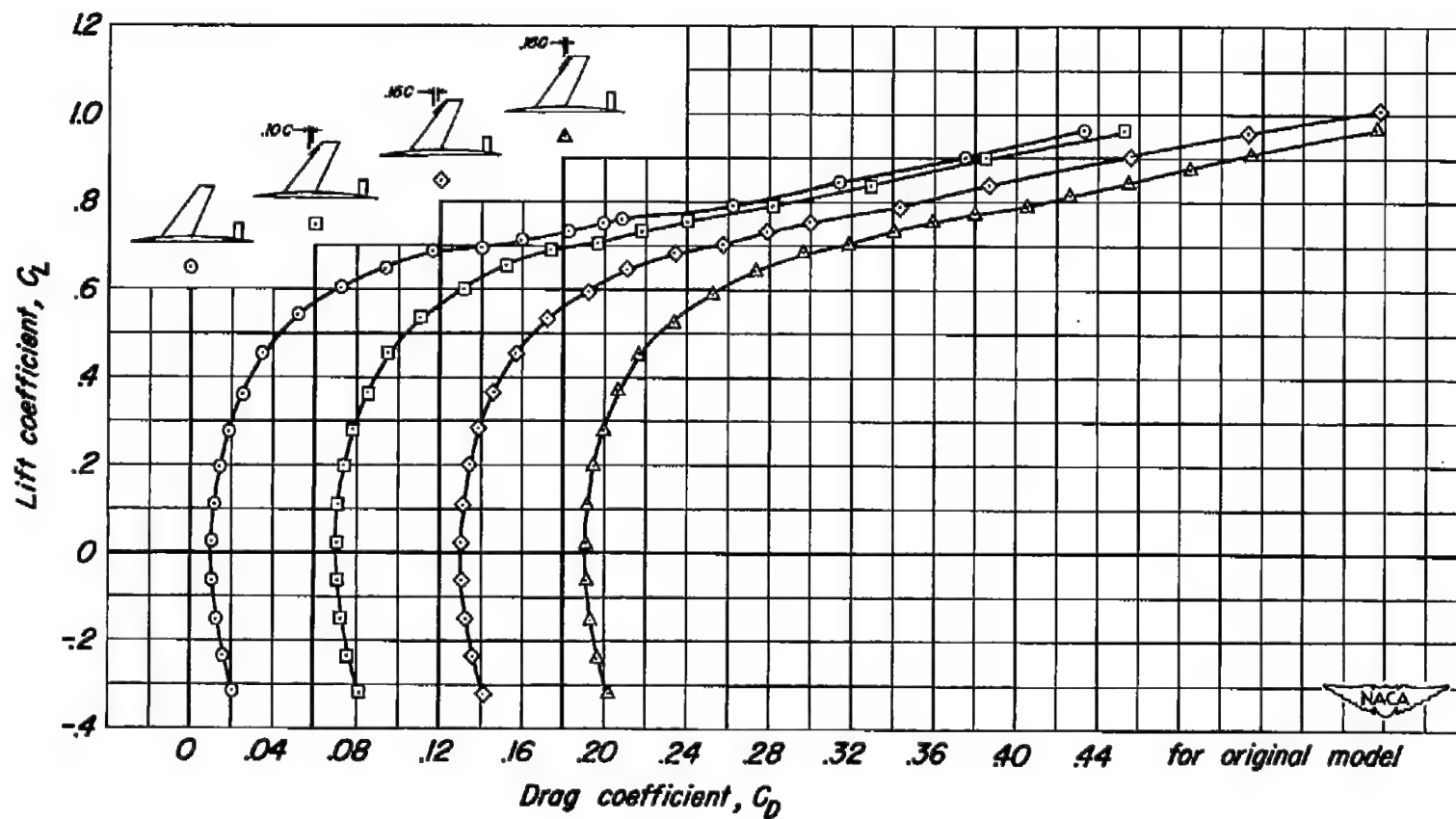
(b)  $C_L$  vs  $C_D$

Figure 5.- Concluded.



(a)  $C_L$  vs  $\alpha$ ;  $C_L$  vs  $C_m$

Figure 6.- The aerodynamic characteristics of the complete model with short-span leading-edge extensions at a Mach number of 0.80.  $R$ , 2,000,000.



(b)  $C_L$  vs  $C_D$

Figure 6.- Concluded.

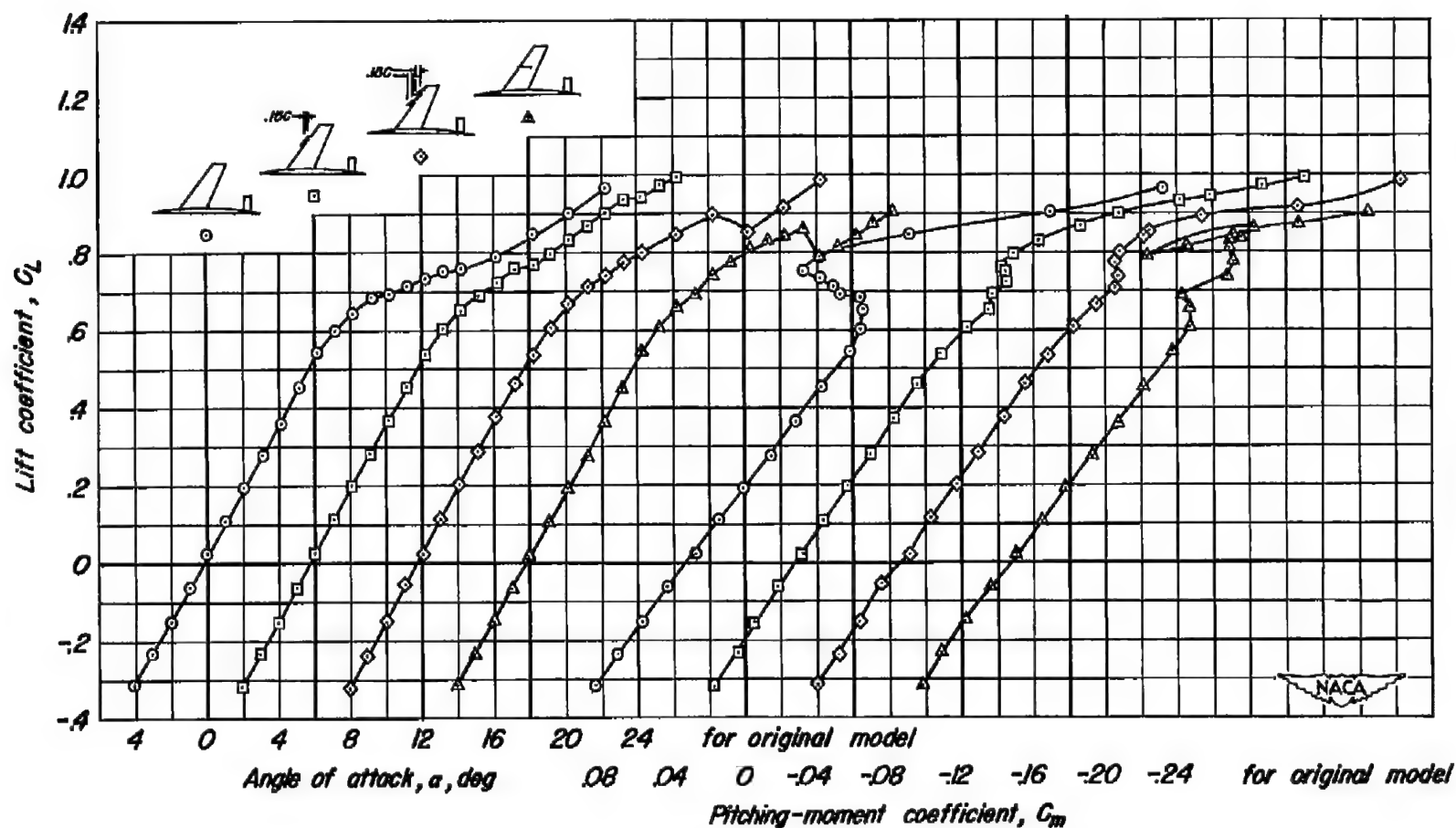
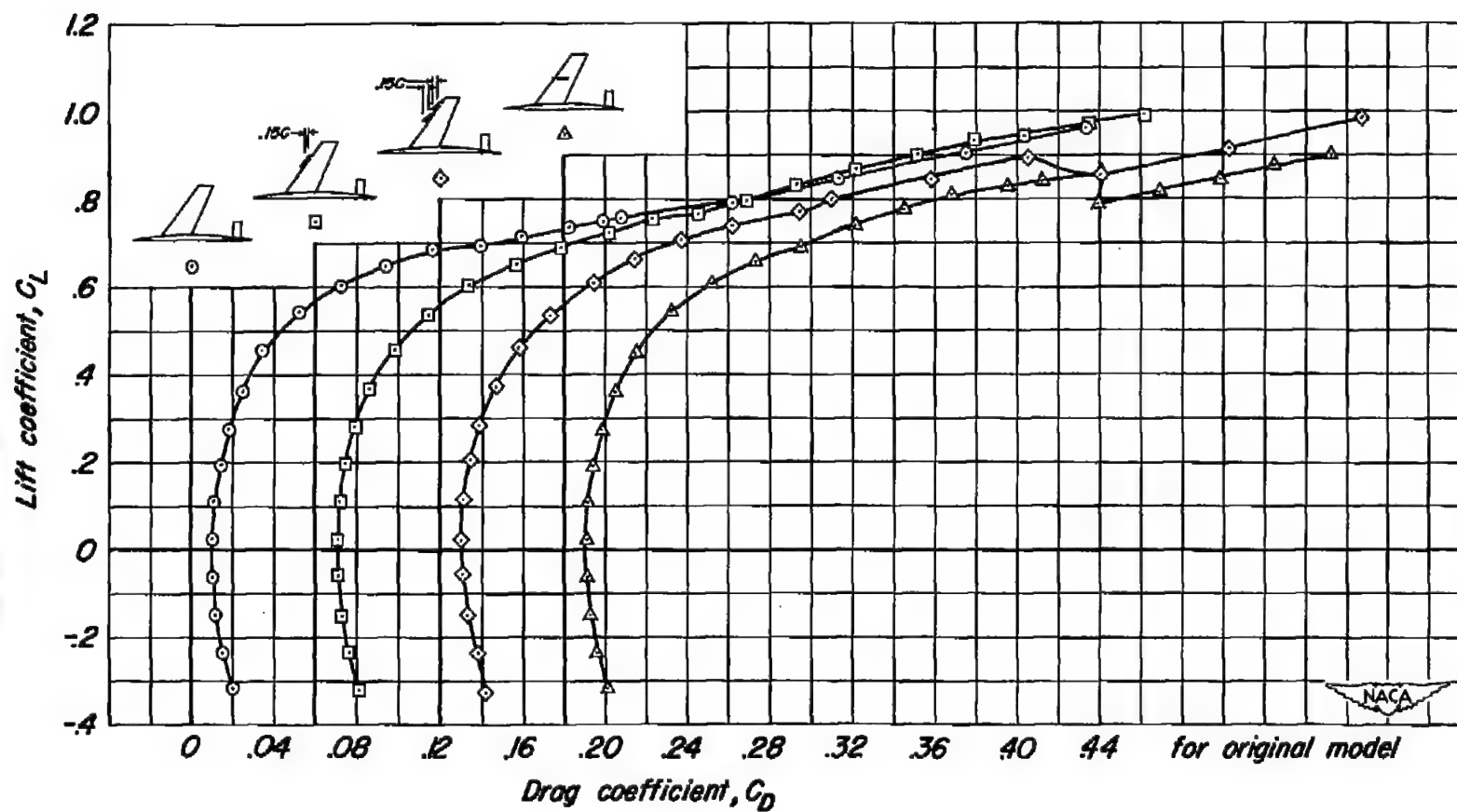
(a)  $C_L$  vs  $\alpha$ ;  $C_L$  vs  $C_m$ 

Figure 7.- The aerodynamic characteristics of the complete model with an inner leading-edge extension, a double, tapered extension, and a fence at a Mach number of 0.80.  
 $R, 2,000,000$ .



(b)  $C_L$  vs  $C_D$

Figure 7.- Concluded.

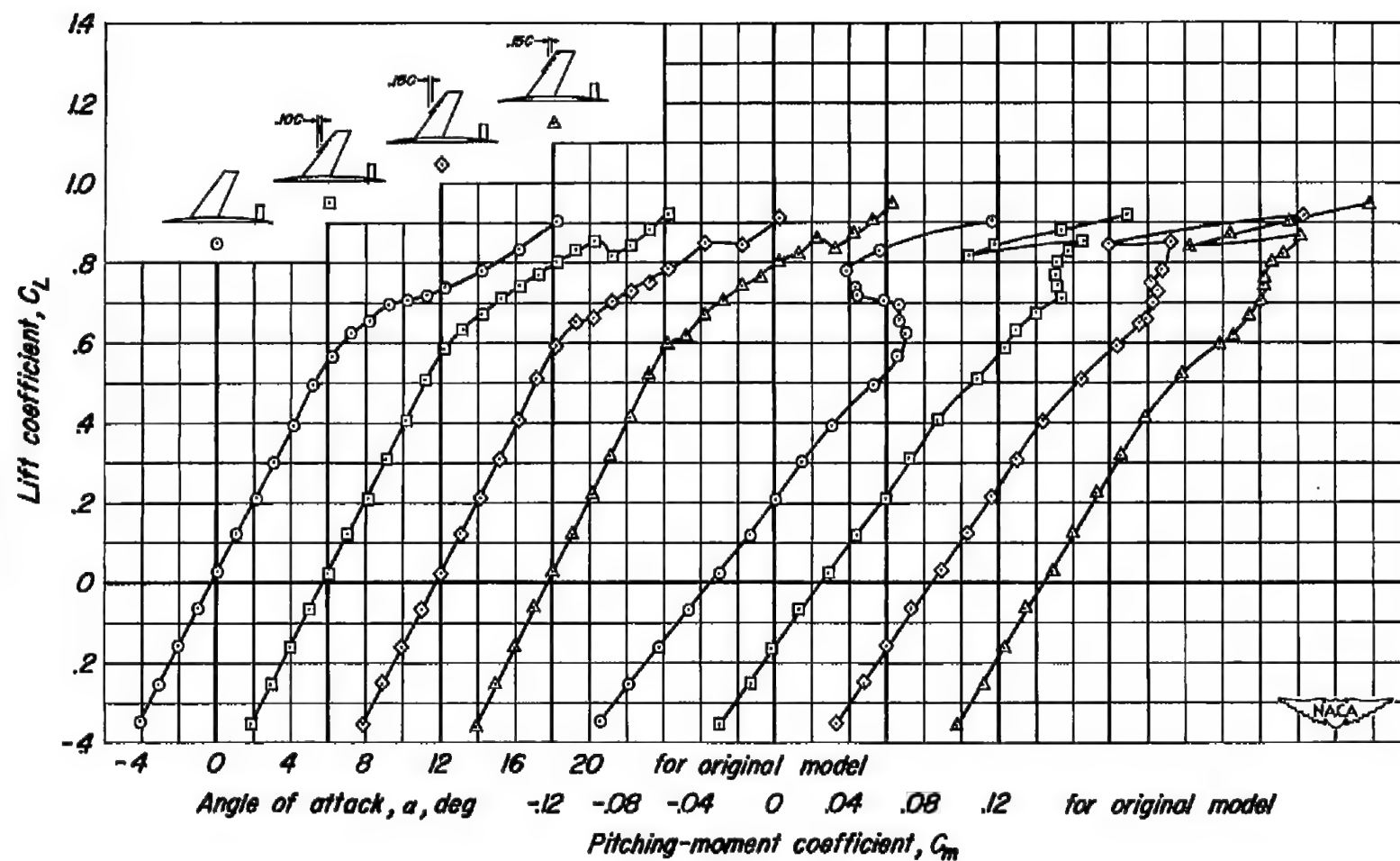
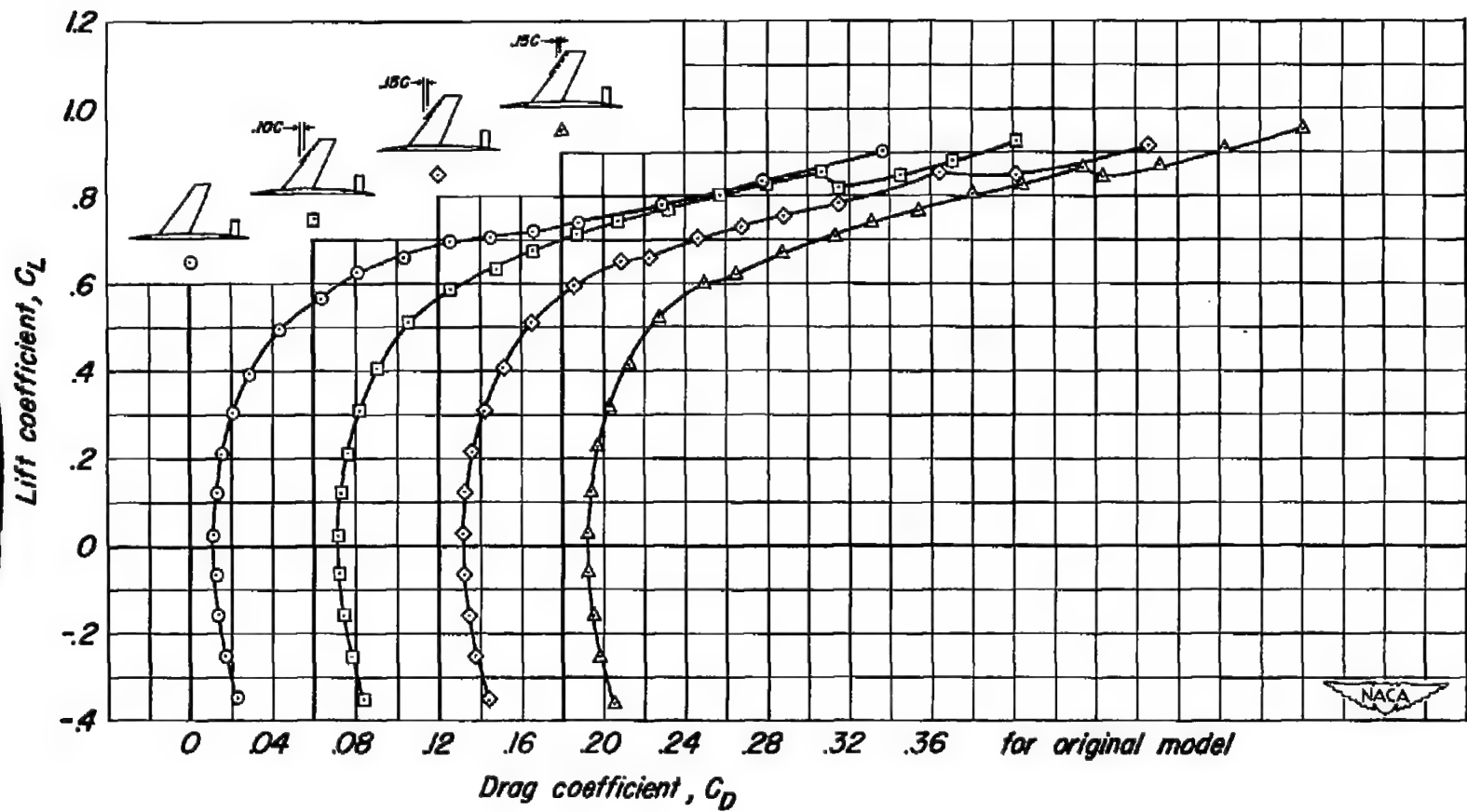
(a)  $C_L$  vs  $\alpha$ ;  $C_L$  vs  $C_m$ 

Figure 8.- The aerodynamic characteristics of the complete model with long-span leading-edge extensions at a Mach number of 0.85.  $R$ , 2,000,000.



(b)  $C_L$  vs  $C_D$

Figure 8.- Concluded.

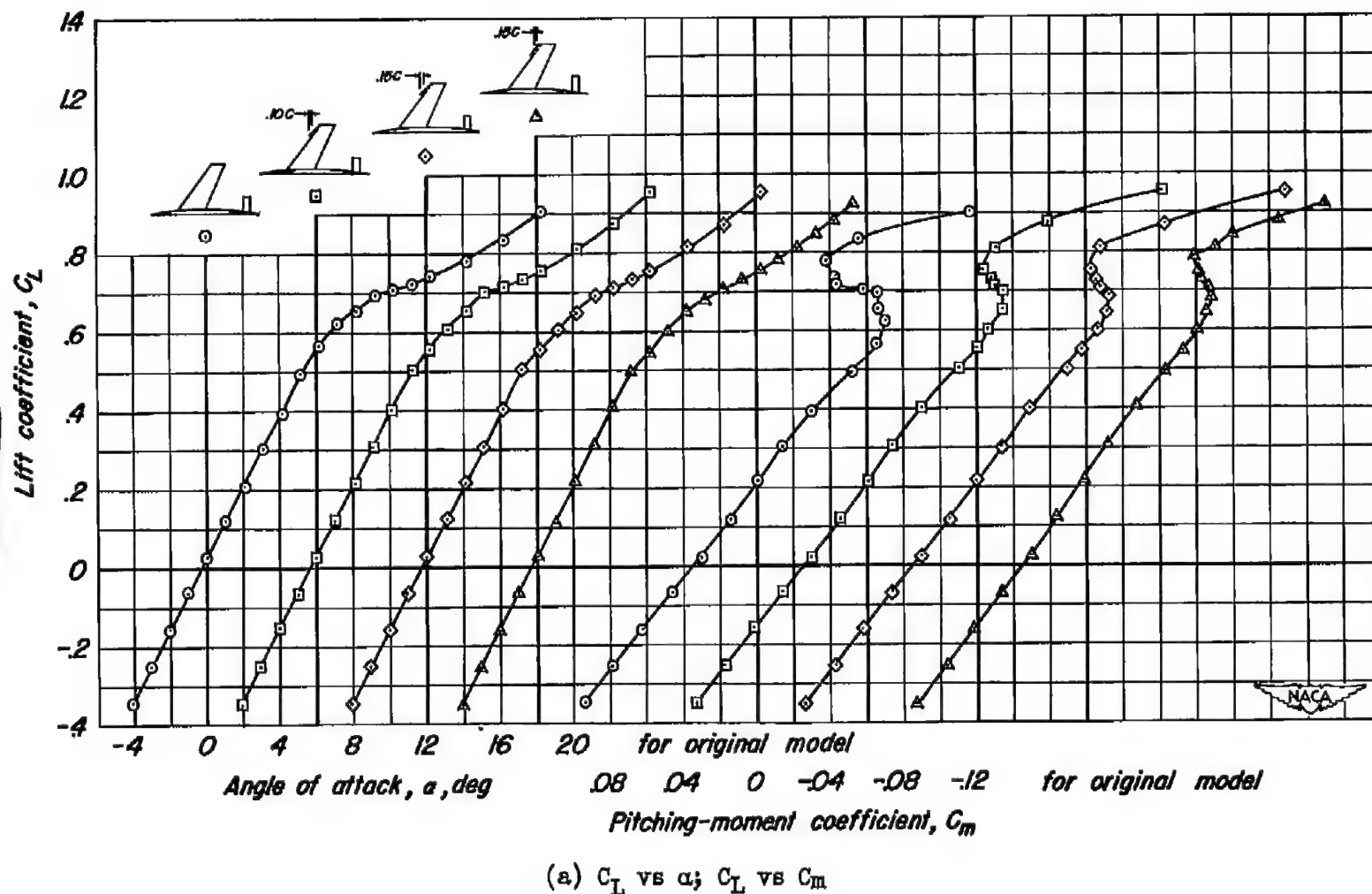
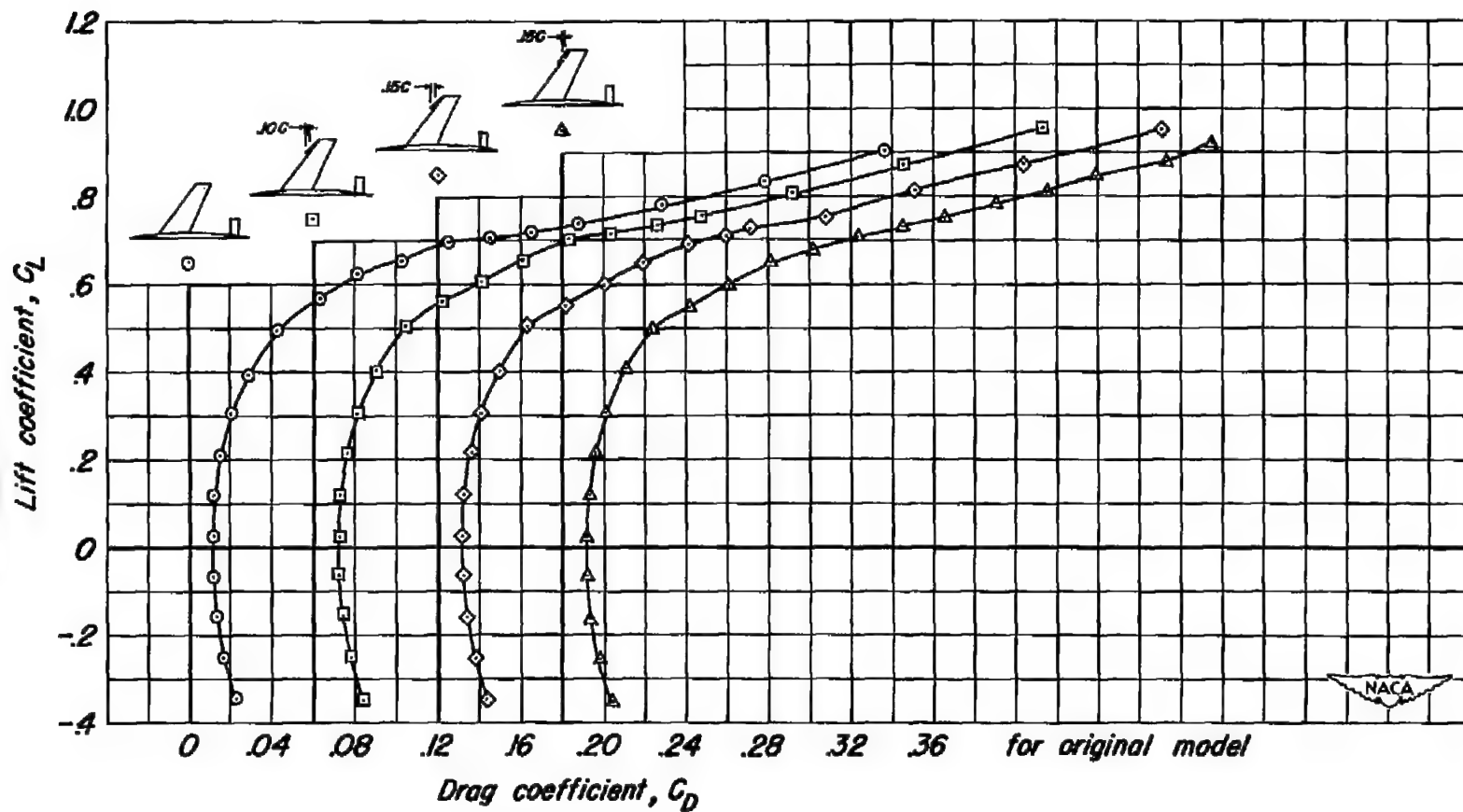


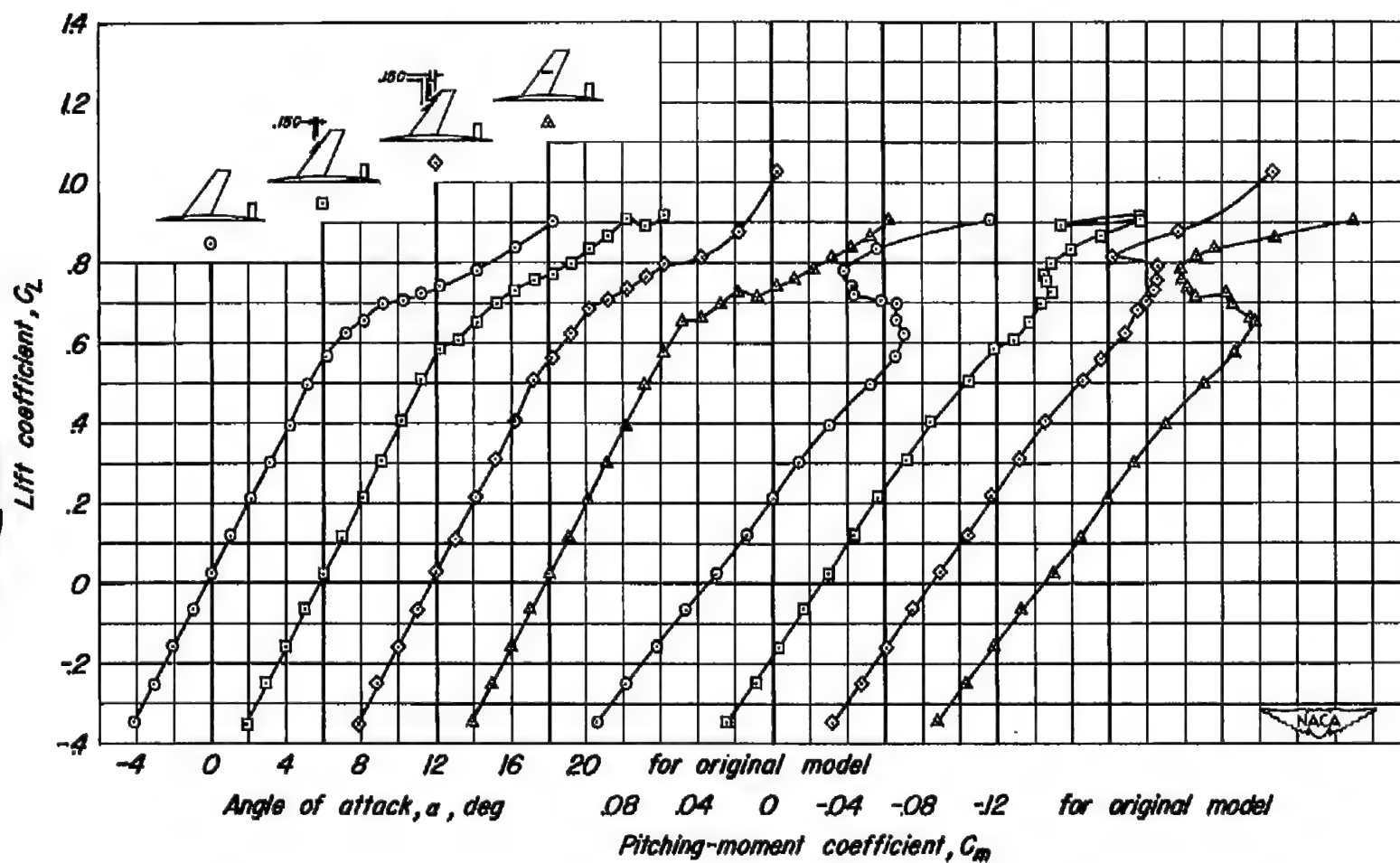
Figure 9.- The aerodynamic characteristics of the complete model with short-span leading-edge extensions at a Mach number of 0.85.  $R$ , 2,000,000.





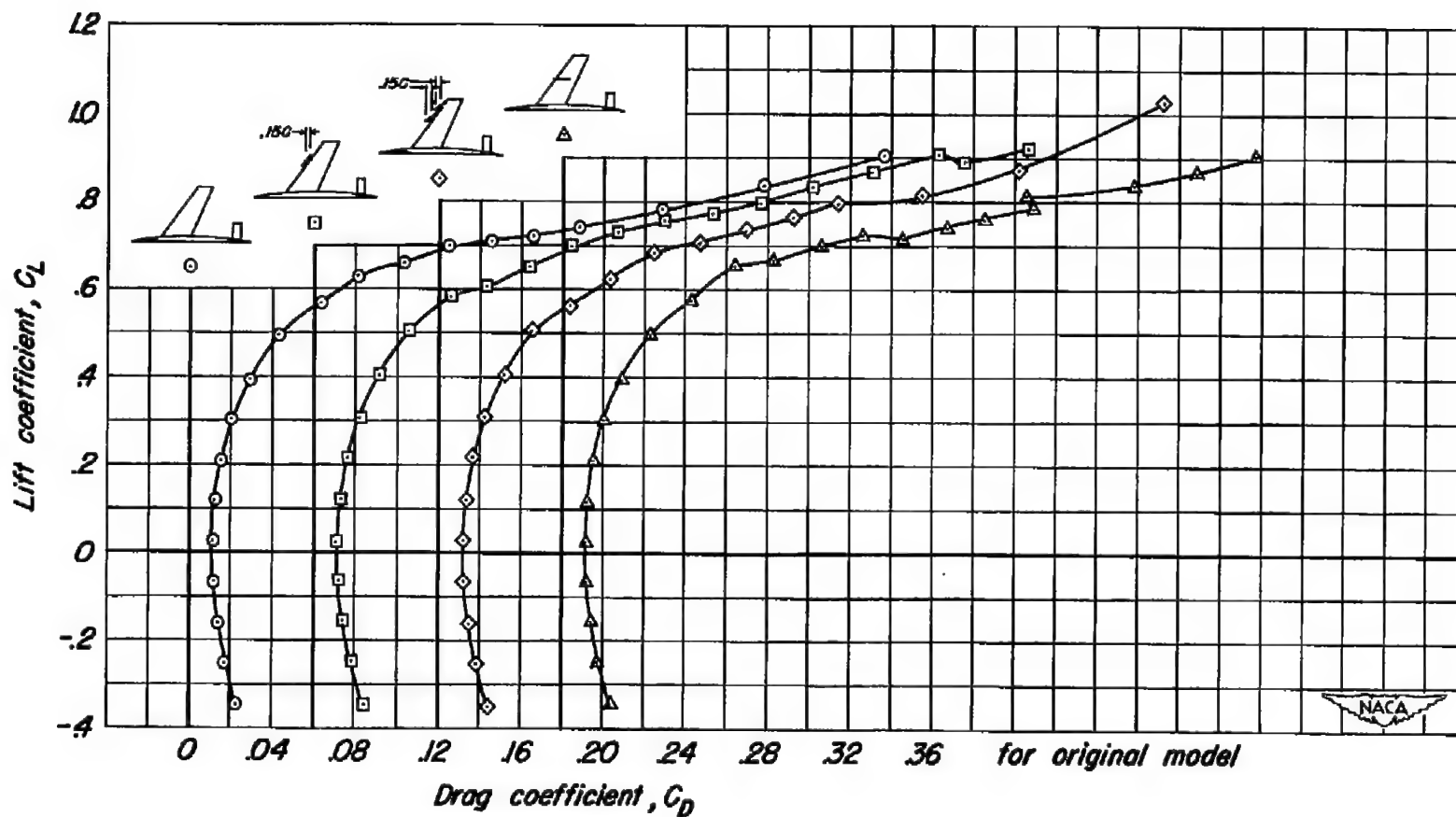
(b)  $C_L$  vs  $C_D$

Figure 9.- Concluded.



(a)  $C_L$  vs  $\alpha$ ;  $C_L$  vs  $C_m$

Figure 10.- The aerodynamic characteristics of the complete model with an inner leading-edge extension, a double, tapered extension, and a fence at a Mach number of 0.85.  $R, 2,000,000$ .



(b)  $C_L$  vs  $C_D$

Figure 10.- Concluded.

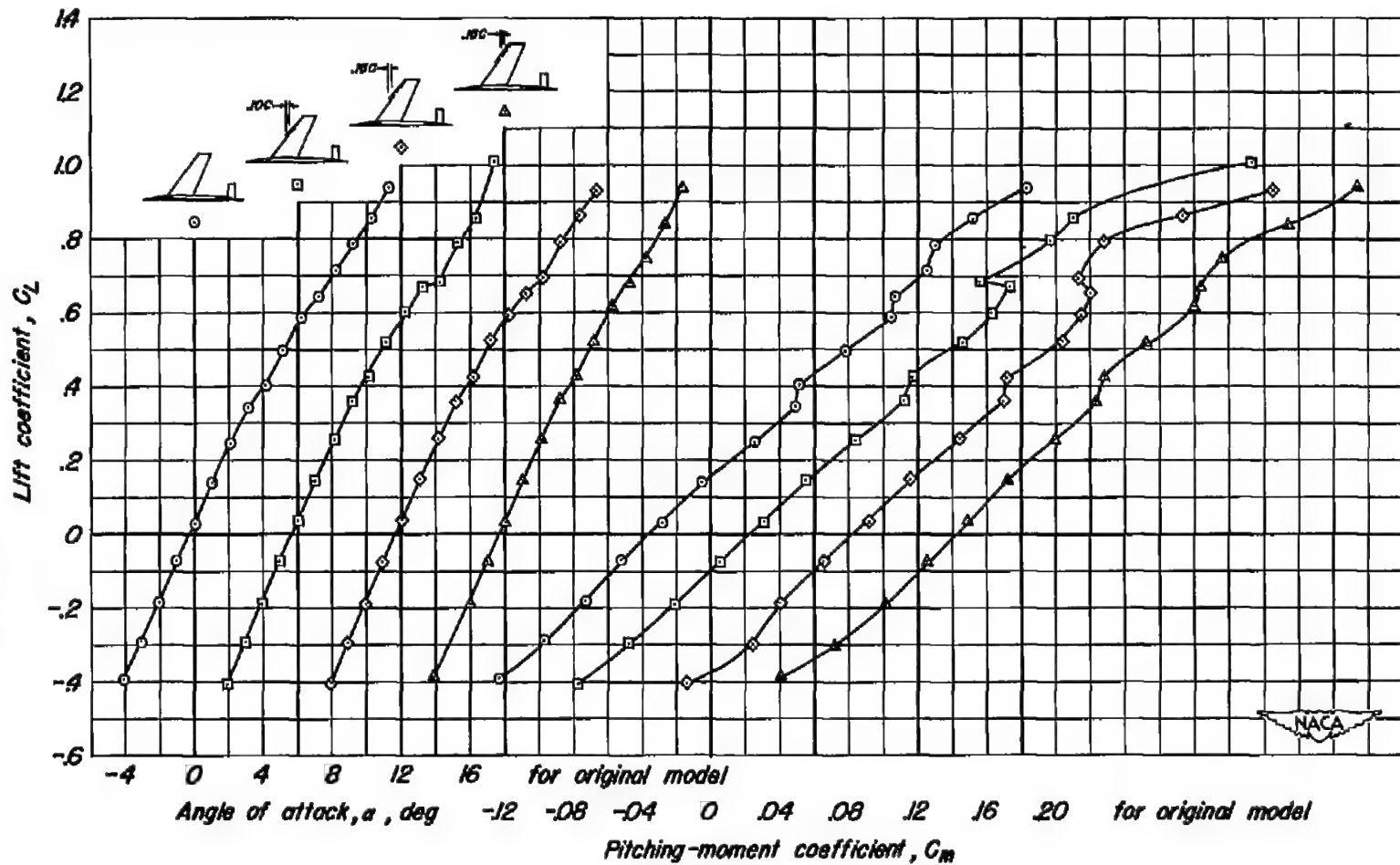
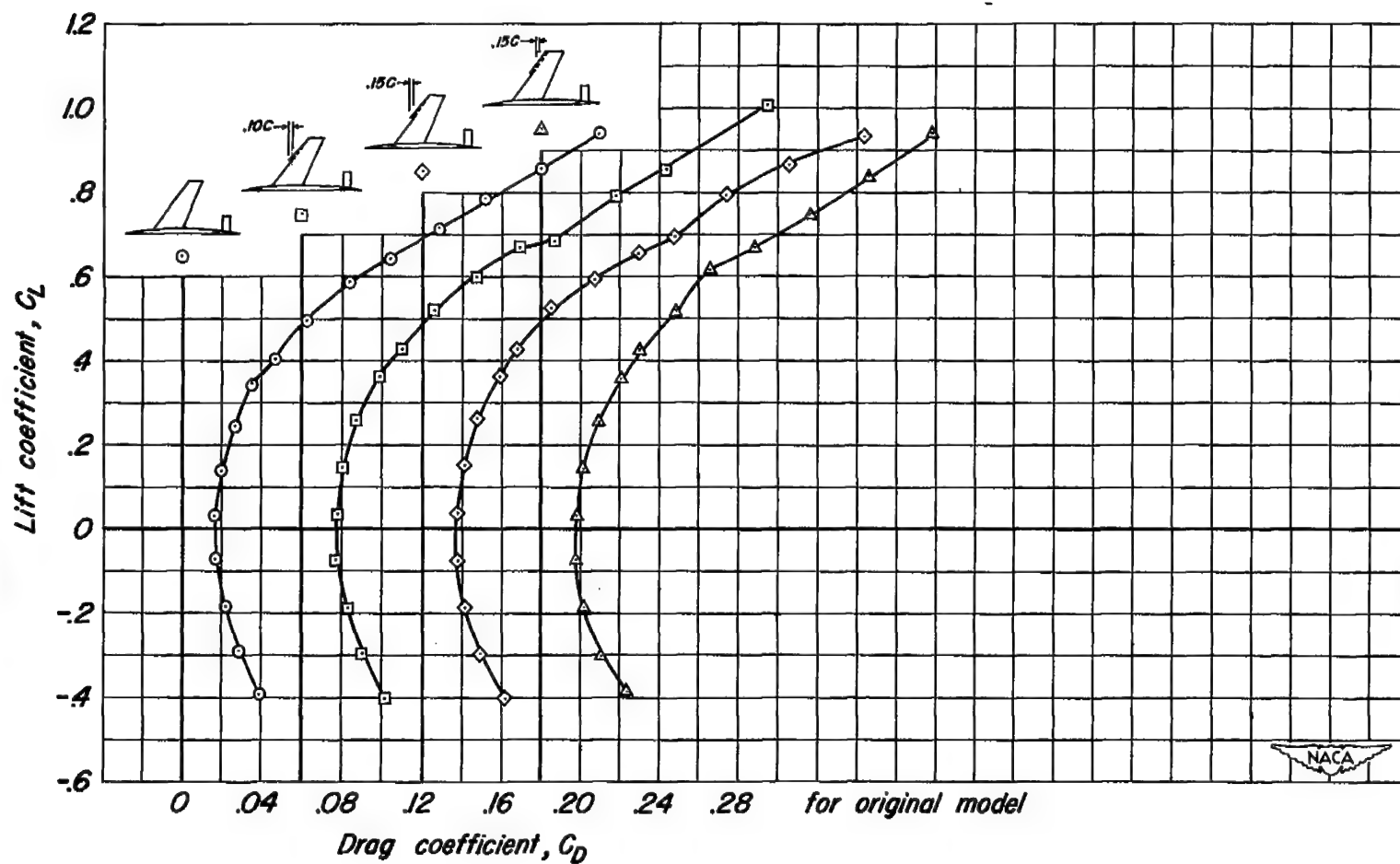
(a)  $C_L$  vs  $\alpha$ ;  $C_L$  vs  $C_m$ 

Figure 11.- The aerodynamic characteristics of the complete model with long-span leading-edge extensions at a Mach number of 0.92.  $R$ , 2,000,000.



(b)  $C_L$  vs  $C_D$ .

Figure 11.- Concluded.

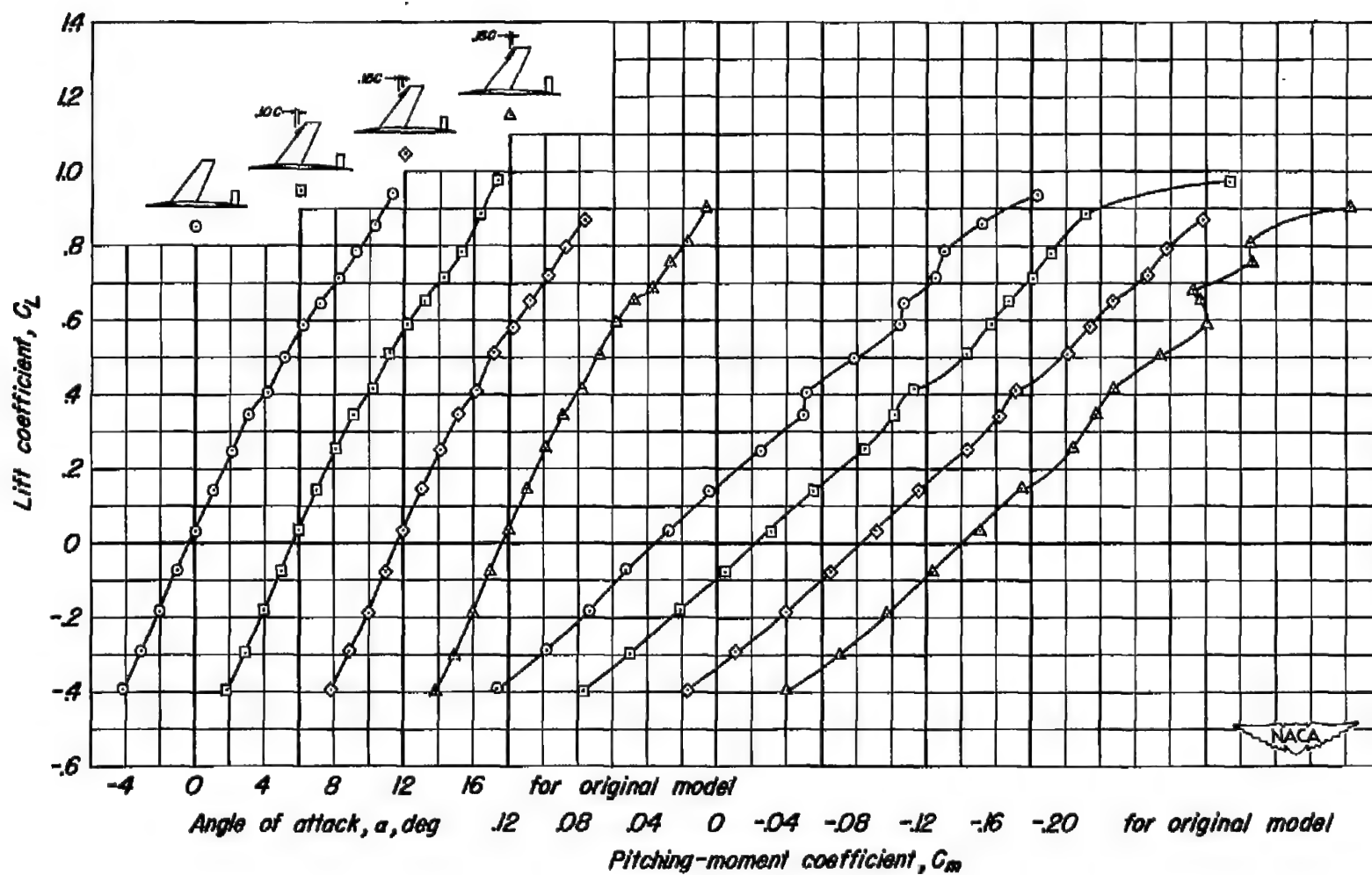
(a)  $C_L$  vs  $\alpha$ ;  $C_L$  vs  $C_m$ 

Figure 12.- The aerodynamic characteristics of the complete model with short-span leading-edge extensions at a Mach number of 0.92.  $R$ , 2,000,000.

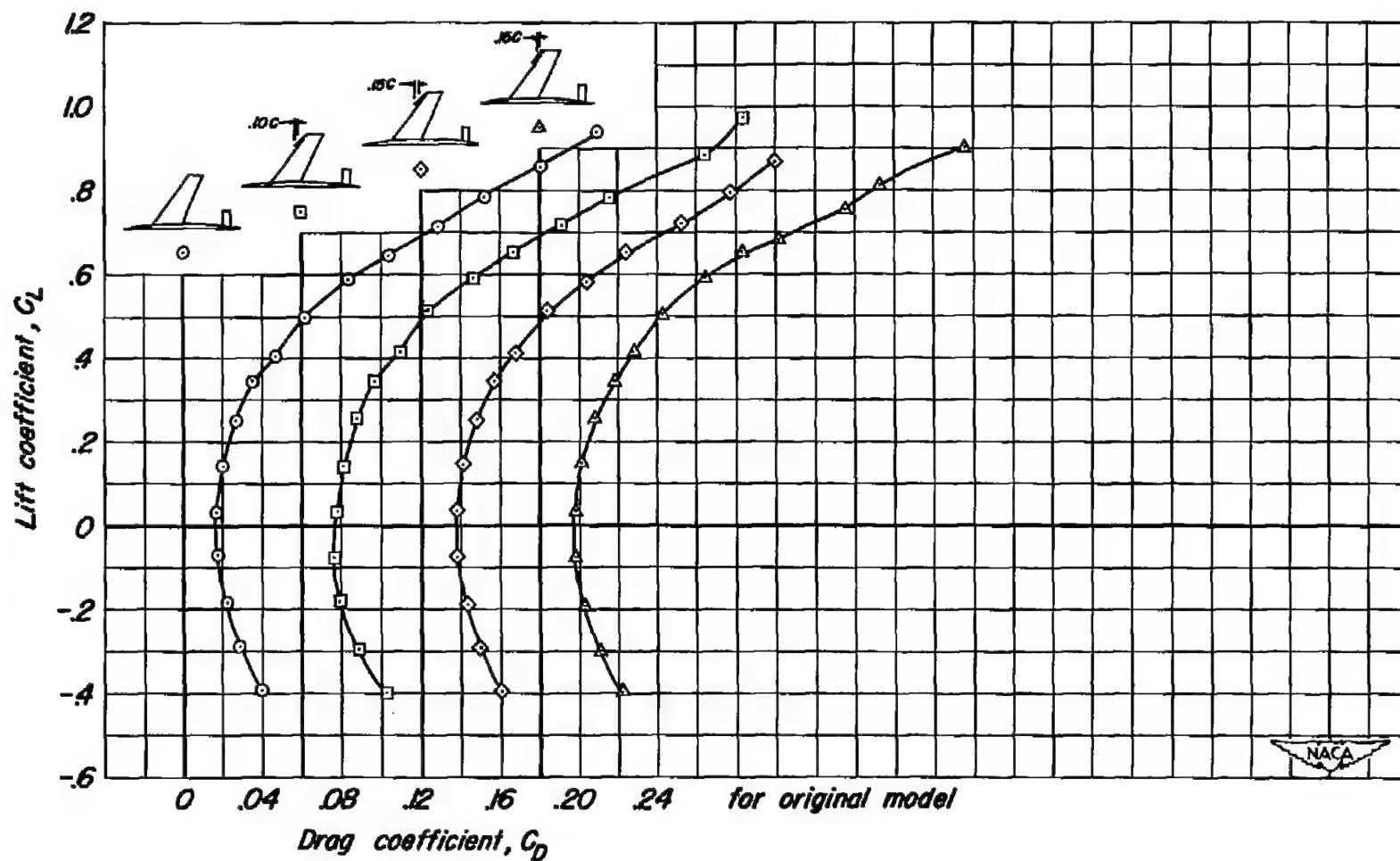
(b)  $C_L$  vs  $C_D$ 

Figure 12.- Concluded.

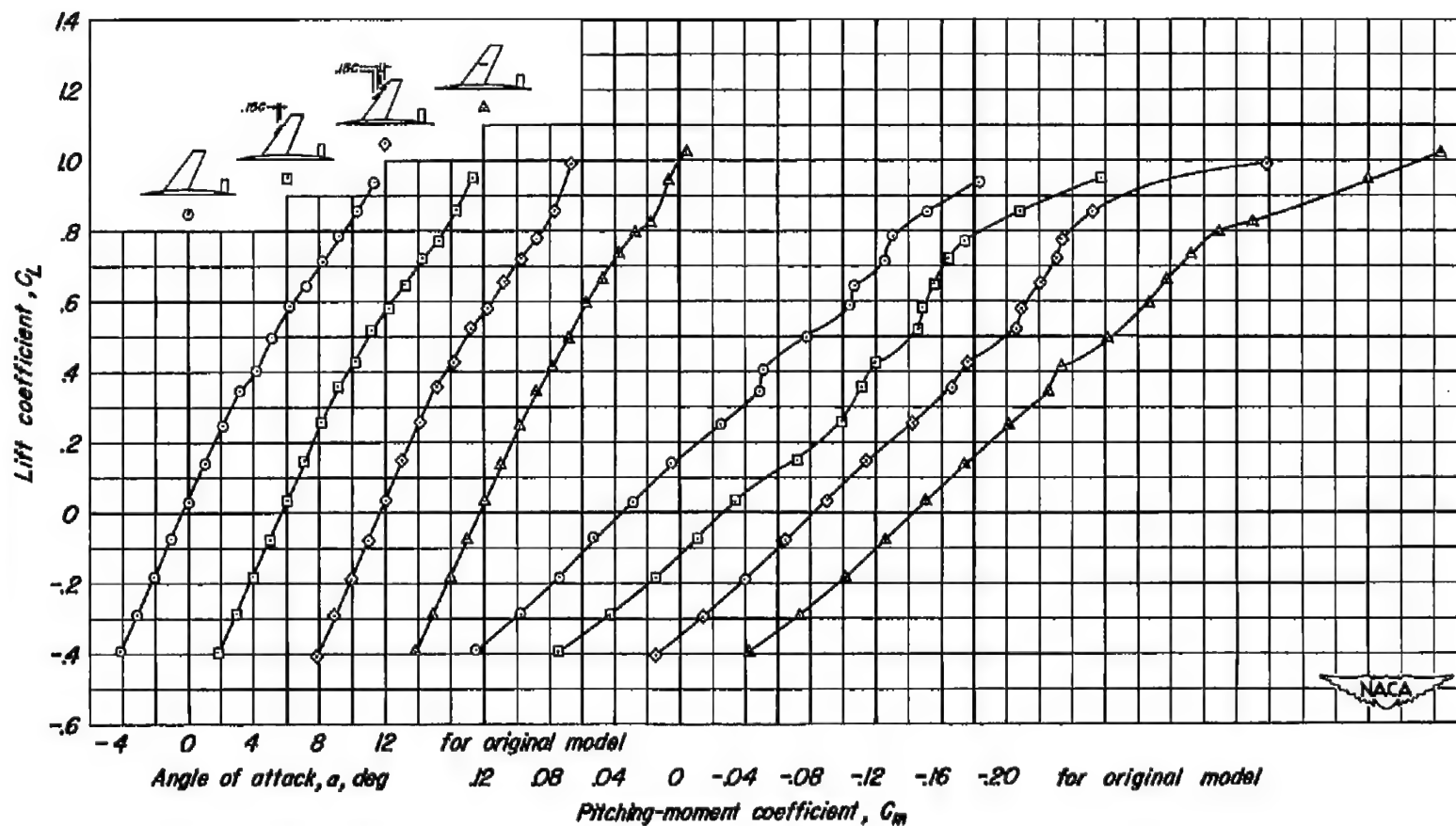
(a)  $C_L$  vs  $\alpha$ ;  $C_L$  vs  $C_m$ 

Figure 13.- The aerodynamic characteristics of the complete model with an inner leading-edge extension, a double, tapered extension, and a fence at a Mach number of 0.92.  $R, 2,000,000$ .



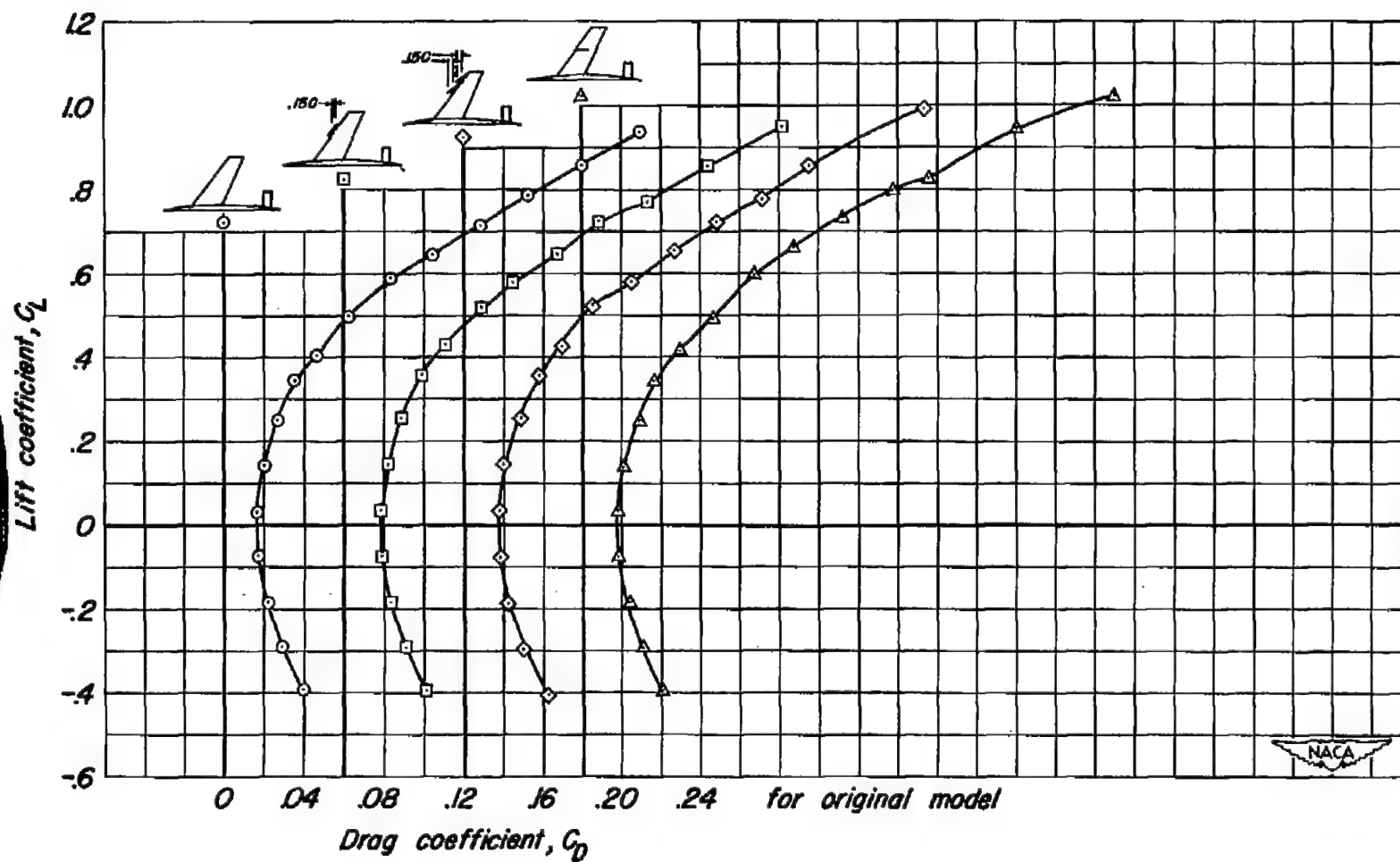
(b)  $C_L$  vs  $C_D$ 

Figure 13.- Concluded.

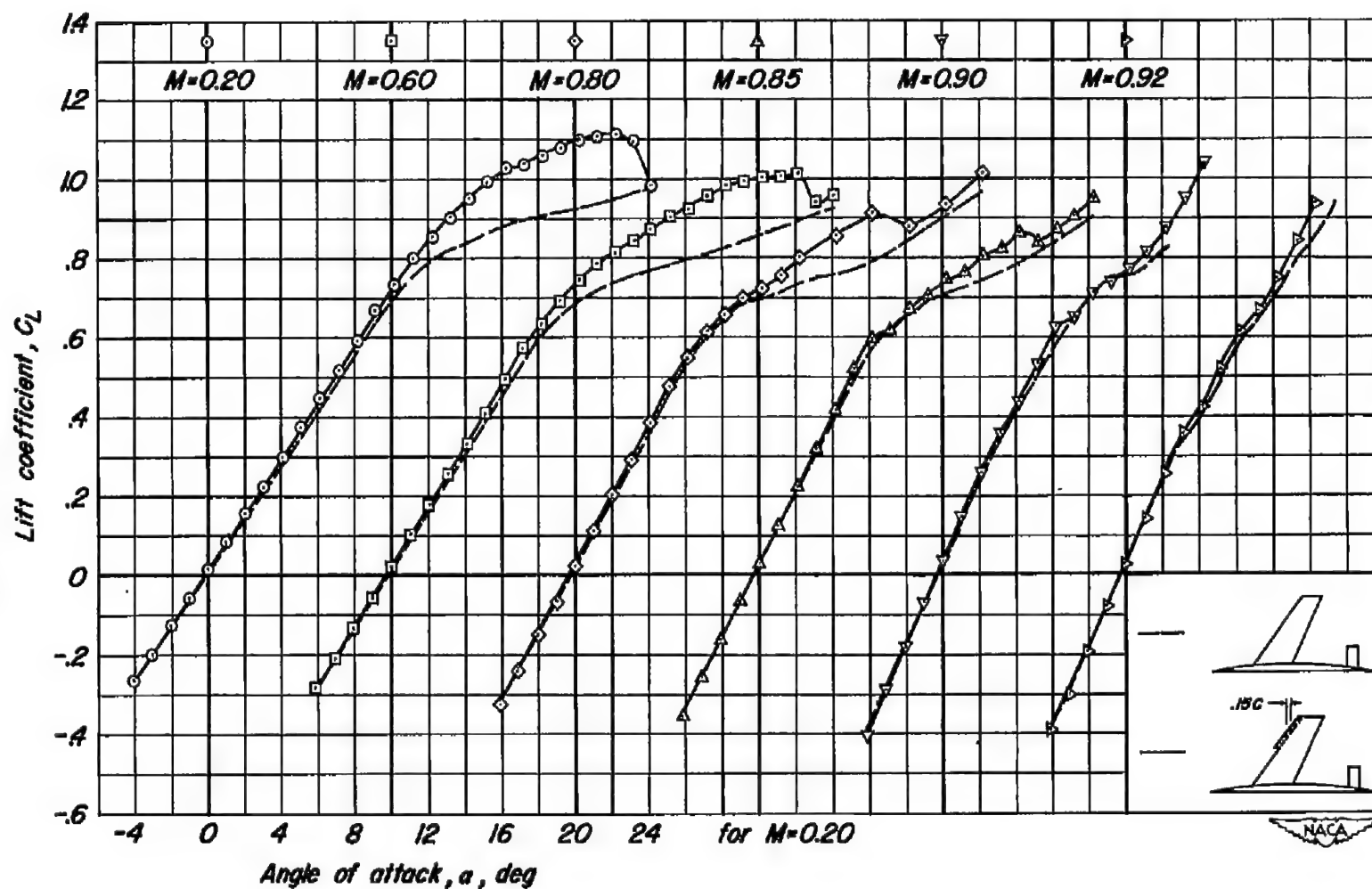
(a)  $C_L$  vs  $\alpha$ 

Figure 14.- The effect of a long-span leading-edge extension on the aerodynamic characteristics of the complete model at various Mach numbers.  $R, 2,000,000$ .

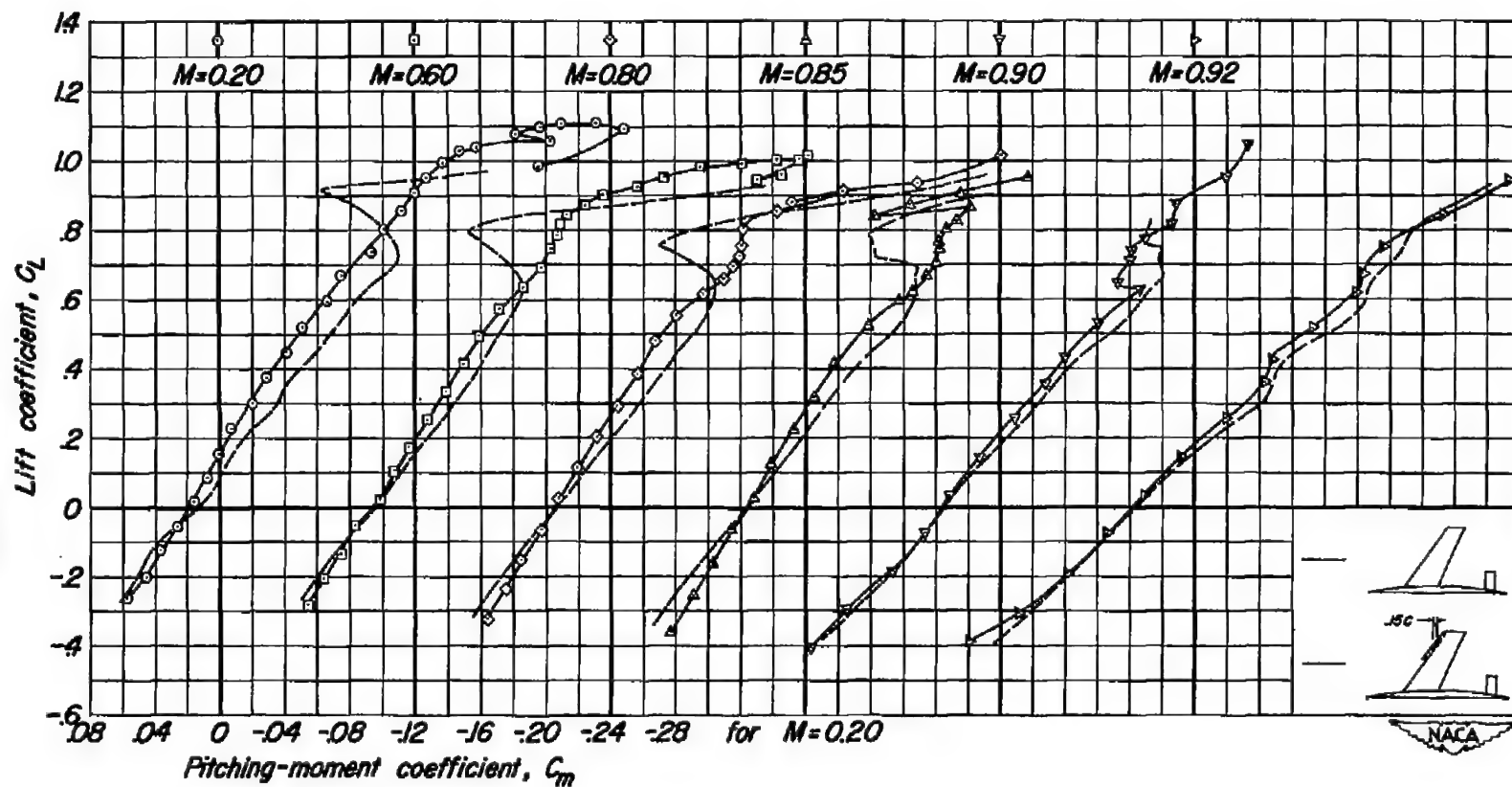
(b)  $C_L$  vs  $C_m$ 

Figure 14.- Continued.

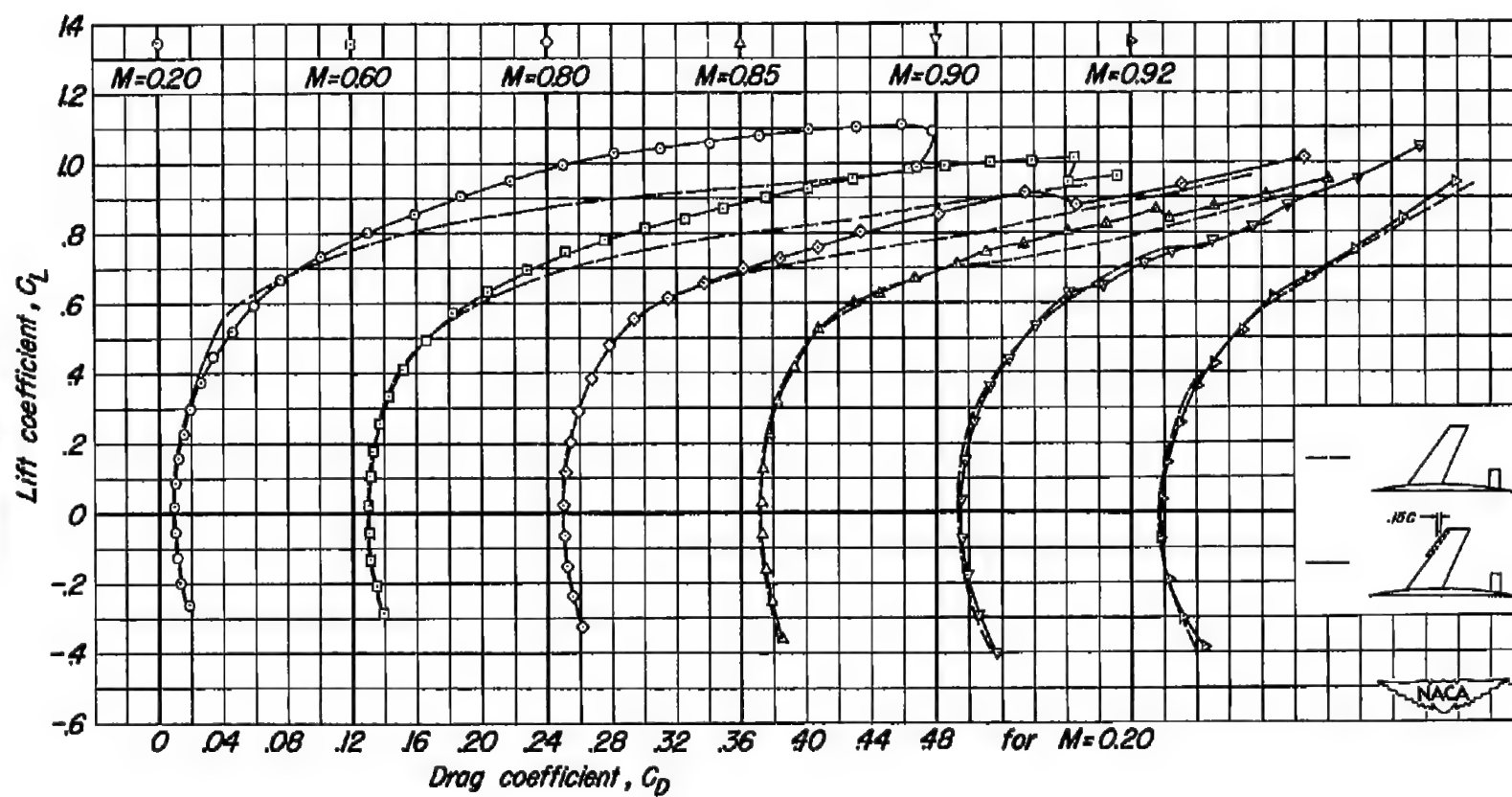
(c)  $C_L$  vs  $C_D$ 

Figure 14.- Concluded.

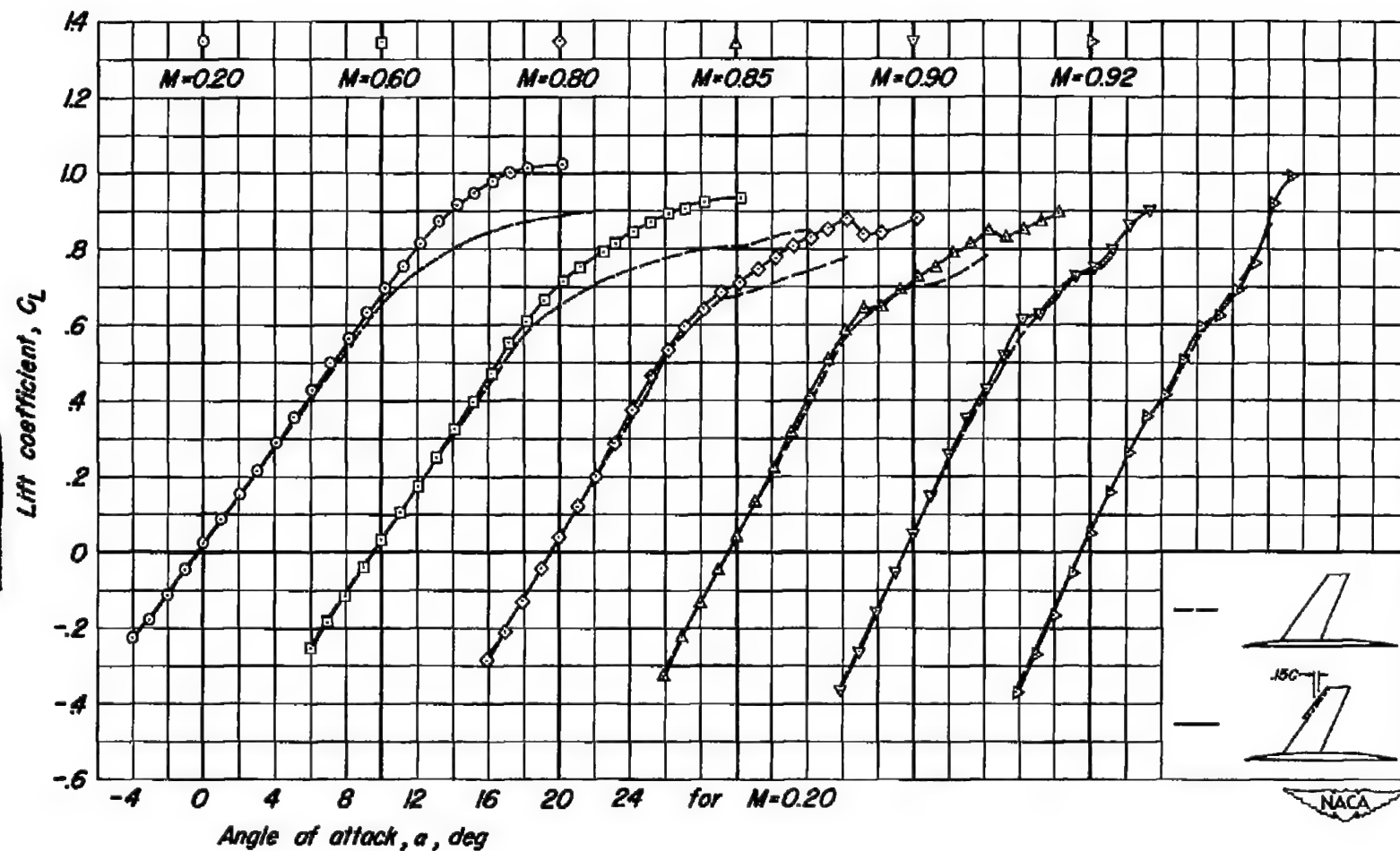
(a)  $C_L$  vs  $\alpha$ 

Figure 15.- The effect of a long-span leading-edge extension on the aerodynamic characteristics of the model without tail at various Mach numbers.  $R$ , 2,000,000.

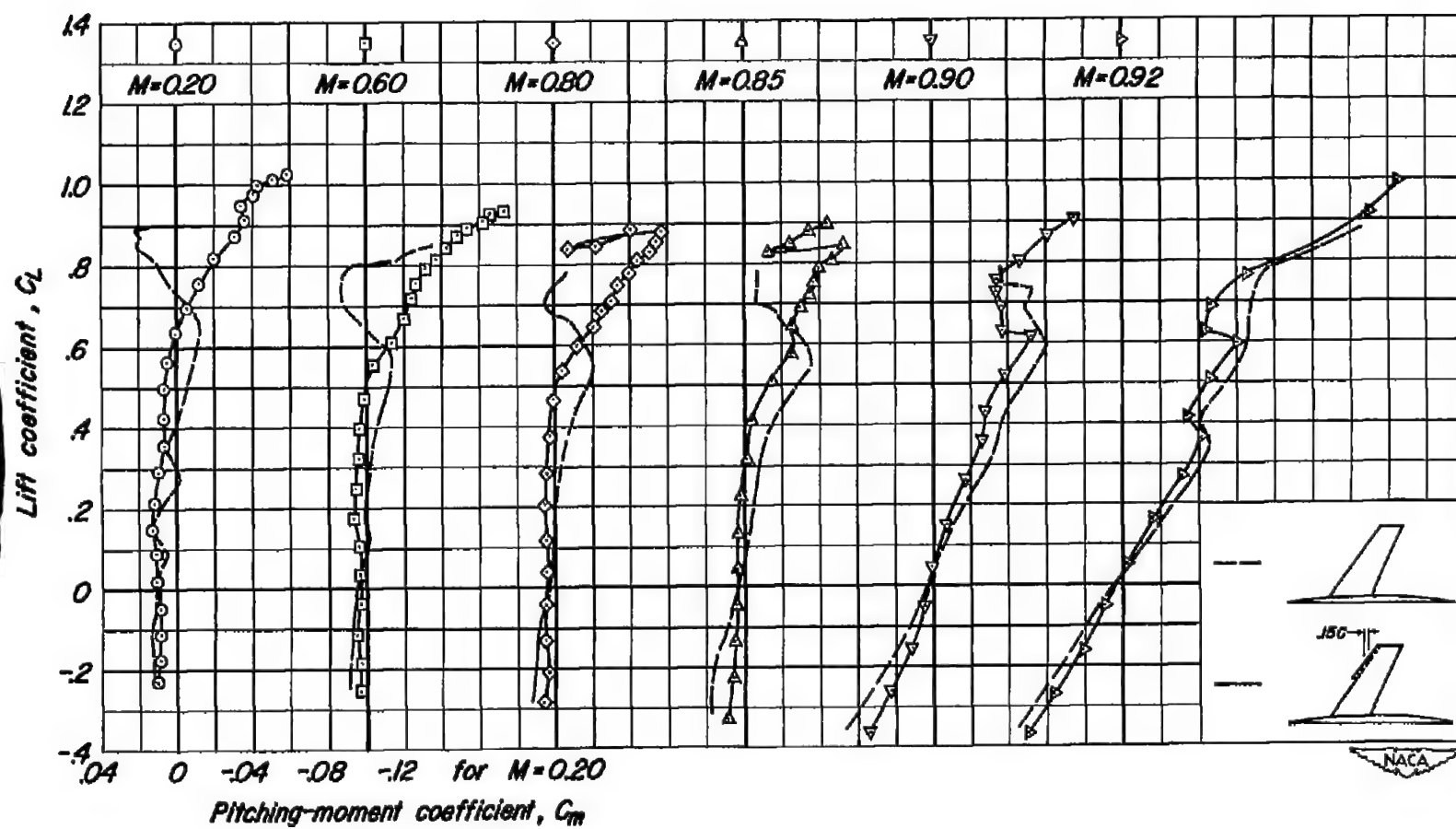
(b)  $C_L$  vs  $C_m$ 

Figure 15.- Continued.

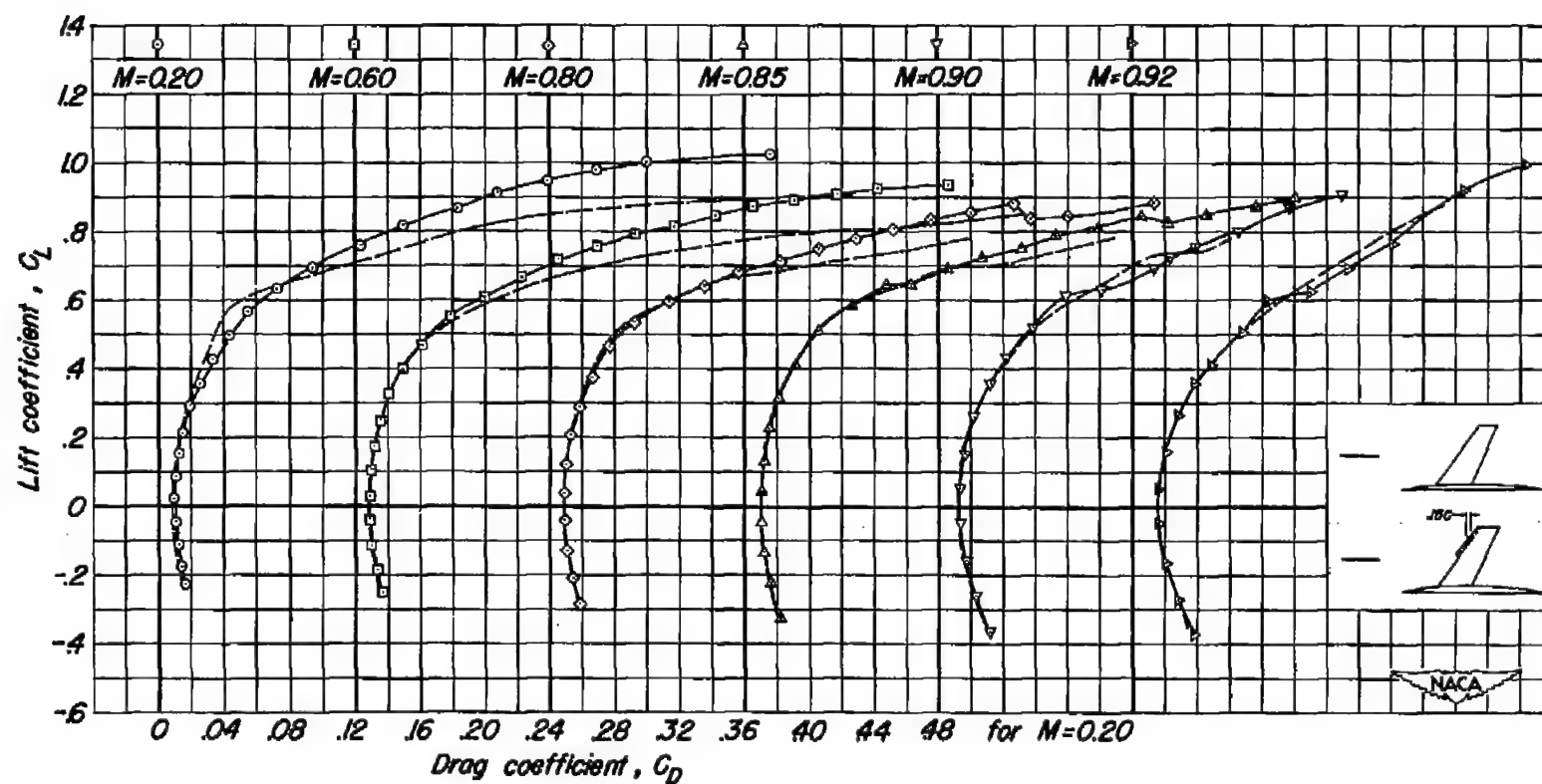
(c)  $C_L$  vs  $C_D$ 

Figure 15.- Concluded.

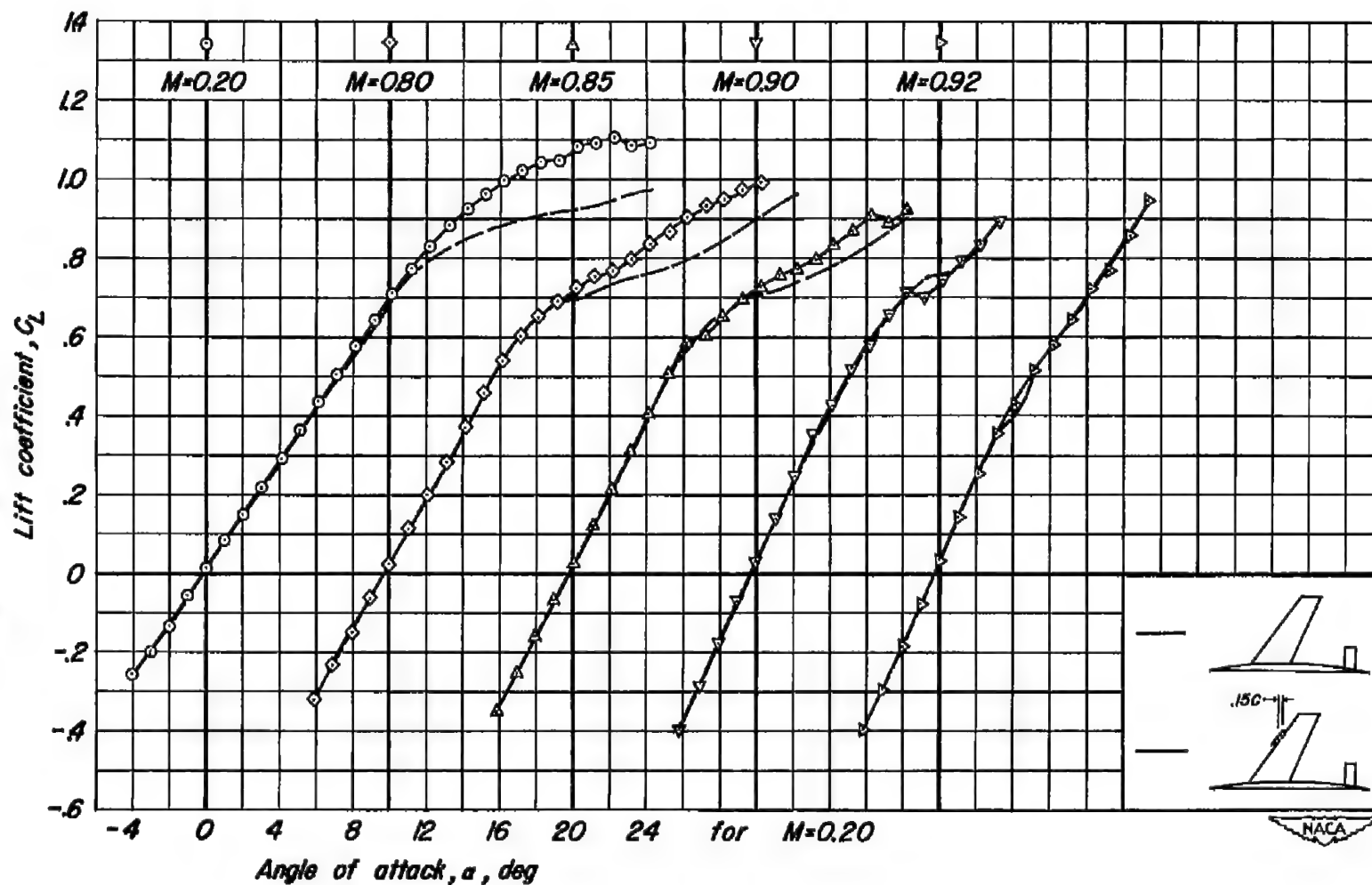
(a)  $C_L$  vs  $\alpha$ 

Figure 16.- The effect of an inner, short-span leading-edge extension on the aerodynamic characteristics of the complete model at various Mach numbers.  $R, 2,000,000$ .



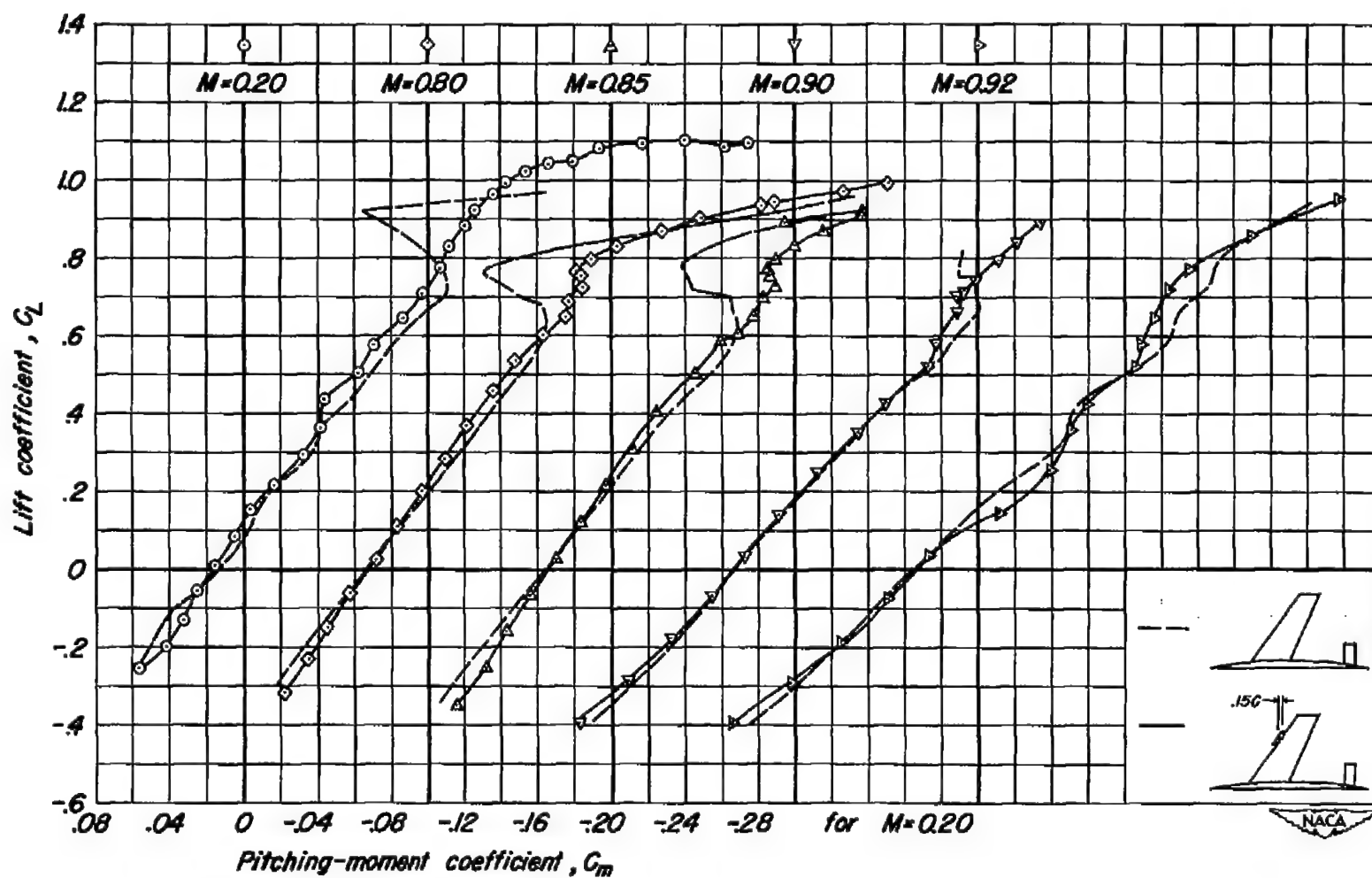
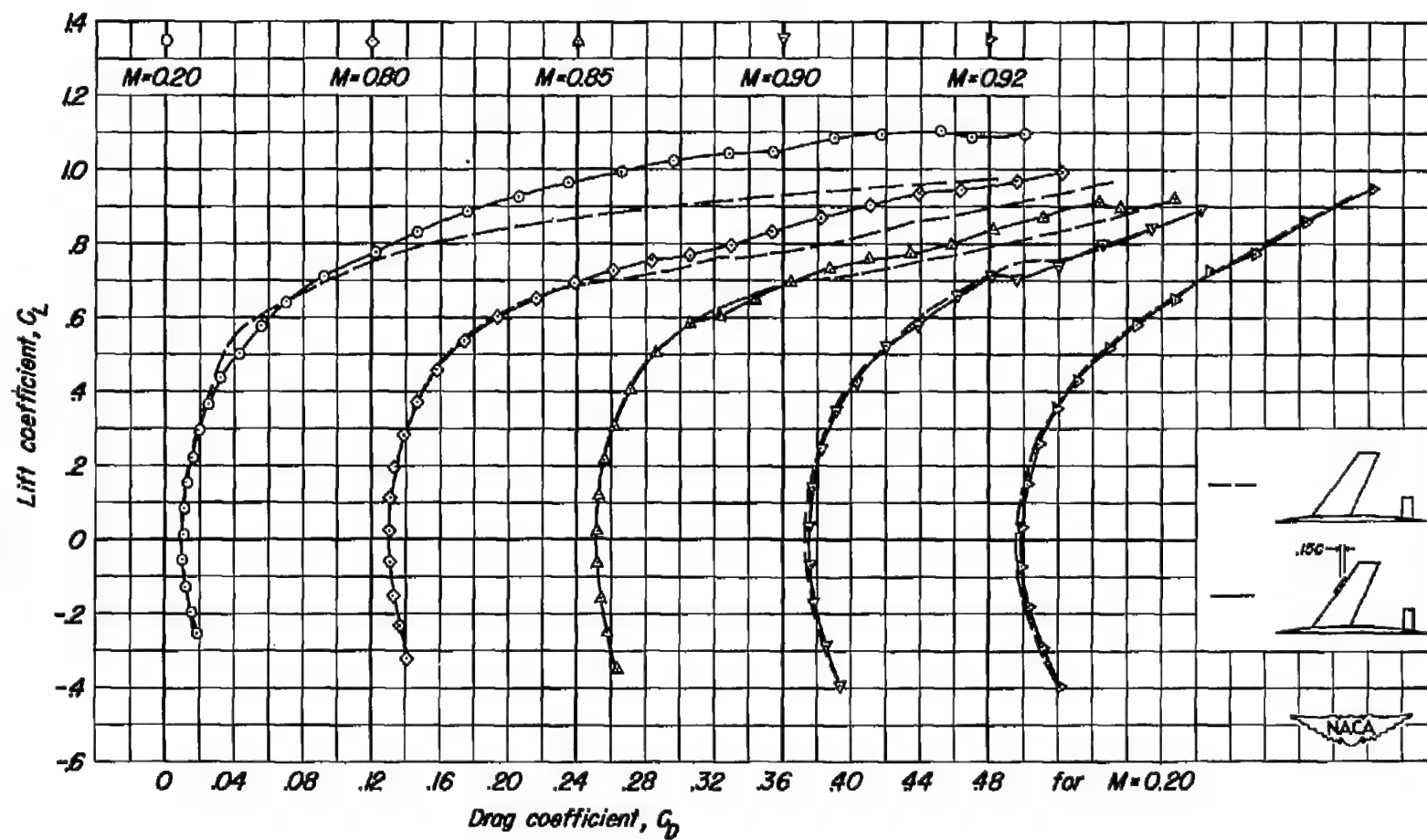
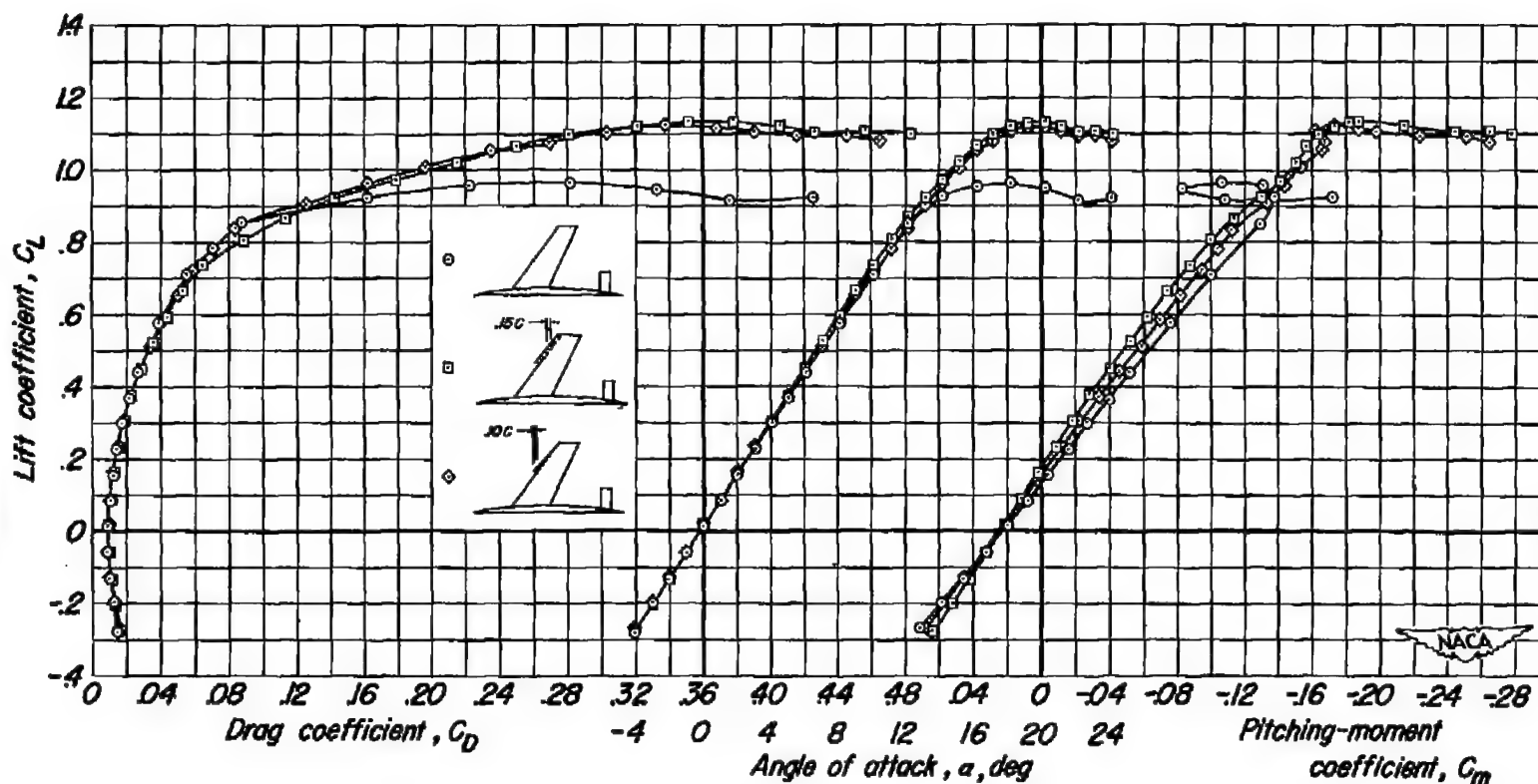
(b)  $C_L$  vs  $C_m$ 

Figure 16.- Continued.



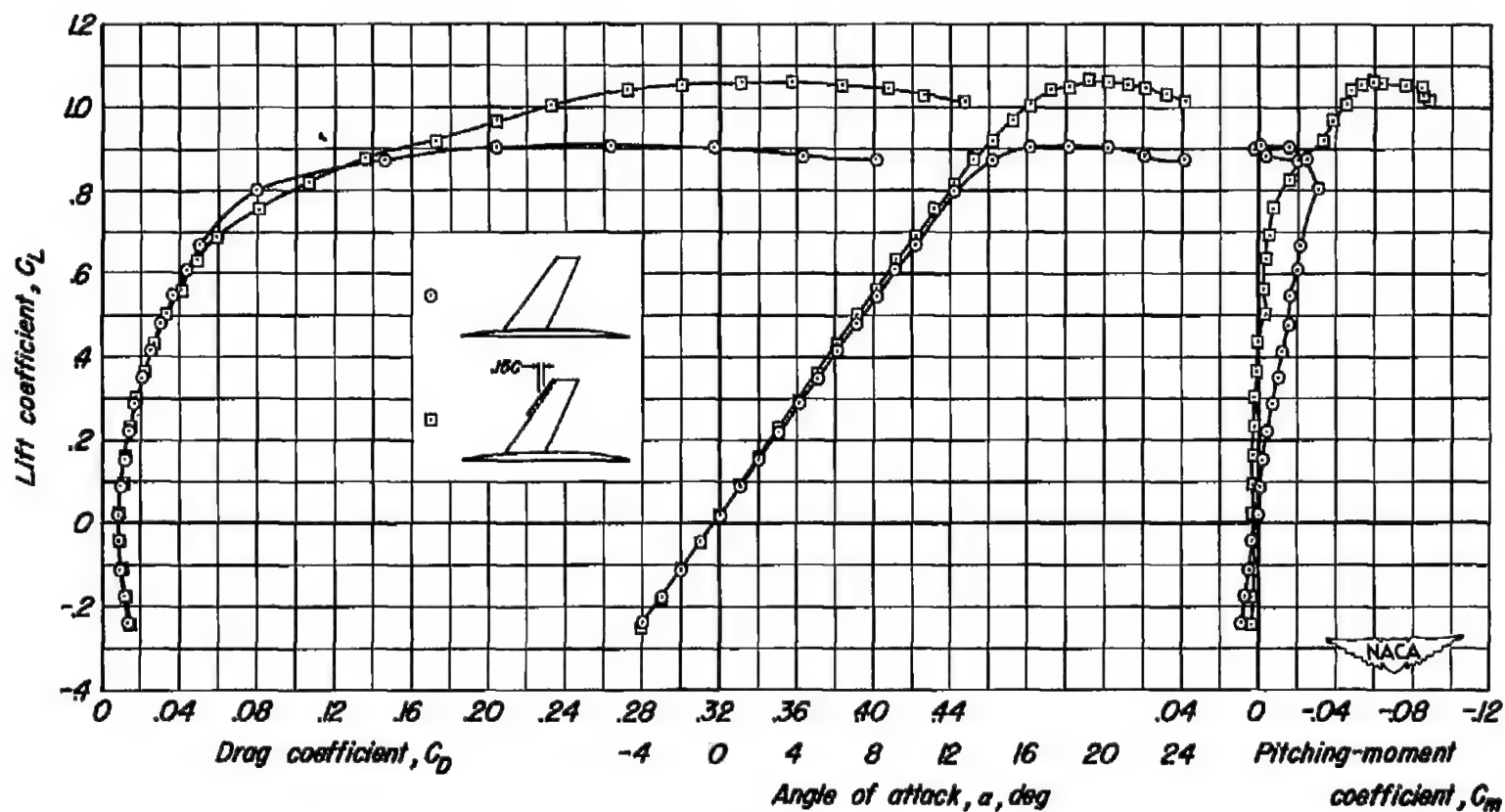
(c)  $C_L$  vs  $C_D$

Figure 16.- Concluded.



(a) Complete model.

Figure 17.- The aerodynamic characteristics of the model with long-span, leading-edge extensions at a Reynolds number of 11,000,000.  $M$ , 0.20.



(b) Model without tail.

Figure 17.- Concluded.

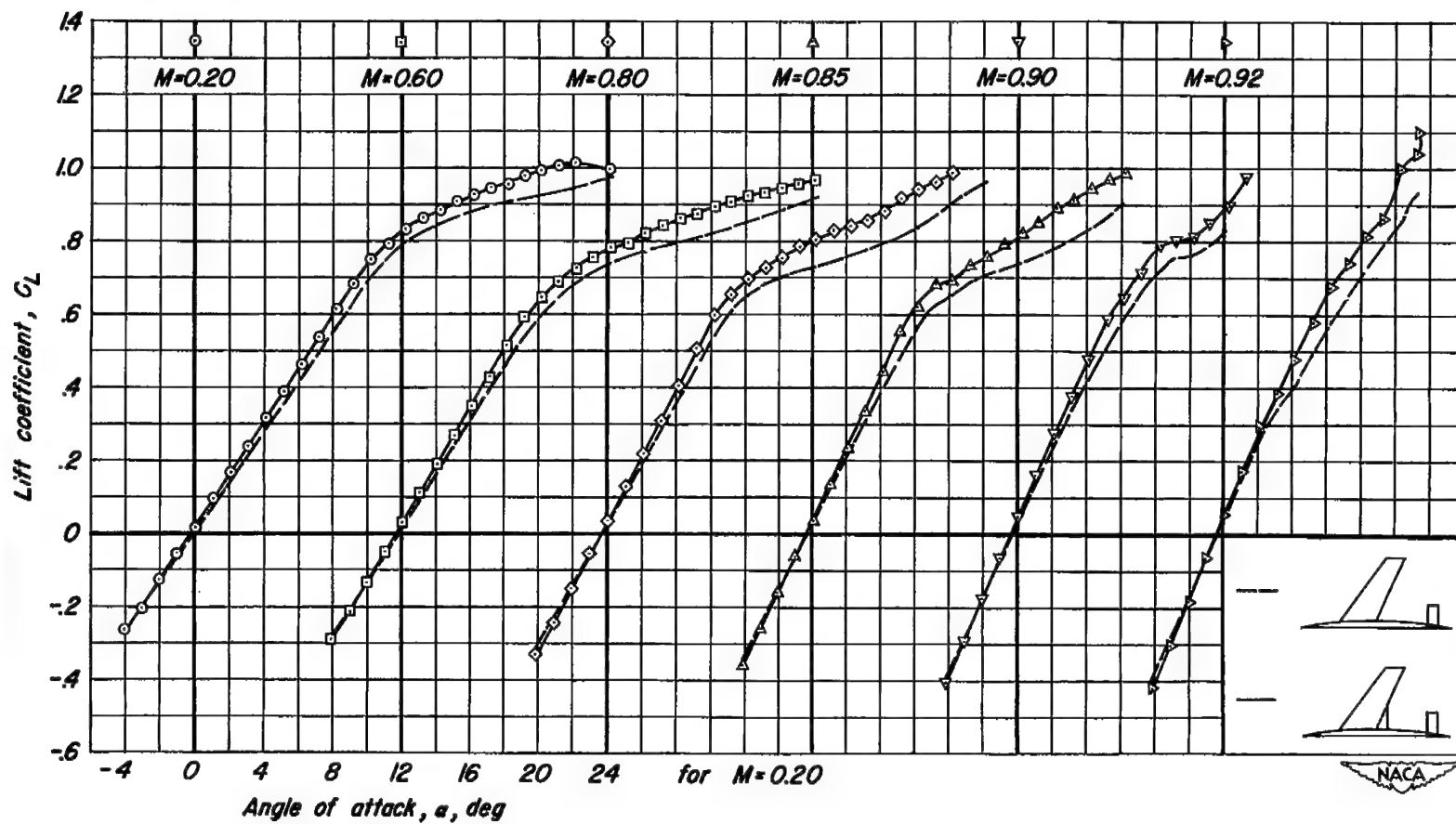
(a)  $C_L$  vs  $\alpha$ 

Figure 18.- The effect of a trailing-edge root-chord extension on the aerodynamic characteristics of the complete model at various Mach numbers. R, 2,000,000.

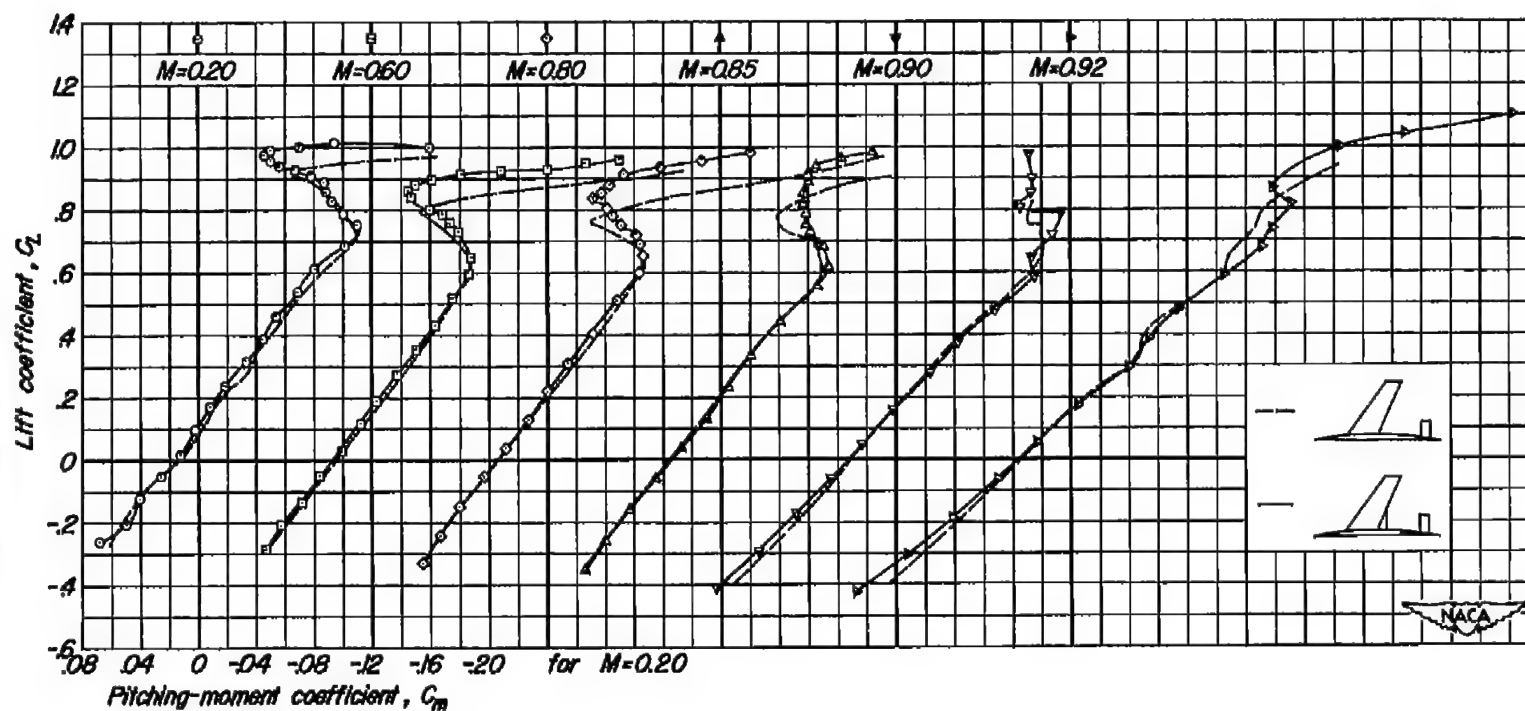
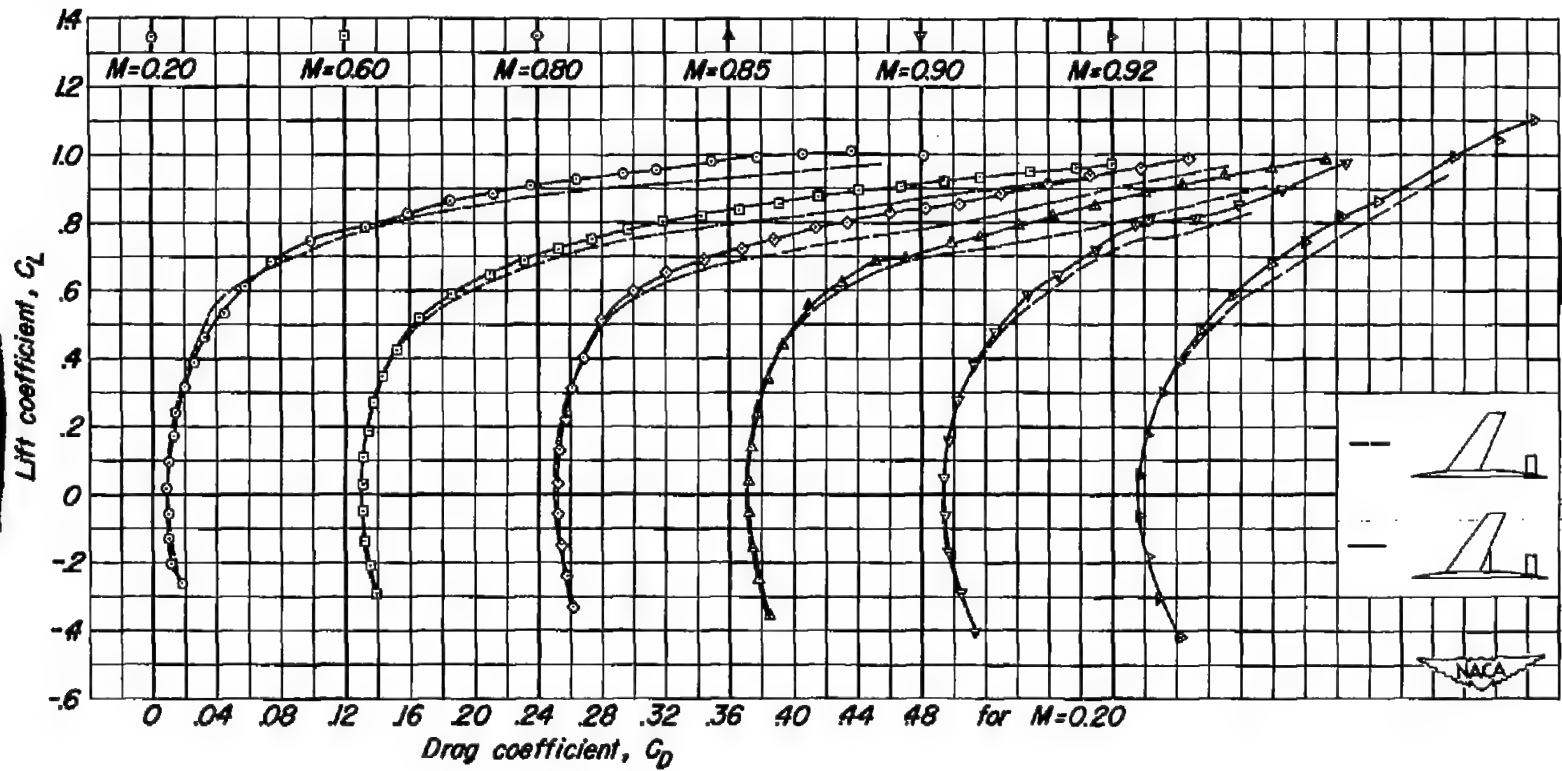
(b)  $C_L$  vs  $C_m$ 

Figure 18.- Continued.



(c)  $C_L$  vs  $C_D$

Figure 18.- Concluded.

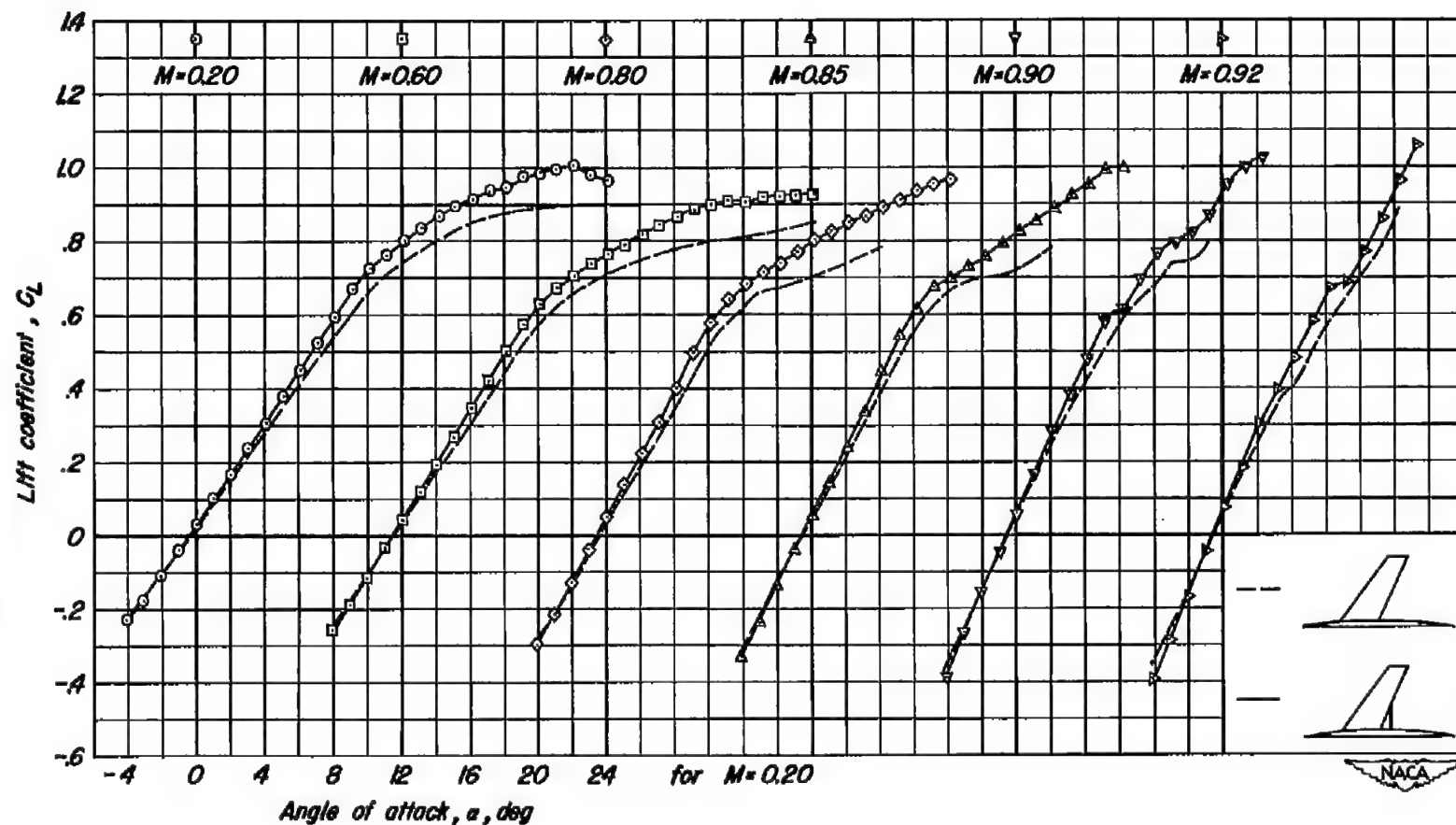
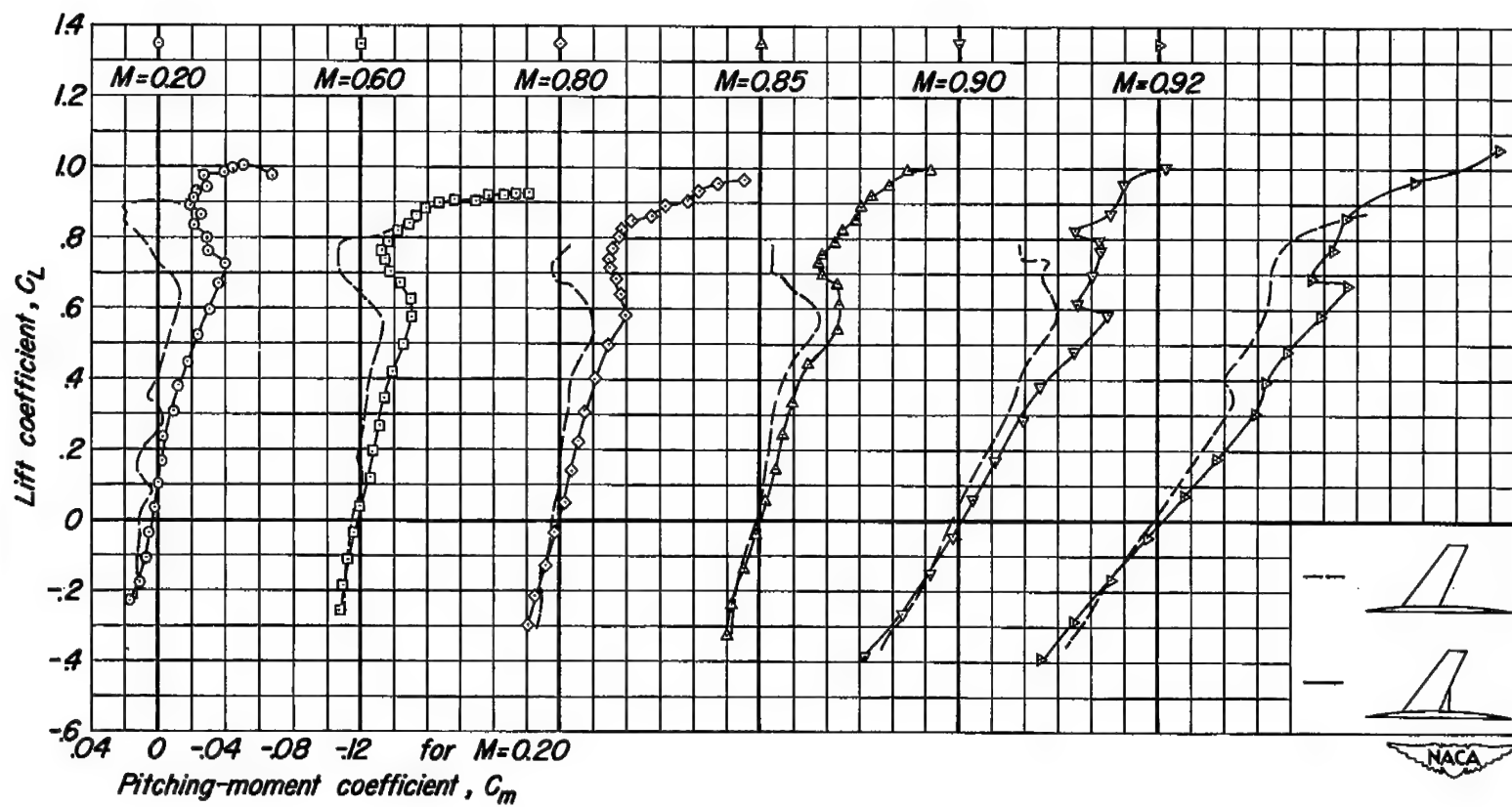
(a)  $C_L$  vs  $\alpha$ 

Figure 19.- The effect of a trailing-edge root-chord extension on the aerodynamic characteristics of the model without tail at various Mach numbers.  $R, 2,000,000$ .





(b)  $C_L$  vs  $C_m$

Figure 19.- Continued.

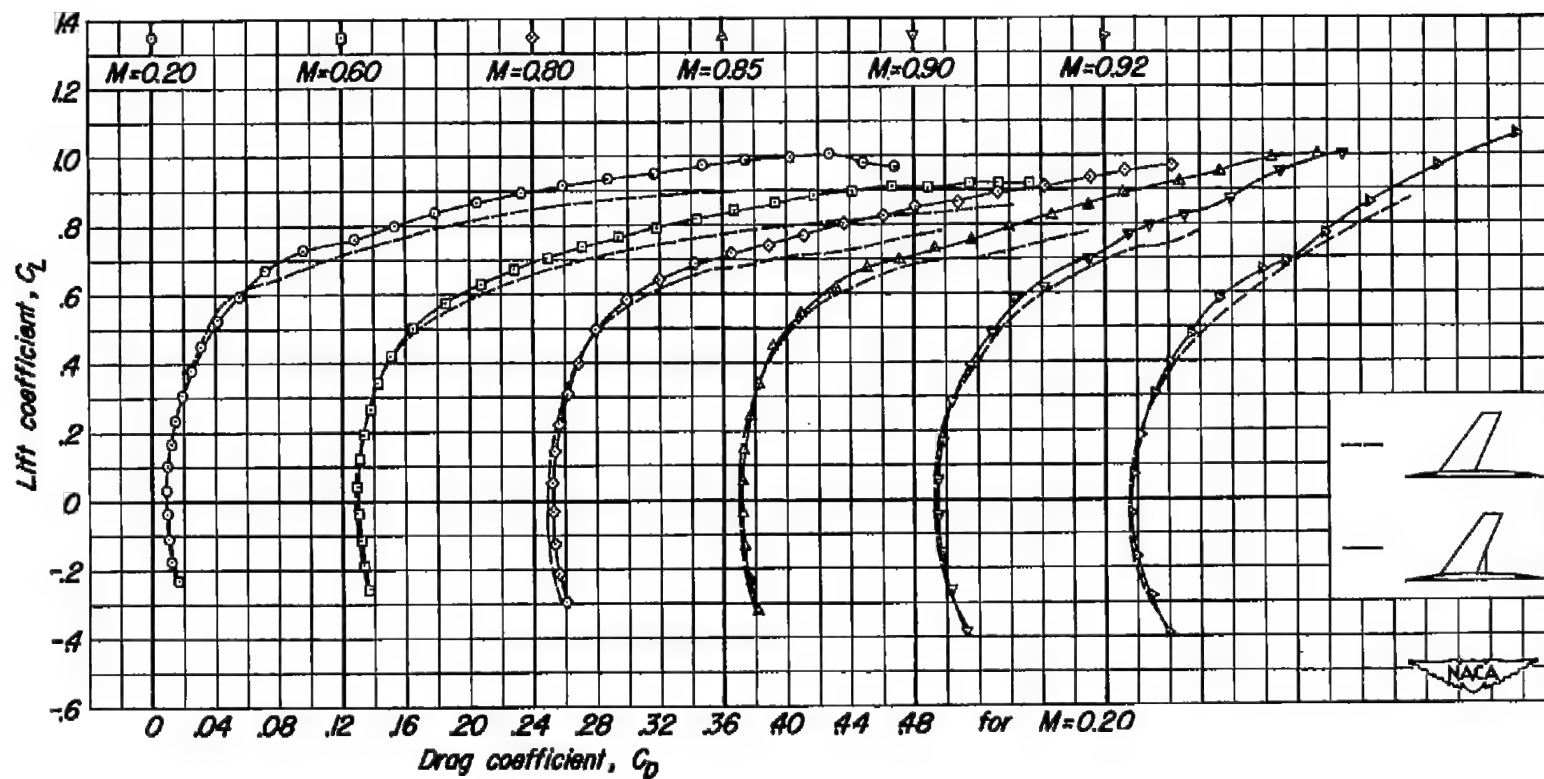
(c)  $C_L$  vs  $C_D$ 

Figure 19.- Concluded.

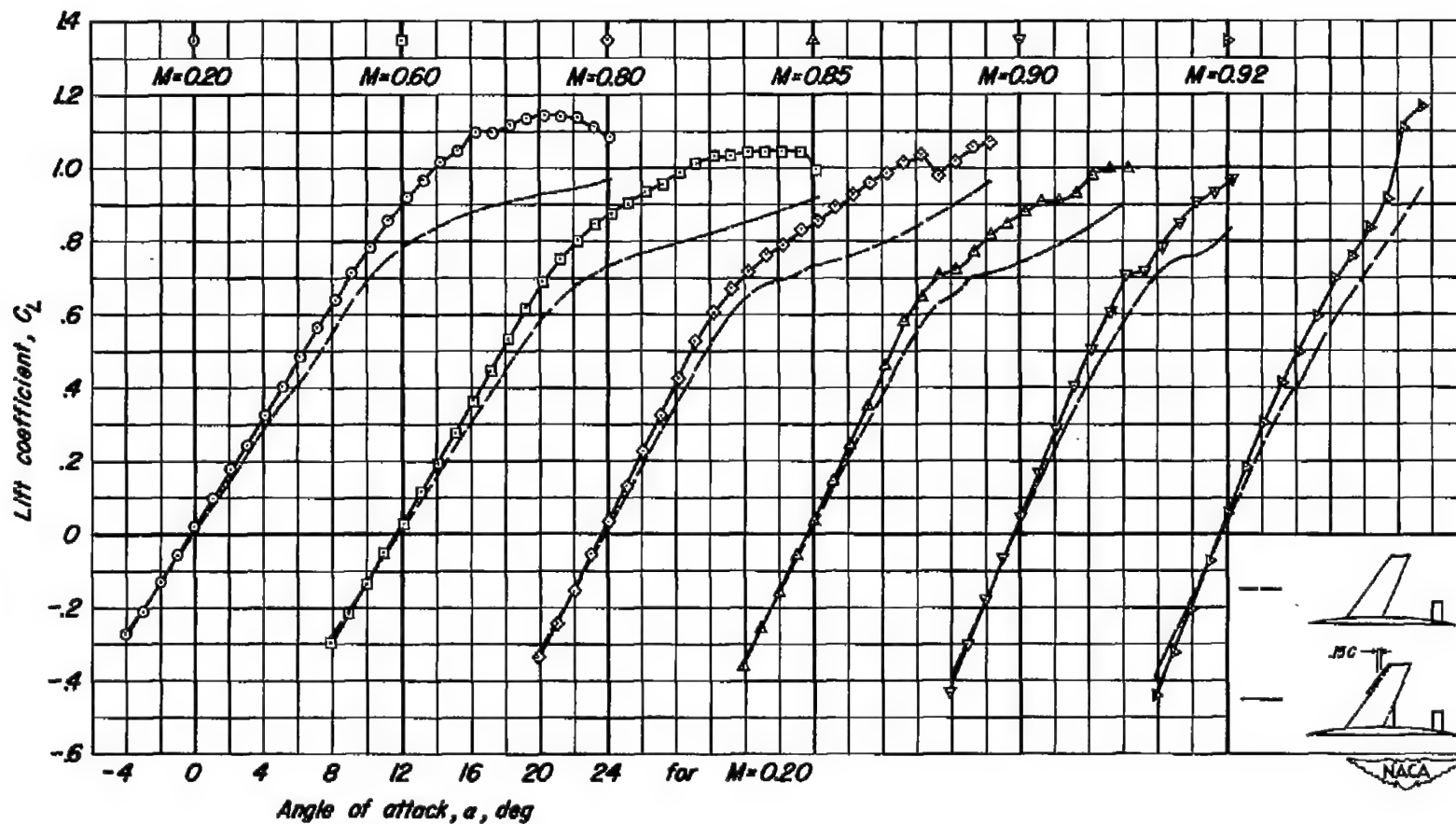
(a)  $C_L$  vs  $\alpha$ 

Figure 20.- The effect of a trailing-edge root-chord extension in combination with a long-span leading-edge extension on the aerodynamic characteristics of the complete model at various Mach numbers.  $R$ , 2,000,000.

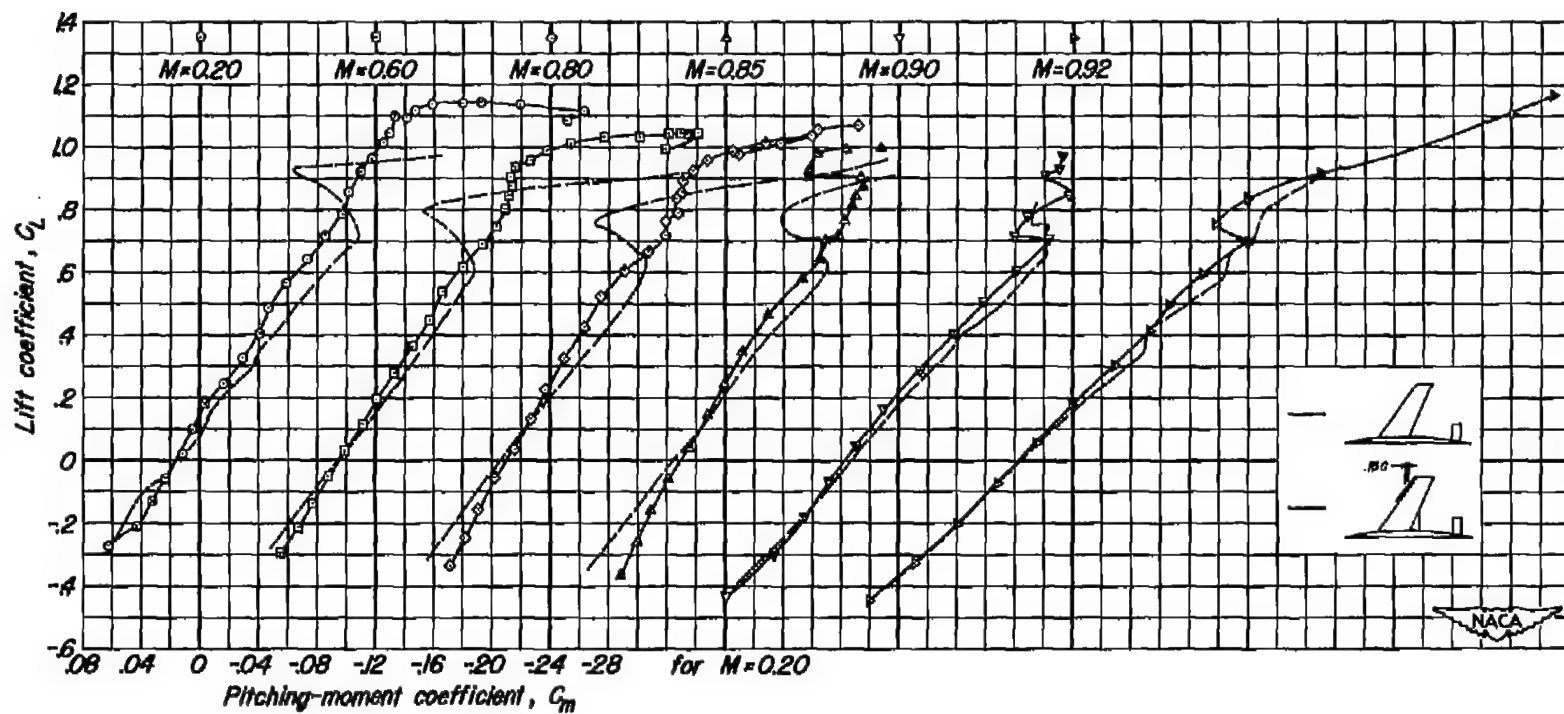
(b)  $C_L$  vs  $C_m$ 

Figure 20.- Continued.

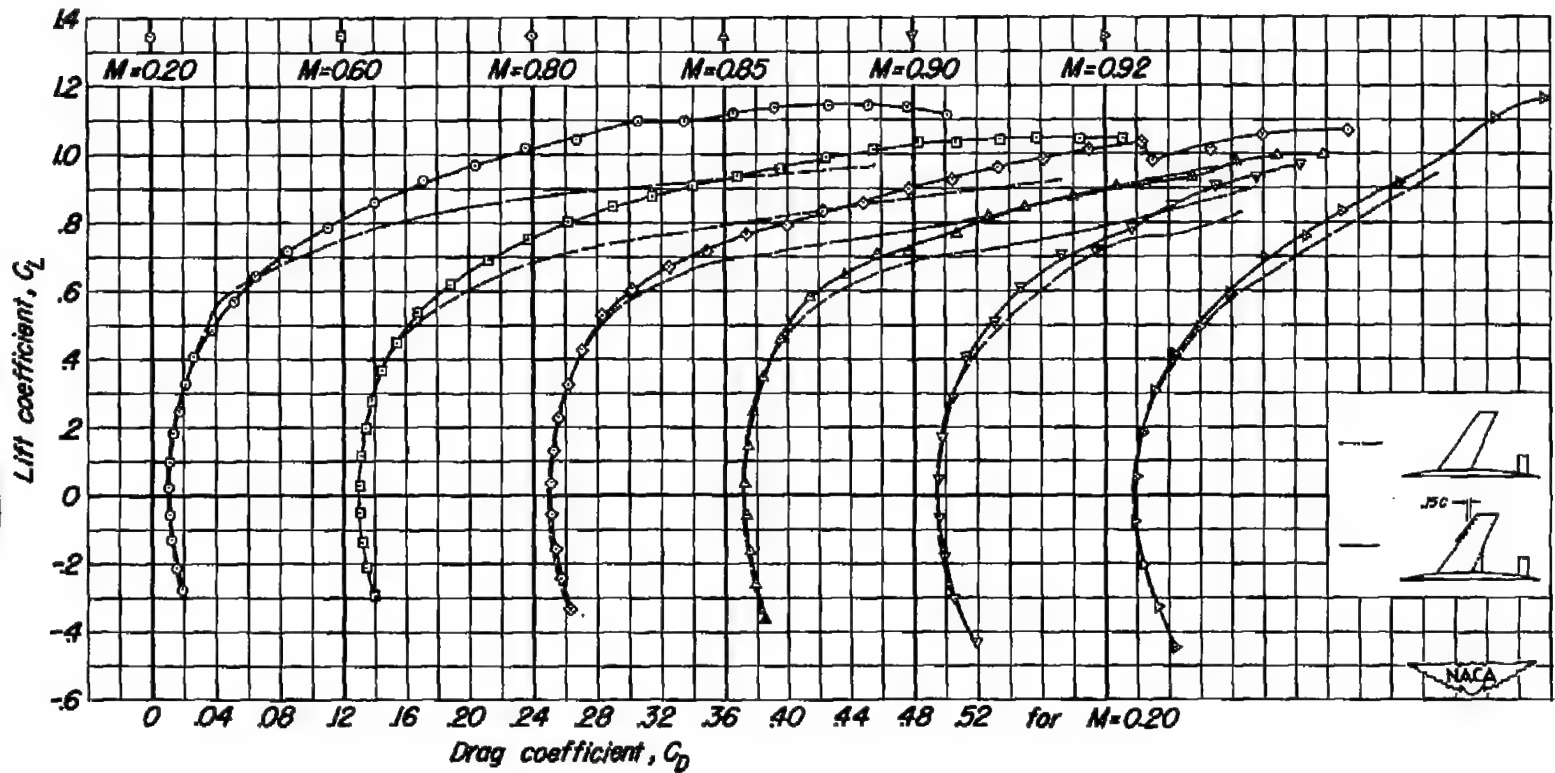
(c)  $C_L$  vs  $C_D$ 

Figure 20.- Concluded.

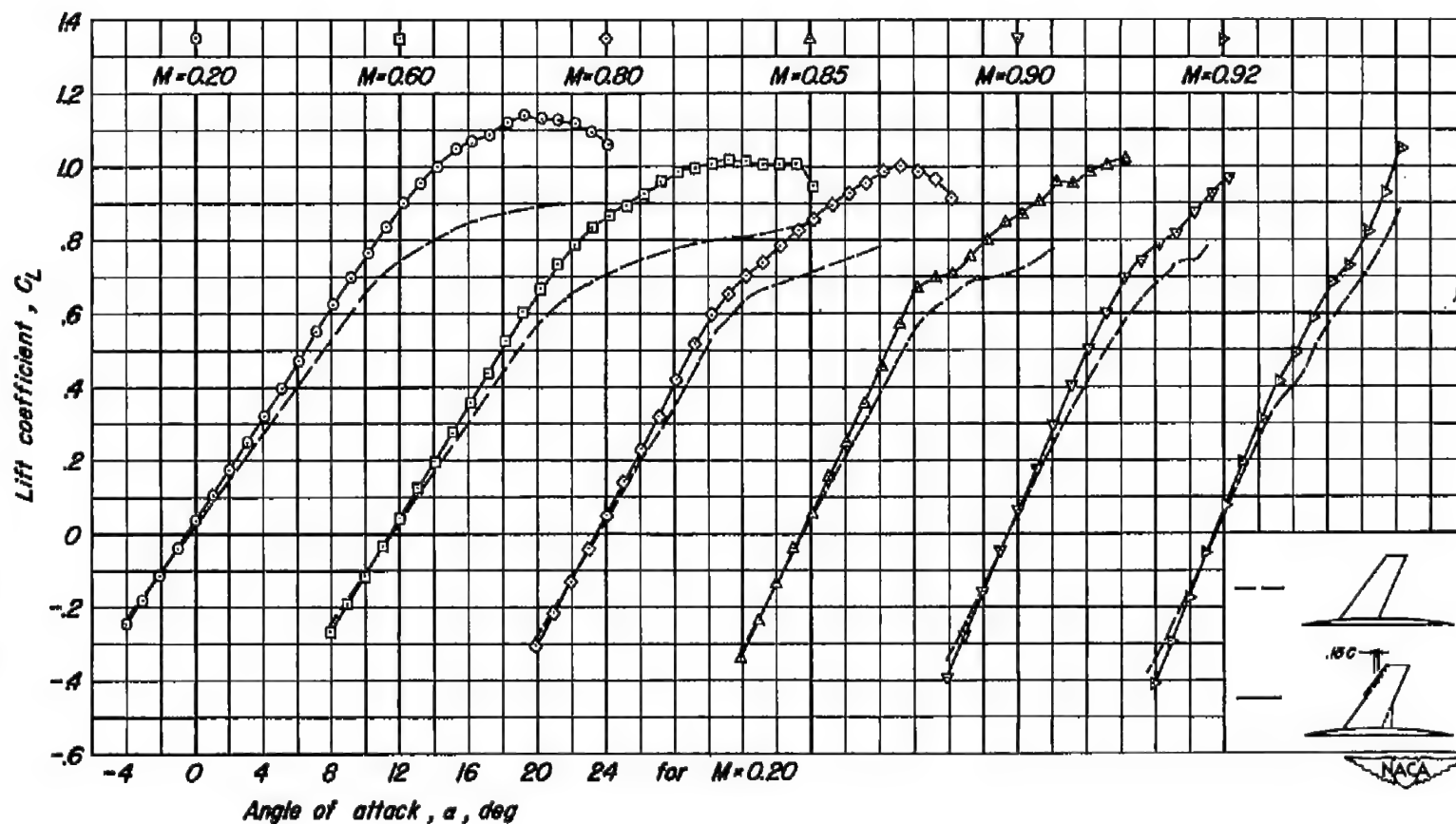
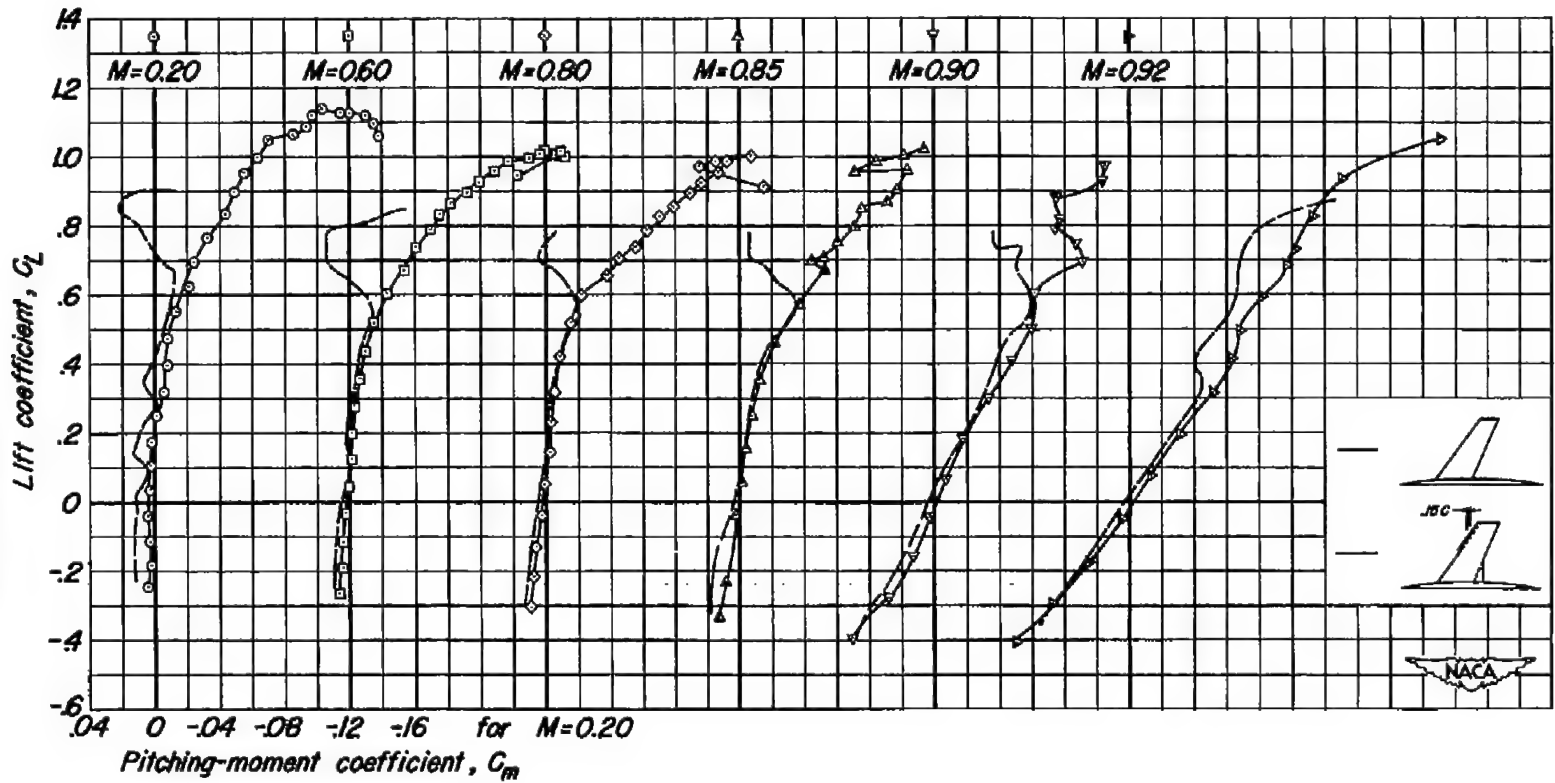
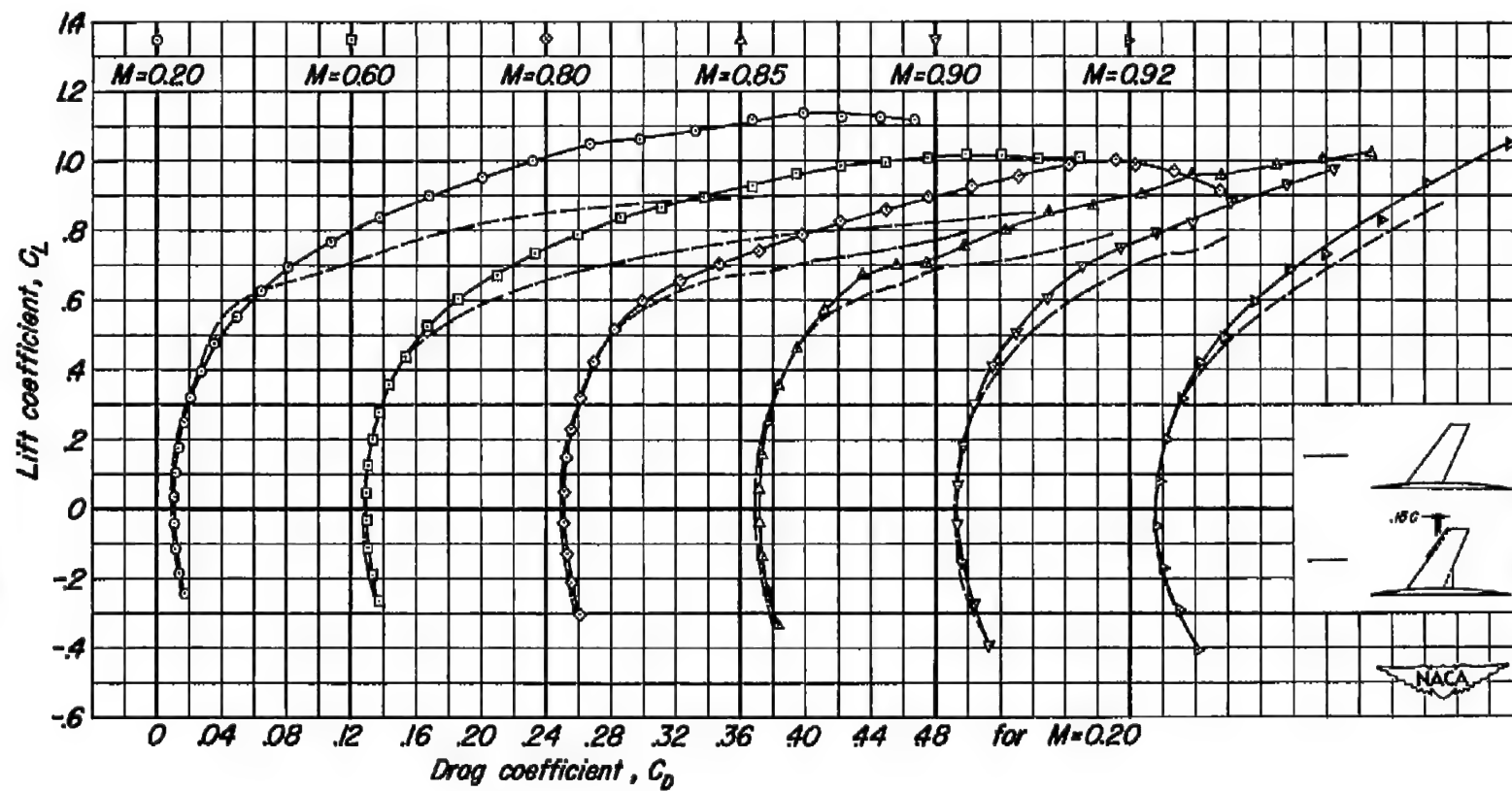
(a)  $C_L$  vs  $\alpha$ 

Figure 21.- The effect of a trailing-edge root-chord extension in combination with a long-span leading-edge extension on the aerodynamic characteristics of the model without tail at various Mach numbers.  $R, 2,000,000$ .



(b)  $C_L$  vs  $C_m$

Figure 21.- Continued.



(c)  $C_L$  vs  $C_D$

Figure 21.- Concluded.



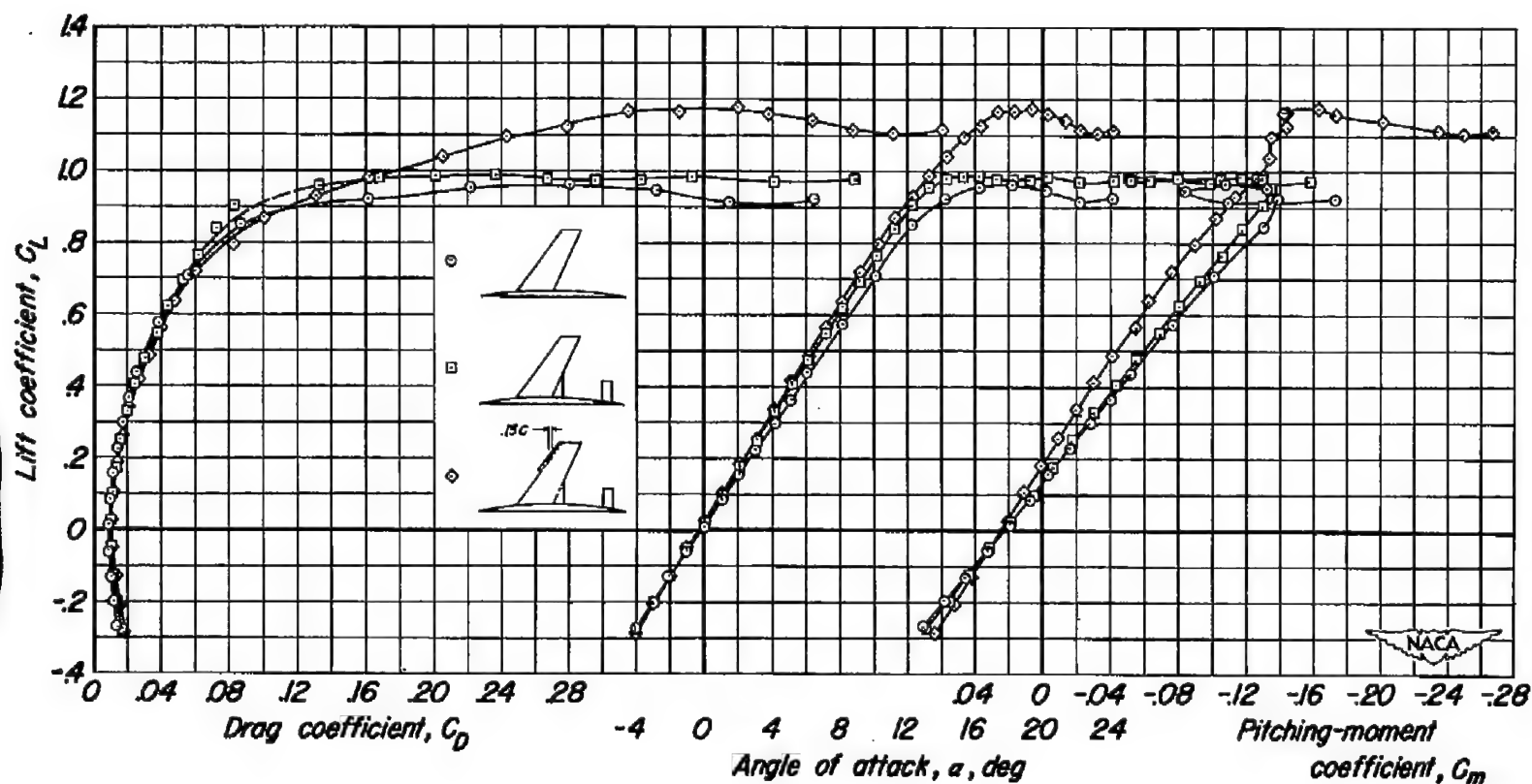


Figure 22.- The effect of a trailing-edge root-chord extension alone and in combination with a long-span leading-edge extension on the aerodynamic characteristics of the complete model at a Reynolds number of 11,000,000.  $M$ , 0.20.

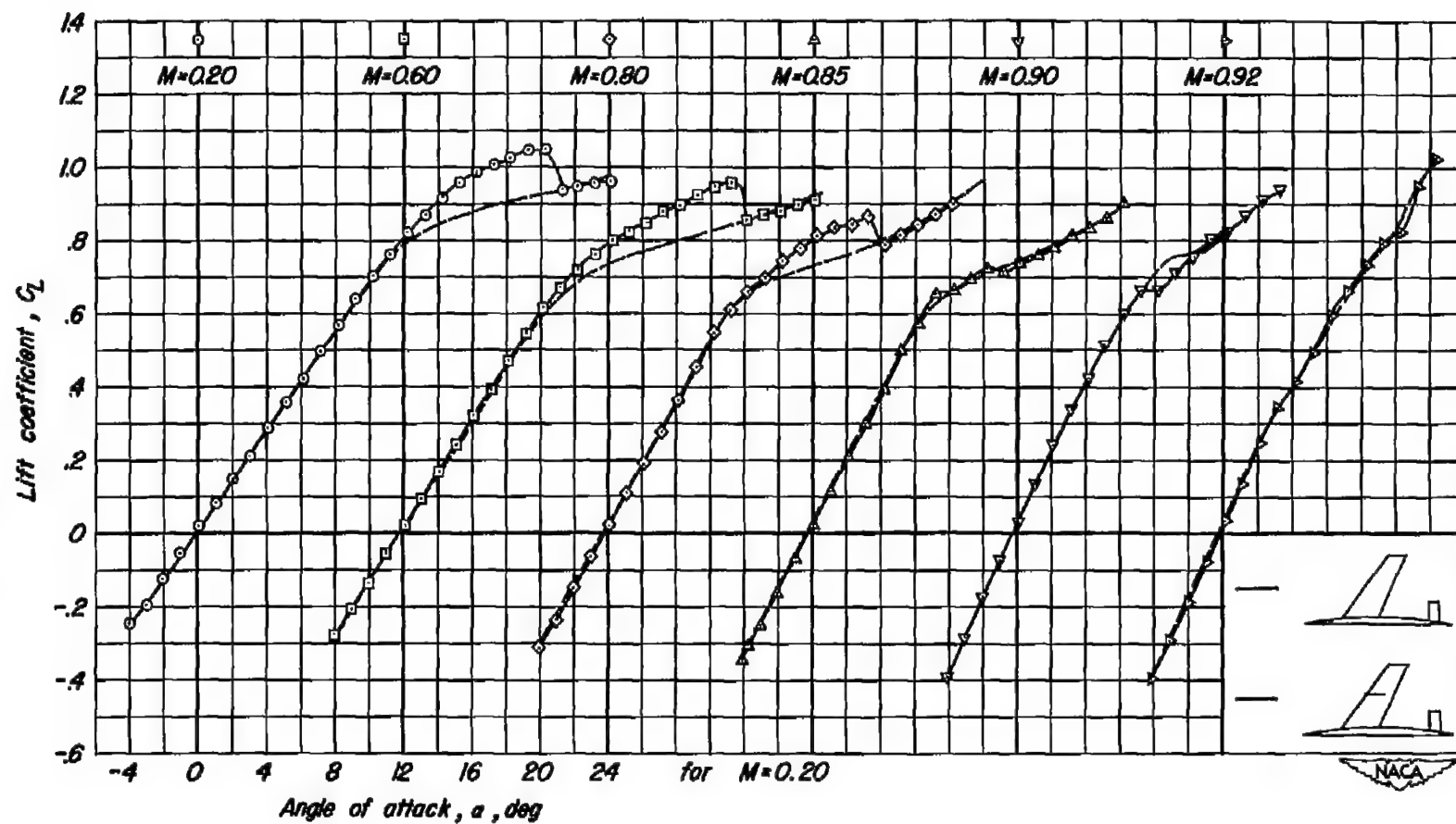
(a)  $C_L$  vs  $\alpha$ 

Figure 23.- The effect of a leading-edge fence on the aerodynamic characteristics of the complete model at various Mach numbers.  $R, 2,000,000$ .

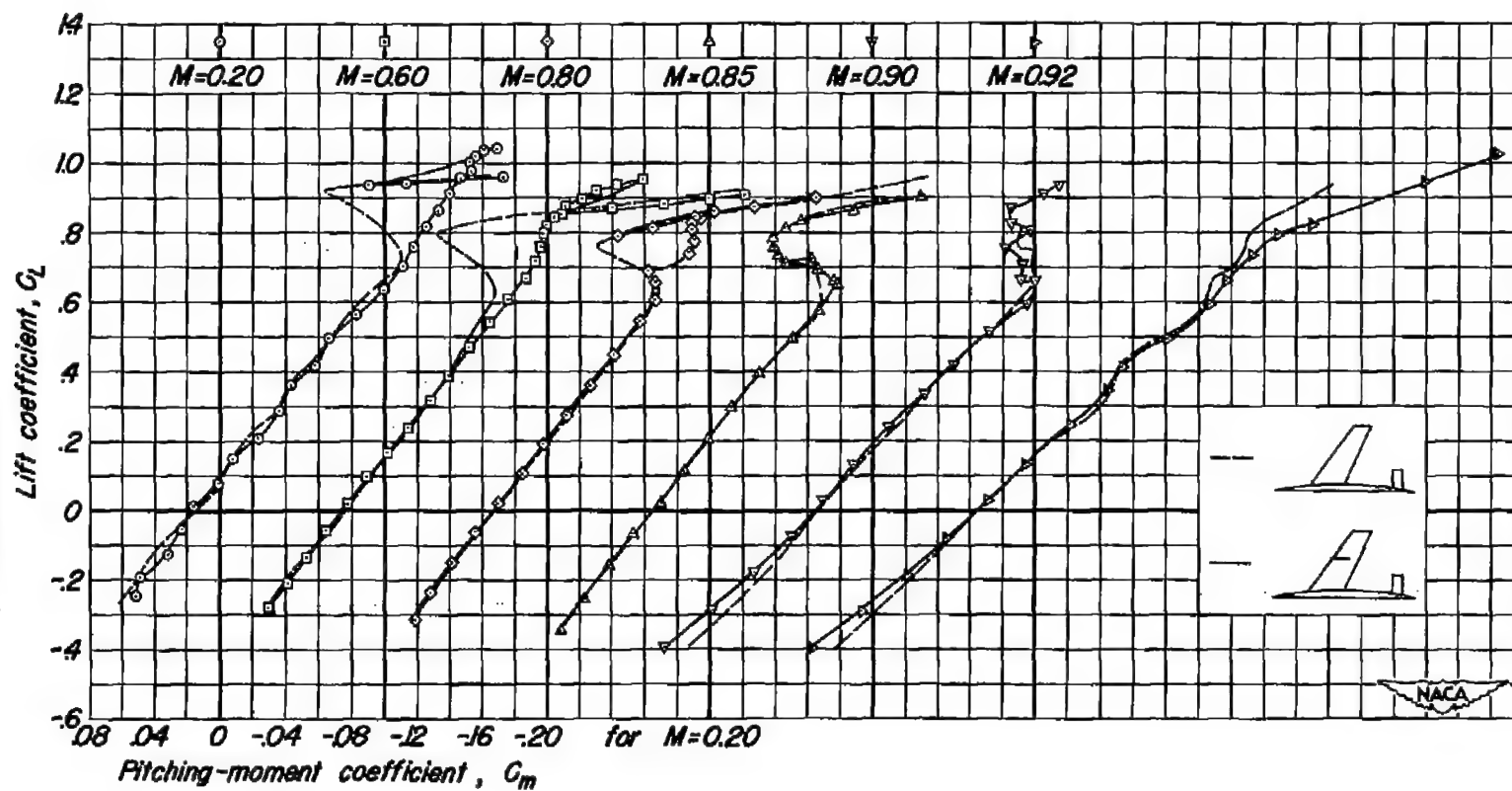
(b)  $C_L$  vs  $C_m$ 

Figure 23.- Continued.

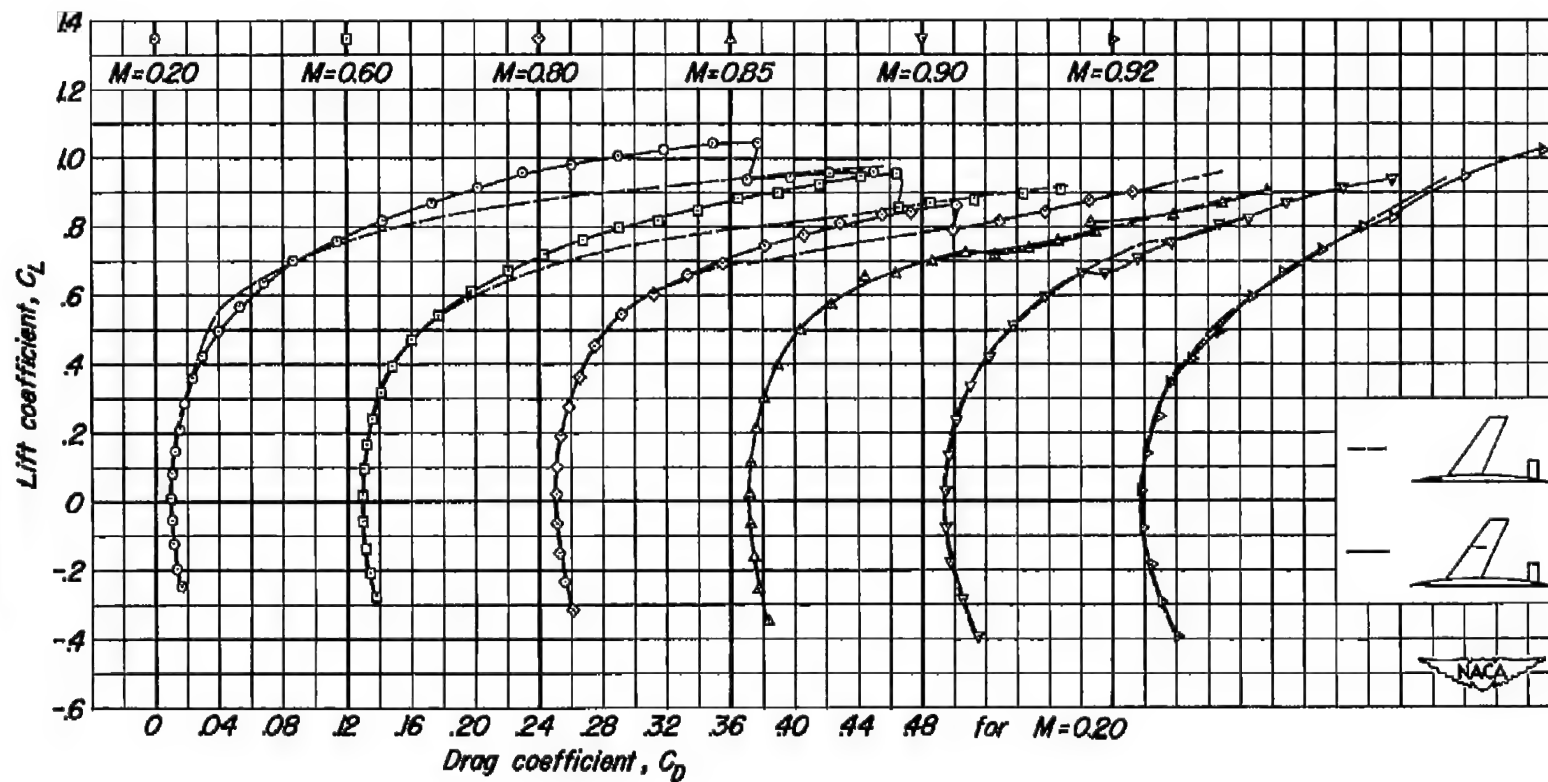
(c)  $C_L$  vs  $C_D$ 

Figure 23.- Concluded.

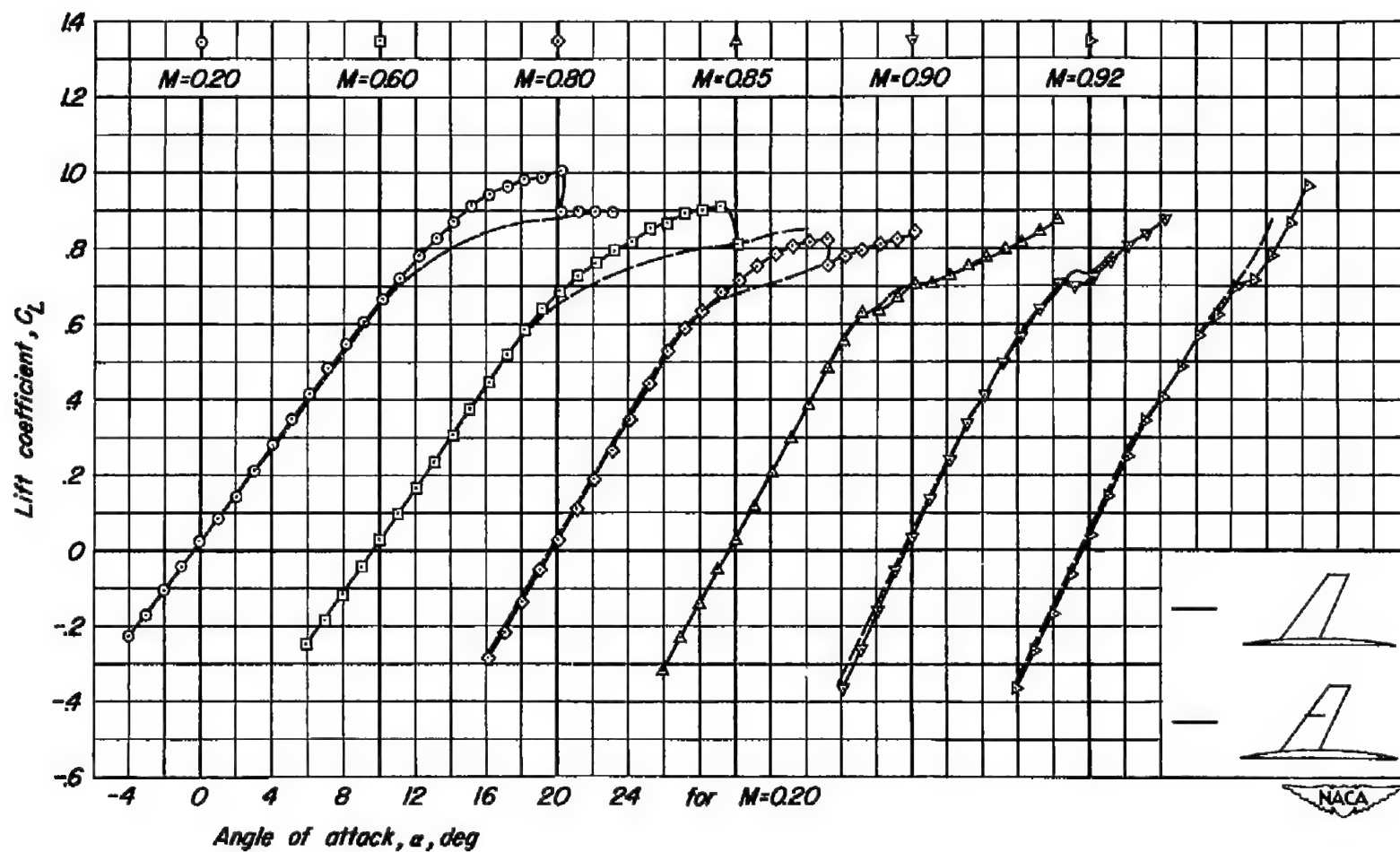
(a)  $C_L$  vs  $\alpha$ 

Figure 24.- The effect of a leading-edge fence on the aerodynamic characteristics of the model without tail at various Mach numbers.  $R, 2,000,000$ .

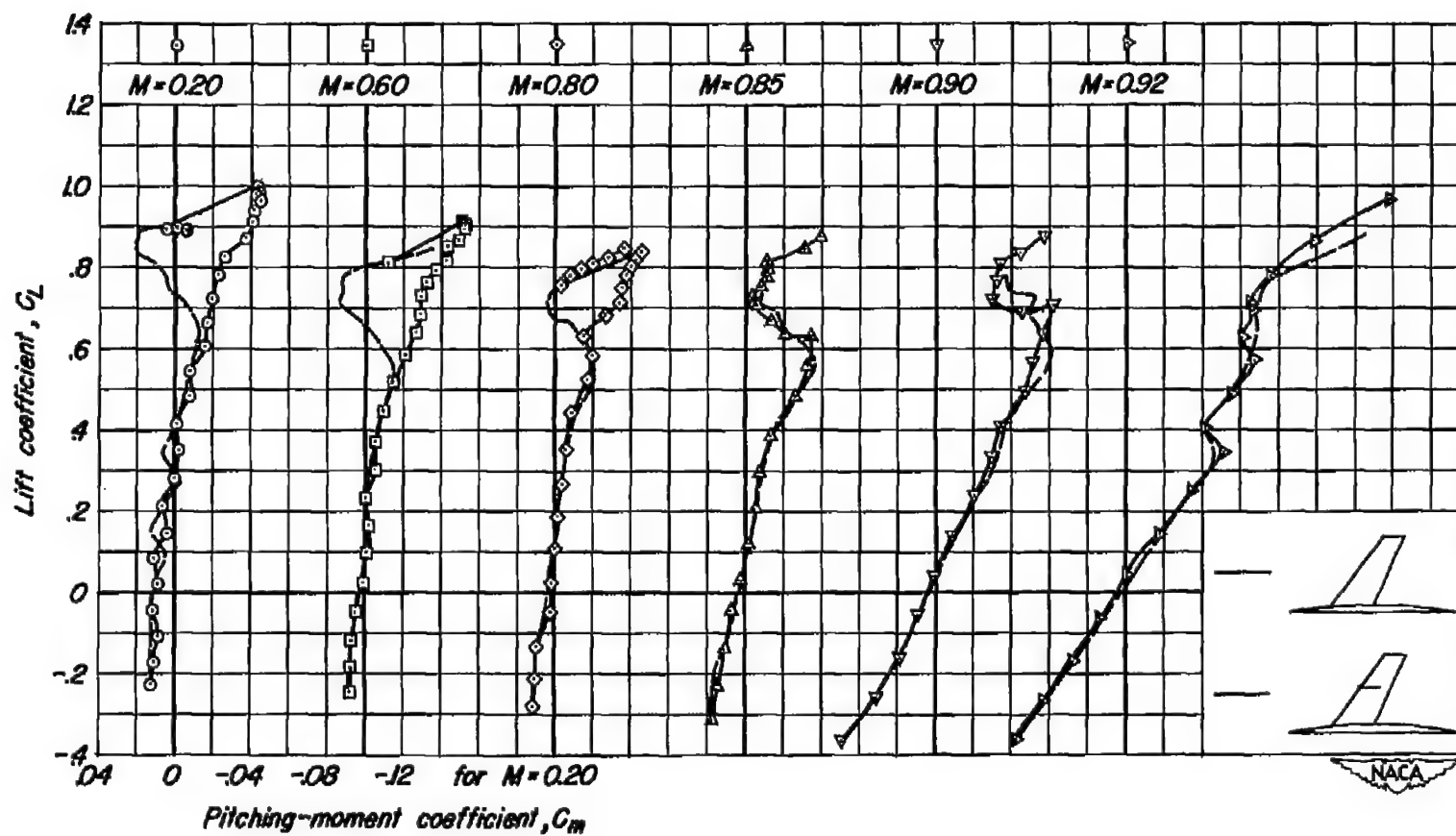
(b)  $C_L$  vs  $C_m$ 

Figure 24.- Continued.

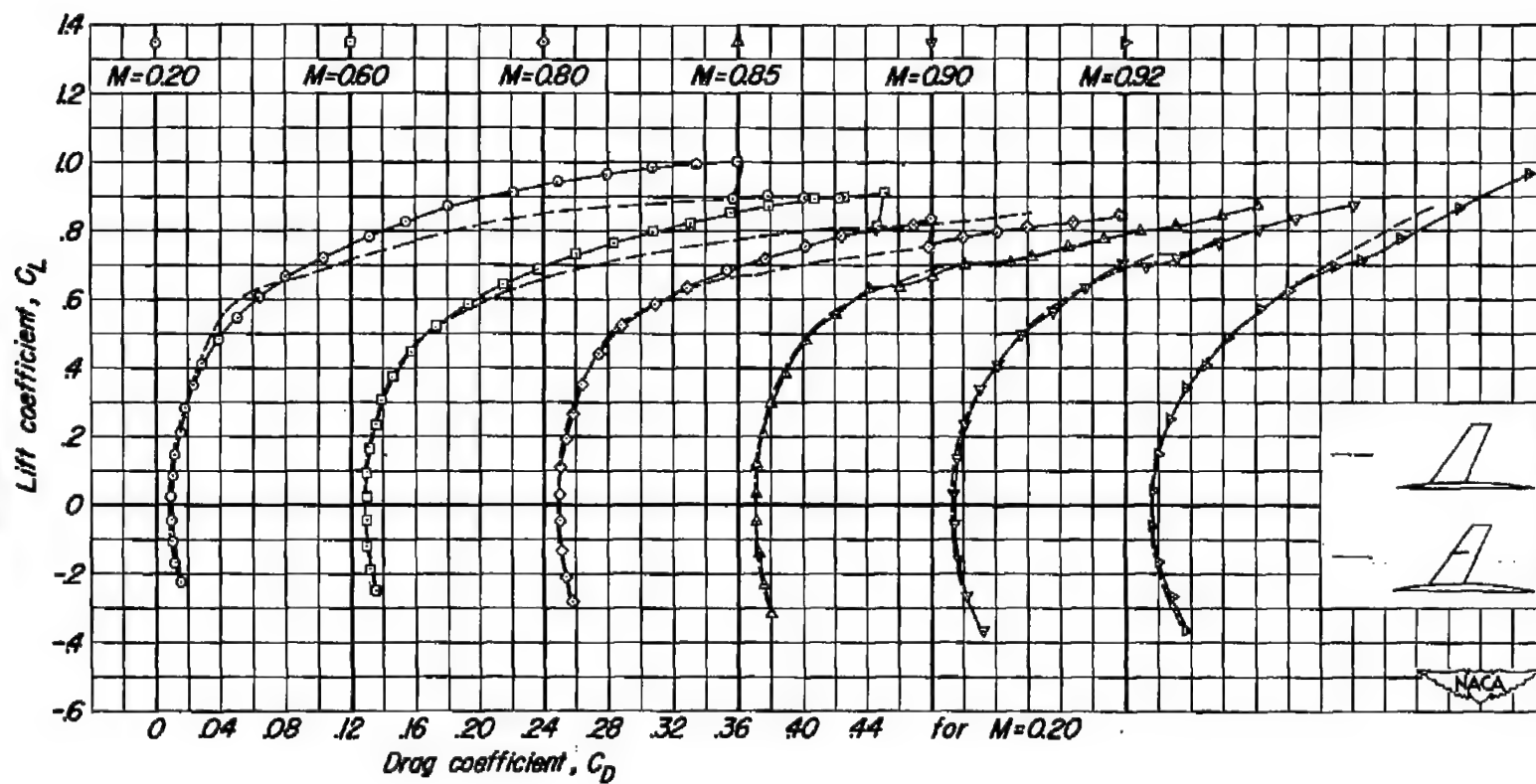
(c)  $C_L$  vs  $C_D$ 

Figure 24.- Concluded.

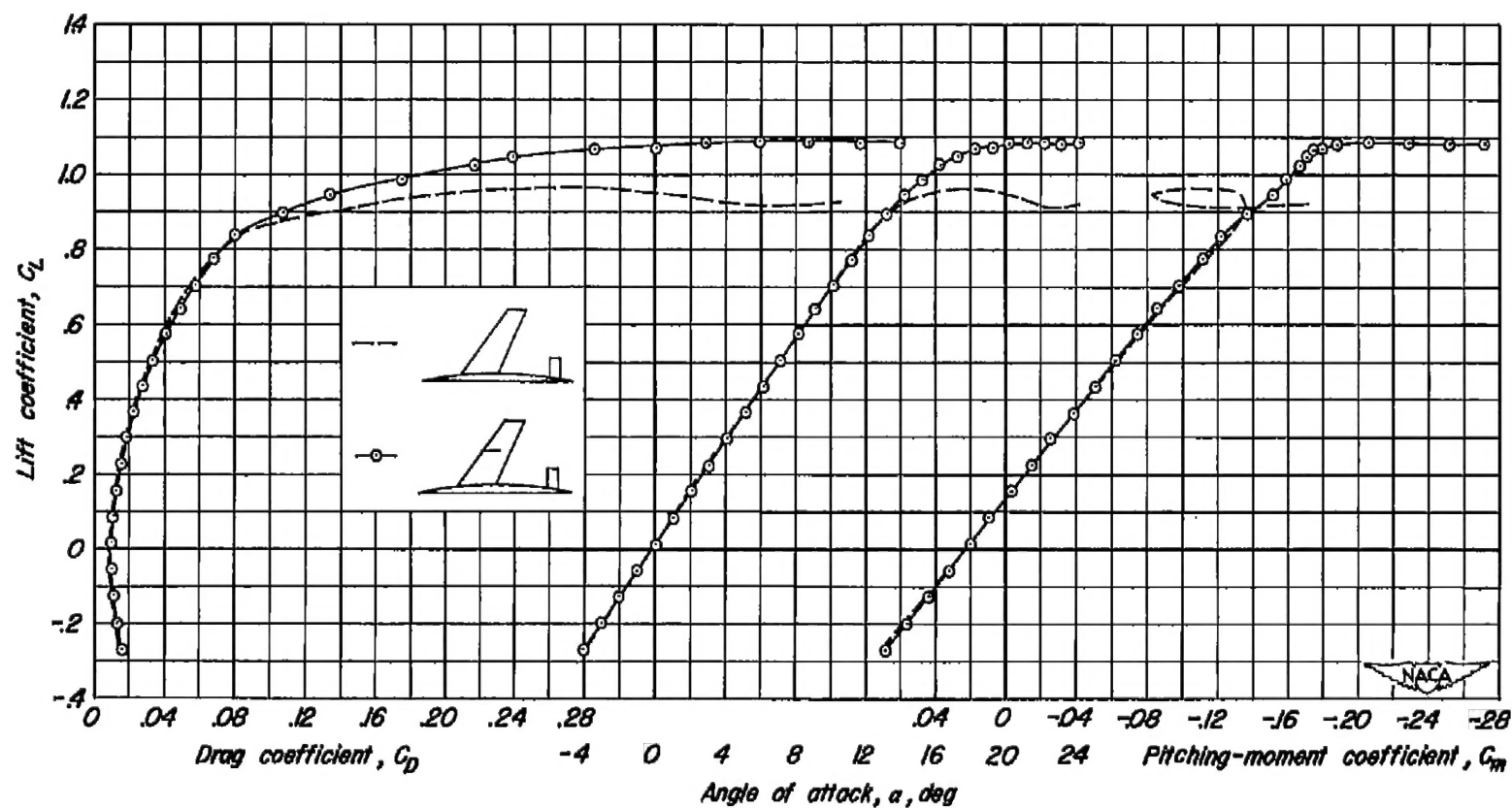


Figure 25.- The effect of a leading-edge fence on the aerodynamic characteristics of the complete model at a Reynolds number of 11,000,000.  $M$ , 0.20.



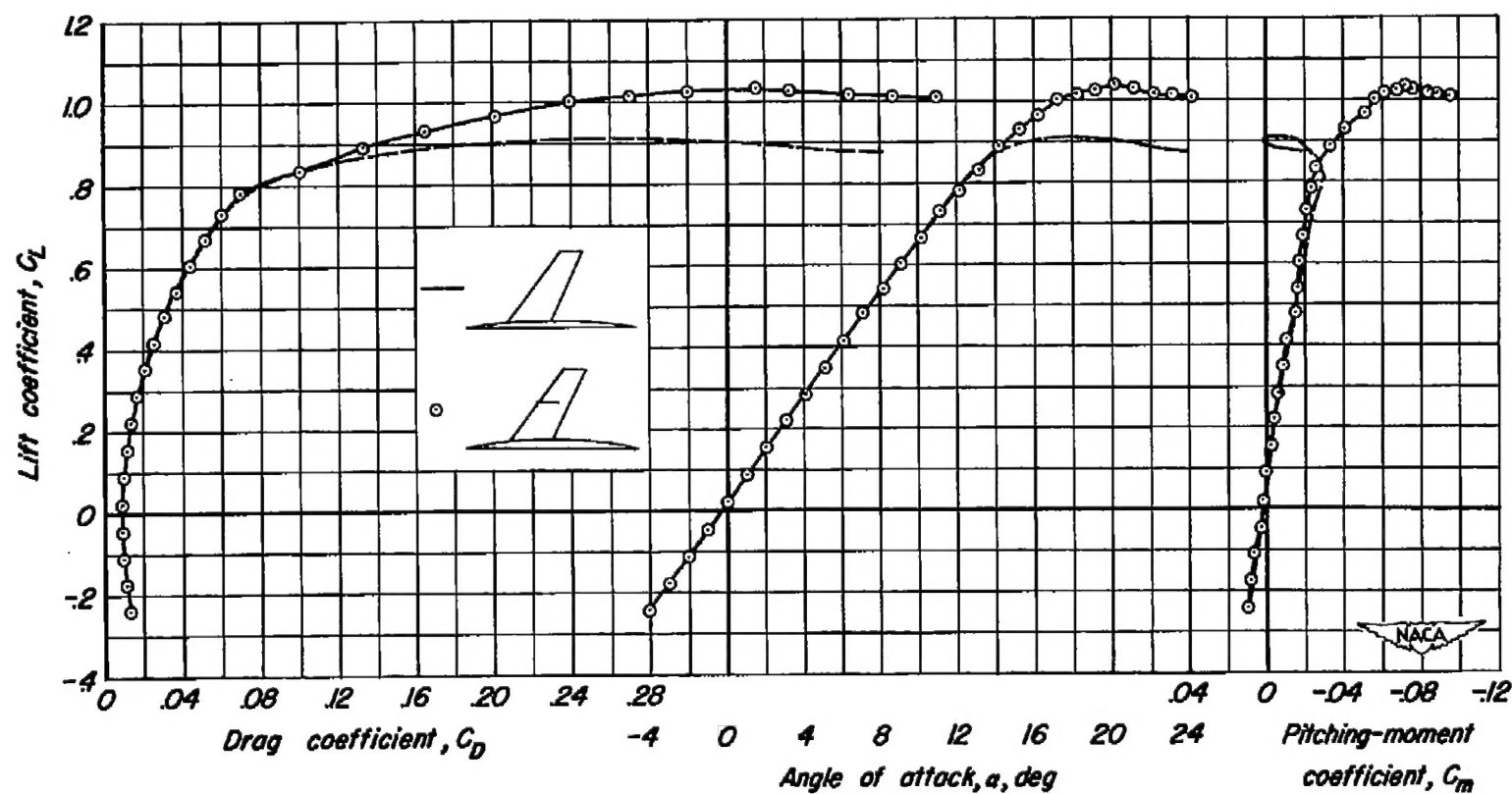


Figure 26.- The effect of a leading-edge fence on the aerodynamic characteristics of the model without tail at a Reynolds number of 11,000,000.  $M$ , 0.20.

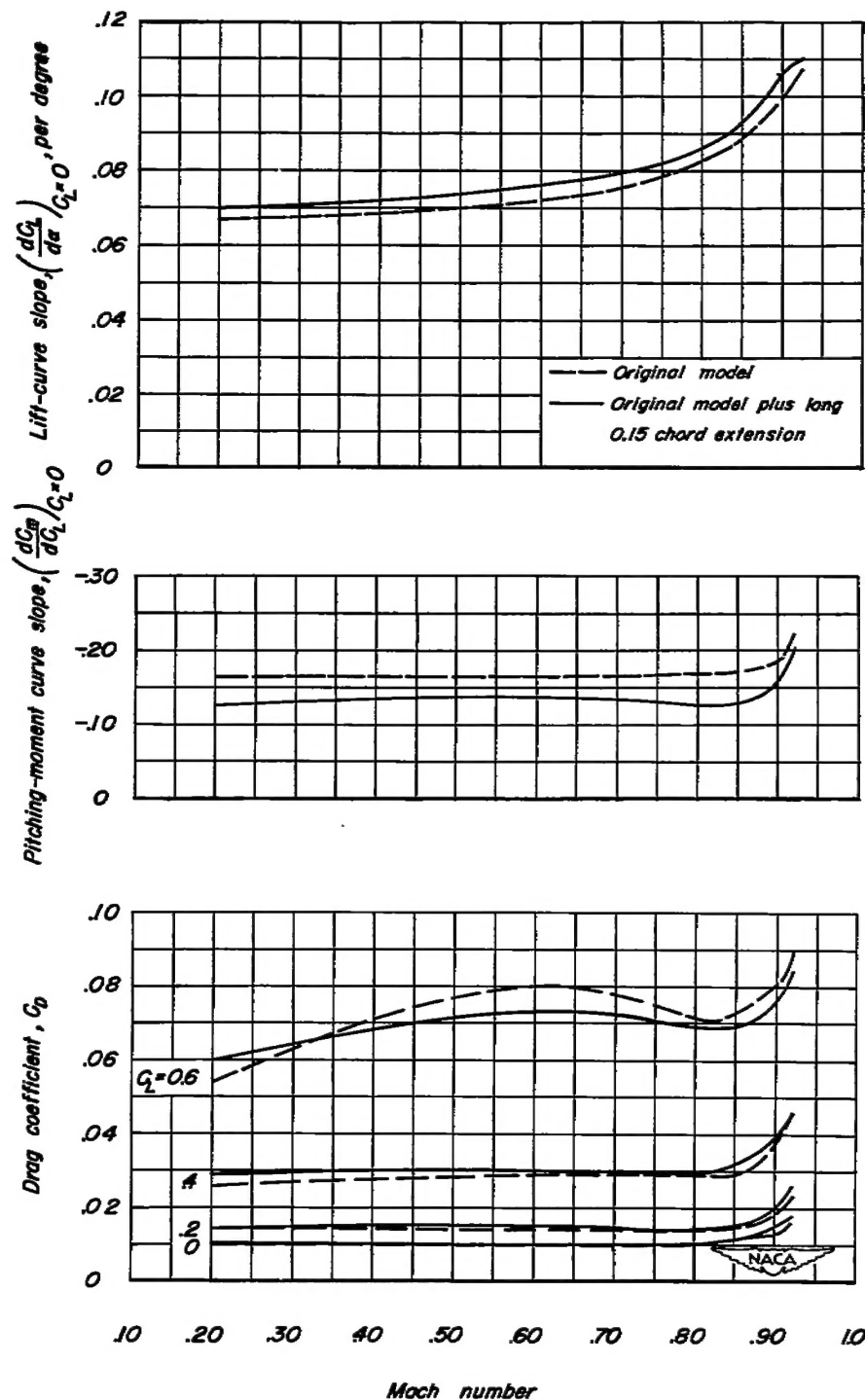


Figure 27.- The variation with Mach number of lift-curve slope, pitching-moment-curve slope, and drag coefficient for the complete model with and without a long-span, constant 15-percent-chord, leading-edge extension. R, 2,000,000.

SECURITY INFORMATION



[REDACTED]

[REDACTED]